Carbon cycling and calcification in hypersaline microbial mats

Dissertation zur Erlangung des Doktorgrades
der Naturwissenschaften

- Dr. rer. nat.-

Dem Fachbereich Biologie/Chemie
der Universität Bremen vorgelegt von

Rebecca Ludwig

Bremen
März 2004

Die vorliegende Arbeit wurde in der Zeit von Oktober 2000 bis März 2004 am Max-Planck-Institut für marine Mikrobiologie in Bremen angefertigt.

Gutachter

Prof. Dr. Bo Barker Jørgensen
Prof. Dr. Gunter O. Kirst

Prüfer

Prof. Dr. Friederike Koenig
Dr. Henk M. Jonkers

Tag des Promotionskolloqiums: 14. Mai 2004

Table of contents

Thesis outline **v**

1 Introduction **1**

Prologue 3
Carbon cycle in microbial mats: Organisms and metabolism 8
Gradients and adaptations to diel changes 17
Calcification 20
Principles and applications of microsensors 22
Sampling/study sites 28

2 Structure and function of Chiprana mats **37**

Structural and functional analysis of a microbial mat ecosystem from a unique permanent hypersaline inland lake: 'La Salada de Chiprana' (NE Spain)

3 Rate limitation in microbial mats **71**

Limitation of oxygenic photosynthesis and respiration by phosphate and organic nitrogen in a hypersaline mat: A microsensor study

4 Effect of salinity on benthic photosynthesis **89**

Reduced gas diffusivity and solubility limit metabolic rates in benthic phototrophs at high salinities

5 Calcification mechanism in a microbial mat **109**

Photosynthesis controlled calcification in a hypersaline microbial mat

6 Stromatolite calcification and bioerosion **127**

Balance between microbial calcification and metazoan bioerosion in modern stromatolitic oncolites

Discussion **145**

Summary **151**

Zusammenfassung **153**

Appendix **155**

Danksagung 155
List of publications 157

Thesis outline

Five manuscripts are included in this thesis that investigate the carbon cycle in microbial mats with a special emphasis on community carbon flow and mechanisms of microbial calcification.
The introduction **(chapter 1)** provides background information about organisms and processes involved in the carbon cycle in microbial mats. Emphasis was placed on oxygenic photosynthesis, the dominant primary production process in mats, and its relation to the organic carbon cycle.

Chapter 2 describes the microbial mats from "La Salada de Chiprana" with special emphasis on the structural and functional analysis of the microbial community with respect to the carbon cycle.
Concept developed by Rebecca Ludwig and H. Jonkers, execution and data analysis by Rebecca Ludwig and H. Jonkers with help of the respective co-authors. The manuscript was written by H. Jonkers with editorial help from Rebecca Ludwig. Published in FEMS Microbial Ecology.

Objective of the study presented in **chapter 3** was the identification of factors that limit oxygenic photosynthesis and respiration in microbial mats of "La Salada de Chiprana".
The study was initiated by H. Jonkers and O. Pringault. Rebecca Ludwig was responsible for the execution, data analysis and interpretation. The manuscript was written by Rebecca Ludwig with editorial help from H. Jonkers. The manuscript has been prepared for submission to FEMS Microbial Ecology.

Chapter 4 compares the influence of salinity on photosynthesis and respiration between planktonic and benthic model cultures of *Cyanothece* sp. (PCC 7418).
The concept was developed by F. Garcia-Pichel and Rebecca Ludwig. The experiments were executed by Rebecca Ludwig. The manuscript was written by Rebecca Ludwig with editorial help from F. Garcia-Pichel. The manuscript is in preparation for submission to L&O.

The study described in **chapter 5** investigated whether calcification in mats from "La Salada de Chiprana" is driven by photosynthetic or heterotrophic processes.
Rebecca Ludwig and H. Jonkers developed the concept. Execution, data analysis and interpretation by Rebecca Ludwig. The manuscript was written by Rebecca Ludwig with inputs from the co-authors. This manuscript is to be submitted to L&O.

Chapter 6 examines the balance between calcification and metazoan grazing in stromatolitic microbialites from Cuatro Cienegas, Mexico.
The study was initiated by F. Garcia-Pichel. Rebecca Ludwig and F. Al Horani were responsible for concept, execution and data analysis of microsensor measurements. All authors contributed equally to this work. Published in Geobiology (in press).

Chapter 1

Introduction

1

Prologue: Ancient and modern microbial mats

Microbial mats are dense aggregations of microorganisms and their viscous excretion products that form a laminated system at the boundary between a substratum (typically the sediment surface) and water[1]. The lamination of phototrophic microbial mats originates in the vertical distribution of pigmented bacteria, which orient themselves to zones where they find optimal conditions. Mats harbour a large diversity of microbes, which by their metabolic activity create steep chemical gradients[2]. Microbial mats are considered to be analogues of ancient stromatolites (Fig. 1) and have been extensively researched in order to better understand the formation of the latter (Van Gemerden 1993). While similar to microbial mats, stromatolites are solid structures as a consequence of heavy calcification or sediment trapping.

Stromatolites represent the first fossilised evidence for life on earth, and have been found in rocks as old as 3.2 Ga (1 Ga = 10^9 years) (Nisbet & Fowler 1999). Stromatolites claimed to be older than that might be structural analogues of abiotic origin (Lowe 1994). Geological evidence suggests that life originated even earlier, around 3.8 – 4 Ga, without leaving a fossilised trace (Nisbet & Sleep 2001; Nisbet & Fowler 2003). Where exactly life originated, what kind of metabolism was used and what early life looked like are topics heavily disputed and controversially discussed. Due to scarce evidence these questions might never be answered unambiguously and scientists are left to develop scenarios for the evolution of life based on indirect evidence about early earth (i.e. ancient relics, modern descendants, models) (Nisbet & Fowler 2003). The best way to avoid misinterpretation of the scarce evidence might be the integration of evidence from geology, biochemistry and (molecular) biology. As recent microbial mats are often considered as analogues of ancient stromatolites this prologue presents some aspects of the environmental conditions ancient stromatolites probably experienced and the metabolic processes that might have taken place.

Soon after the origin of earth around 4.6 Ga the earth was very hot and reached core temperatures of around 2000°C, the melting temperature of iron. Due to gravitation,

[1] While this is also true for biofilms, most researchers reserve the term mat for a system with a visible lamination.

[2] For a more detailed description of organism and processes in microbial mats the reader is referred to the following section.

the heavy liquid iron accumulated in the core, while lighter material got transported towards the surface where it cooled down and built a thin crust. To our present knowledge, the existence of liquid water and an atmosphere is essential for the existence of life. Both the gaseous atmosphere and liquid water are thought to have gassed out from the hot core of earth, where they were present in elemental form (Press & Siever 1995). The exact nature of this prebiological atmosphere is heavily debated, but the favoured hypothesis today is that it was mildly reducing with N_2 as the major constituent but also containing CO_2 and H_2O (Wayne 2000). It had been assumed previously that the prebiological atmosphere mainly contained NH_3 and CH_4 and was strongly reducing, but recent research suggests that these constituents did not last long, if they were present at all (Wayne 2000; Nisbet & Sleep 2001). This is supported by highly metamorphosed sediments in Isua, West Greenland (3.8 Ga), that are thought to be formed in the presence of H_2O and CO_2, but without abundant methane (Wayne 2000).

As mentioned above, life probably originated around 3.8 – 4 Ga, but whether this happened in hydrothermal or mesophilic environments is heavily debated[3]. While this question cannot be fully answered based on the evidence known so far, one possible scenario for the evolution of life, namely the evolution of mats around hydrothermal vents, will be described[4]. Hydrothermal vents would have allowed chemolithoautotrophs to thrive as they transport reduced compounds like H_2, H_2S, CH_4 from the earth's core to the more oxidised ocean waters (Nisbet & Fowler 2003). The earliest organisms might have been using FeS and H_2S to gain energy or H_2 and CO_2 for methanogenesis. As death should have been part of life from its start, the biomass of these bacteria would for example enable fermenters to live on dead organic material. This might indeed have been an important source of organic carbon, as the existence of a primaeval soup of organic carbon is challenged by geologists (Martin & Russell 2003; Nisbet & Fowler 2003). Some sulphate and nitrate was probably provided via the atmosphere (Nisbet & Fowler 2003) and allowed anaerobic respiration e.g. by sulphate reducers which might have had evolved around 3.5 Ga ago (Shen et al. 2001). Anaerobic respiration in turn would have provided reduced

[3] One argument used to support a hyperthermophilic origin is that the most deeply rooted organisms of the universal phylogenetic tree are high temperature adapted (Pace 1997; Woese 2000; Nisbet & Fowler 2003), however, the inferred GC content of the universal ancestor and the unstability of RNA at high temperatures has been considered as incompatible with a hyperthermal habitat of the universal ancestor (Forterre & Philippe 1999; Galtier et al. 1999).

[4] The reader is referred to Fuerst (1995) and Nisbet & Fowler (2003) for descriptions of the early evolution and possible habitats of planktonic cells.

substances like H_2S and CH_4 in addition to that from hydrothermal vents. The implications of diverse geological evidence is that hyperthermal habitats around hot vents were probably populated by microbial mats by the mid-Archean (Nisbet & Fowler 2003). The next step in the evolution of mats would have been the development of a photoautotrophic process as it used an ubiquitous energy source and e^- donor (light and e.g. water) and was therefore independent of hydrothermal environments (Nealson & Rye 2003). This happened with the onset of photosynthesis. How the crucial step towards photosynthesis exactly happened is still not clear, nor whether oxygenic or anoxygenic photosynthesis evolved first (Blankenship & Hartman 1998; Olson 2001; Nisbet & Fowler 2003). However, evidence is growing that anoxygenic photosynthesis evolved first (Nealson & Rye 2003). Two lines of evidence have been used to infer that oxygenic photosynthesis did evolve around 2.7 Ga. RuBisCO (ribulose bisphosphate carboxylase/oxygenase), the enzyme used by most phototrophs to fix CO_2, leaves organic carbon with a different isotopic signature, when fixed by oxygenic ($\delta^{13}C$~ -28 ‰ to -30 ‰) in contrast to anoxygenic phototrophs ($\delta^{13}C$ around -11 ‰) (Nisbet & Fowler 2003). This RuBisCO fingerprint has provided evidence that oxygenic photosynthesis had evolved by 2.7 – 3.0 Ga. More direct evidence for the presence of cyanobacteria stems from 2.7 Ga when characteristic biomarkers, e.g. 2α-methylhopanes, where found in rocks in Australia (Brocks et al. 1999; Summons et al. 1999). The evolution of oxygenic photosynthesis implies that at least the mat environment itself was oxic and similar cycles to today might have taken place. However it should be kept in mind that the presence of oxygenic photosynthesis does not necessarily mean the presence of an oxidised atmosphere. For a net oxygenation (net production of O_2) of the atmosphere to occur, reducing power has to be removed from the cycle e.g. by burial of organic matter. Cyanobacterial mats possibly also played a role in removing reduced compounds, by producing H_2, which was subsequently lost to space (Hoehler et al. 2001).

Most fossil stromatolites found so far, date from a time when oxygenic photosynthesis had evolved. How similar were these fossils to modern mats? As they consisted of a complex bacterial community and performed oxygenic photosynthesis, they appear to have been very similar to modern mats. However, there might have been some differences to modern microbial mats. In contrast to today, sulphate concentrations might have been very low (< 200 μM) as deduced from minimally fractionised early Archean sedimentary sulphides (Canfield et al. 2000; Habicht et al. 2002). These low sulphate levels might have entailed high rates of methanogenesis, supplying the

atmosphere with CH_4 and making methanogenesis rather than sulphate reduction the main pathway of anaerobic carbon mineralisation.

Figure 1 Left: Fossil stromatolite from the Bell Supergroup, USA (1.3 Ga). Right: Recent stromatolite from the Laguna Mormona, Mexico.

Despite their importance as the first fossils and the intense research stromatolites received, the exact definition of stromatolites has been subject to much confusion since the German Ernst Kalkowsky coined the term stromatolite to describe a layered Buntsandstein formation in the Harz mountains in 1908 (Burne & Moore 1987). According to Awramik (1984) stromatolites are defined as "organosedimentary structures produced by sediment trapping, binding and/or precipitation activity of microorganisms, primarily by cyanobacteria". Although this definition is widely used, it does not include one key feature usually associated with stromatolites: the lamination. Therefore Burne & Moore (1987) suggested the term microbialite to be used as an umbrella term for microbial deposits in general, with stromatolite referring to a laminated texture, thrombolite to a clotted texture and oncolite used for concentrically laminated structures. According to Riding (2000) 'the term stromatolite remained untouched by these clarifications'. The definitions given above, include both fossilised structures and also their recent counterparts, that are still metabolically active like recent stromatolites described by Laval et al. (2000) and Reid et al. (2000).

The fossil record implies that stromatolites were common and widely distributed throughout the Proterozoic. However, the diversity and abundance of stromatolites decreased dramatically in the late Neoproterozoic (see Fig. 2 and Awramik (1971)).

This pronounced decline coincided with the evolution of metazoans, which exposed stromatolites to grazing pressure. Alternative factors that might have triggered the demise of stromatolites include competitive exclusion by macroalgae or changes in seawater chemistry, which decreased calcification rates (Pratt 1982; Grotzinger 1990). Recent microbial mats only thrive in environments where the abundance of grazers is greatly repressed, so that it has been concluded that the onset of metazoan grazing reduced habitats suitable for the stromatolites. Although they are restricted to extreme environments with respect to e.g. temperature and salinity, modern phototrophic mats can be found all over the planet from tropical lagoons to arctic lakes, from thermal springs to deserts.

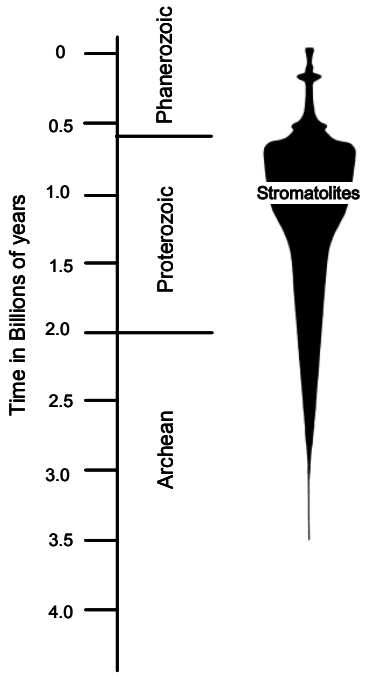

Figure 2 Relative abundance of stromatolites over geological time (redrawn after Awramik (1984)).

Carbon cycle in microbial mats: Organisms and metabolism

This section introduces the different functional groups of microorganisms present in microbial mats and relevant aspects of their metabolism and ecology. The concerted activity of these organisms as well as the internal cycling of metabolites contributes to an effective recycling and thereby to their ability to thrive in oligotrophic environments.

Autotrophy

Oxygenic phototrophs and carbon metabolism

All ecosystems depend on primary producers, autotrophic organisms that fix CO_2 and provide organic carbon for heterotrophic organisms. Organisms capable of using CO_2 as a sole carbon source include phototrophs and chemoautotrophs such as colourless sulphur bacteria, nitrifiers, methanogens and some sulphate-reducing bacteria. The dominant primary producers in shallow water microbial mats are usually oxygenic phototrophs (Paerl et al. 2000; Stal 2000). Phototrophic microbial mats are very productive ecosystems, with the primary production being comparable to tropical rain forest (Guerrero & Mas 1989). (For descriptions of non-phototrophic mats see Belkin & Jannasch (1989), Sarbu et al. (1994), and Krüger et al. (2003)). Oxygenic phototrophs use light energy to convert CO_2 into organic carbon and generate oxygen. In microbial mats this process is performed by diatoms (Eukaryotes) and cyanobacteria (Prokaryotes). Oxygenic photosynthesis will be described in more detail in the following paragraphs.

Linear electron transport and CO_2 fixation using RuBisCO Oxygenic phototrophs fix CO_2 with the Calvin cycle, which depends on ATP and NADPH produced during photosynthetic e^- transport (PET). Pigments (chlorophylls, carotenoids and phycobilins) are involved in absorption of light energy and transferring the excitation energy to the so-called special pair of chlorophyll. In photosystem II (PS II) the photic energy converts P680 into a strong reductant, which donates e^- to pheophytin (see Fig. 3). The remaining $P680^+$ removes electrons from water, generating oxygen, protons and electrons. From pheophytin the e^- are transported along the membrane to the second photosystem (PS I) by a suite of redox reactions. In PS I light energy creates an even stronger reductant ($P700^*$), enabling the cell to produce reducing equivalents in the form of NADPH. Coupled to the e^- transport, protons are transported over the

thylakoid membrane, creating a proton gradient that is for example used to generate ATP.

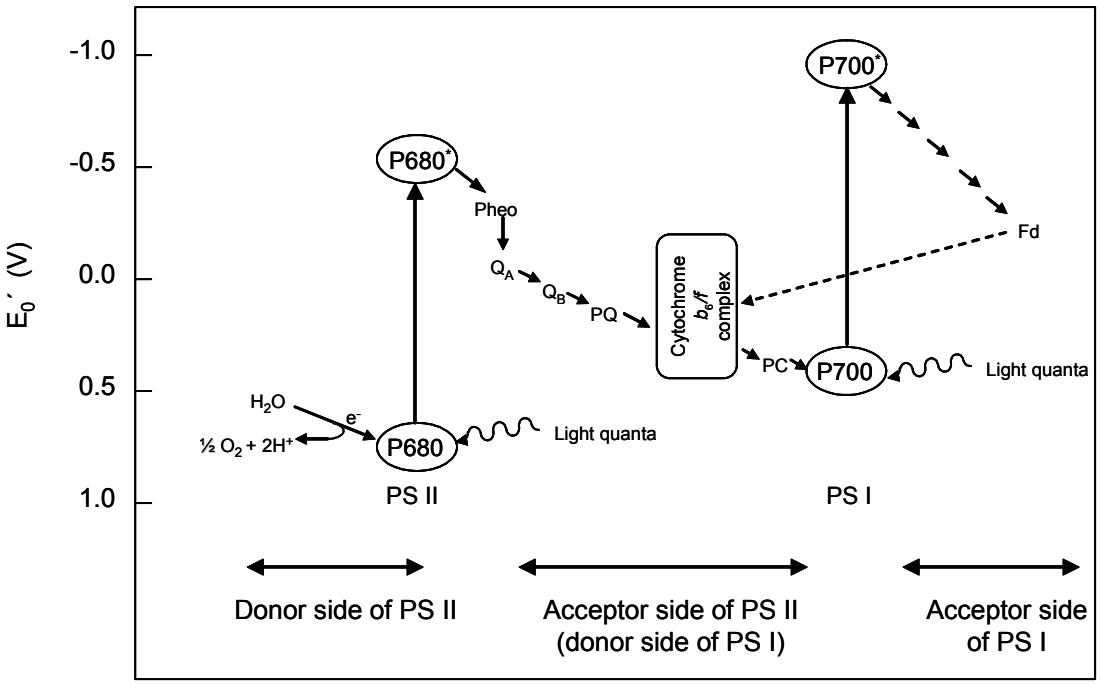

Figure 3 The "z-scheme" of oxygenic photosynthetic e^- transport modified after Falkowski 1997. The e^- carriers are arranged according to their midpoint potential. P680 is the reaction centre of PS II, P700 the reaction centre of PS I. The dashed line depicts the cyclic e^- flow around PS I. Pheo, pheophytin; Q, quinone; PQ, plastoquinone pool; PC, plastocyanin; Fd, ferredoxin.

The above described light-dependent reaction of photosynthesis supplies ATP and NADPH for CO_2 fixation by the Calvin cycle (see Fig. 4). The first step of carbon fixation is the uptake of CO_2. Evidence is growing that cyanobacteria and diatoms not only rely on the diffusional uptake of CO_2, but can also transport inorganic carbon - presumably as HCO_3^- - actively into the cell where it is converted back to CO_2 using carbonic anhydrase (Kaplan et al. 1988; Raven 1997; Rost et al. 2003). The initial step of the Calvin cycle binds CO_2 to ribulose bisphosphate by an enzyme called RuBisCO (ribulose bisphosphate carboxylase/oxygenase), yielding two C3 compounds (phosphoglyceric acid). The following suite of reactions reduce CO_2 and recycle the acceptor molecule. Six runs of this cycle use 6 CO_2 to yield one molecule of fructose-6-phosphate.

$$6\ CO_2 + 12\ NADPH + 18\ ATP \rightarrow C_6H_{12}O_6(PO_3H) + 12\ NADP^+ + 18\ ADP + 17\ P_i$$

Intermediates of the Calvin cycle include a range of C3 to C7 sugars that can be used in anabolism (cell growth) and catabolism (respiration).

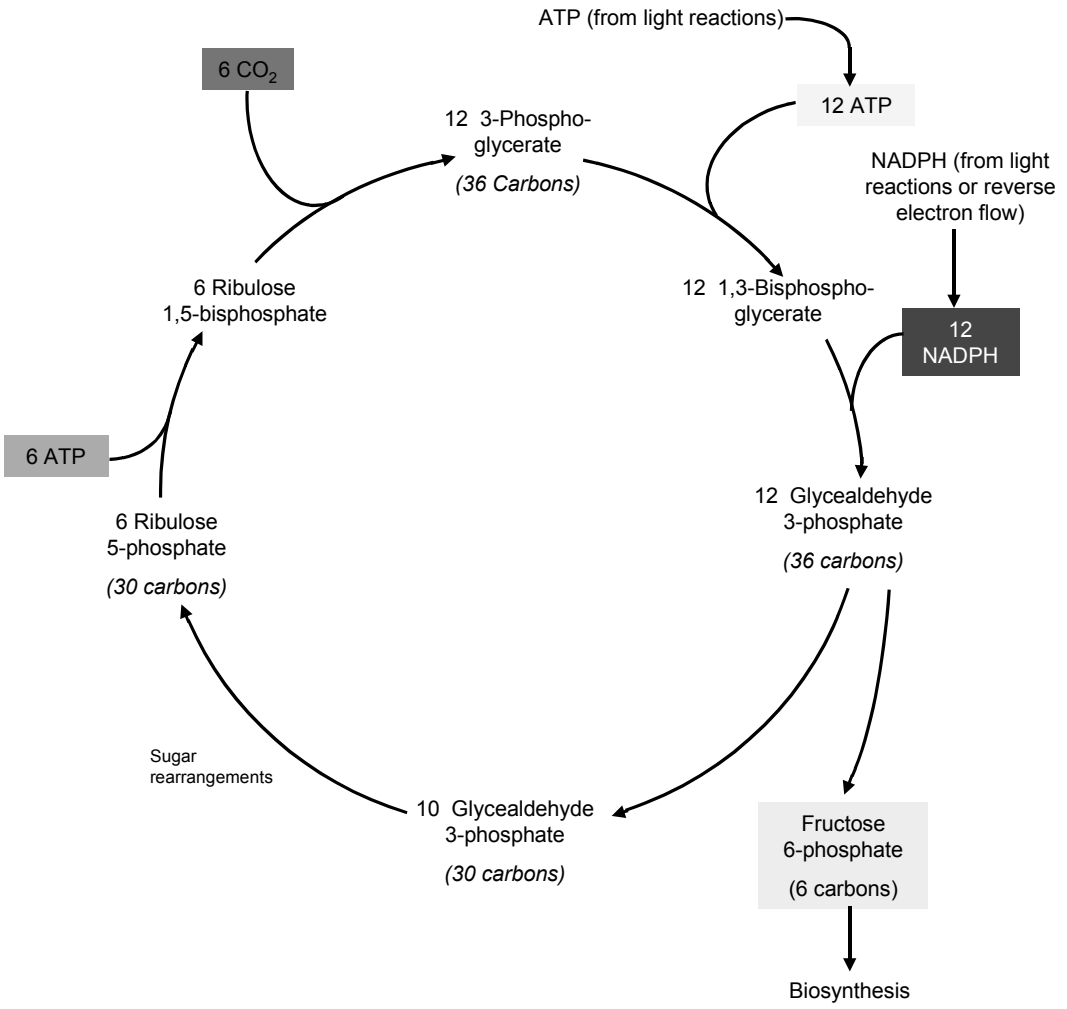

Figure 4 The Calvin cycle. One fructose-6-phosphate is formed per six incorporated CO_2.

Respiration and biosynthesis Photosynthesis supplies hexoses, which can be used for biosynthesis and as an energy source for dark respiration. The oxygen consuming breakdown of hexoses to CO_2 involves four components: 1) glycolysis, 2) oxidative pentose phosphate pathway (PPP) , 3) the tricarboxylic acid cycle (TCA cycle)[5] and 4) respiratory electron transport (RET). To distinguish this oxygen-consuming metabolism from photorespiration, it is often called dark respiration.

Glycolysis provides NADH and ATP as well as small oxidised molecules for the TCA cycle, which is the most important source for NADH. NADH is the e^- donor for respiratory e^- transport, the process where most of the ATP of dark respiration is generated. In cyanobacteria, but not in eukaryotes, NADPH can also donate e^- for respiratory e^- transport. The pentose phosphate pathway provides NADPH in the dark and it converts hexoses to pentoses. Biosynthesis is closely linked to respiration as all

[5] In contrast to Eukaryotes, the TCA cycle in cyanobacteria is incomplete

precursors for biosynthesis can be supplied by dark respiration. A wide range of biomolecules, including amino acids and tetrapyrroles are built from intermediates of the TCA cycle, while other amino acids and purines are built from intermediates of glycolysis or PPP.

While in eukaryotes respiration is spatially separated from photosynthesis, in cyanobacteria both processes are located in the thylakoid membrane and share components e.g. the $cytb_6f$ complex. (Scherer et al. 1988; Schmetterer 1994; Koike & Satoh 1996). This close coupling is challenging for scientists who try to understand the regulation and interaction of photosynthesis and respiration. One possible regulation might include that for many cyanobacterial species dark respiration is inhibited in the light (Scherer et al. 1988).

Effects of limited biosynthesis on PET and CO_2 fixation Insufficient supply of macronutrients (P, N, S) or micronutrients (e.g. Fe, Cu) limits biosynthesis. Nutrient limitation affects the physiology on every level (e.g. inducing chlorosis, degradation of phycobiliproteins, decrease in nucleic acid synthesis) including photosynthetic performance: Nutrient limitation eventually leads to a decrease in protein synthesis, thus also affecting proteins of the e^- transport chain. Especially the D1 protein of PS II requires constant repair and resynthesis in order to be fully functional. Therefore PS II activity is likely to be strongly reduced under nutrient limitation. In addition, due to the decreased demand for organic carbon, the Calvin cycle consumes less NADPH, which reduces the amount of energy needed for carbon fixation (Falkowski & Raven 1997).

When biosynthesis is limited (such as under nutrient limitation) photosynthesis cannot be shut down completely, as e.g. singlet oxygen is created when the absorbed light energy exceeds the amount that can be channelled into the e^- transport chain. Thus, while absorption of light is indispensable to perform photosynthesis, it can also be damaging. Particularly the UV-A and UV-B fraction of light are known to be potent in inducing cell damage (Garcia-Pichel & Castenholz 1994). UV-B is highly damaging to DNA, but it also damages proteins and membranes, while especially the UV-A fraction can also induce damage by generating reactive oxygen species (ROS) like singlet oxygen ($^1O_2{}^*$) and superoxide ($O_2{}^{\bullet -}$).

On the physiological level, modifications of the above-described linear e^- transport and CO_2 fixation pathways are strategies to use photochemical energy that exceeds demands by assimilatory processes such as CO_2 fixation and to decrease oxygen levels. These modifications thereby alleviate the potentially damaging effects of high

rates of photon absorption by PS II and damages related to high oxygen concentration (Falkowski & Raven 1997): These modifications include i) Cyclic e^- transport around PS I (see Fig. 3), which produces ATP, but neither NADPH nor oxygen. An enhanced cyclic e^- transport under nutrient limiting conditions has been described by Grossman et al. (1994). ii) The Mehler reaction (also called pseudocyclic e^- transport) is a linear e^- transport process, where e^- are used to reduce oxygen back to water. This process involves both photosystems and pumps protons, thus generating ATP but no NADPH. The amount of ATP produced by the Mehler reaction, however, can be downregulated for example by disengaging the so-called Q-cycle (which transports H^+ across the membrane) (Falkowski & Raven 1997). iii) At low CO_2/O_2 ratios another oxygen consuming process takes place. RuBisCO, the key enzyme of the Calvin cycle, does not only function as a carboxylase, but also as an oxygenase. The ratio between the two reactions depends on the ratio of CO_2/O_2. The oxygenation reaction of RuBisCO, the so-called photorespiration, yields 3-phosphoglycerate and phosphoglycolate and consumes oxygen. A fraction of the glycolate produced during photorespiration is excreted whereas the rest is further metabolised. As PS I is less susceptible to photooxidative damage than PSII the adaptations also include increases in the ratio of energy transferred to PSI/PSII by so-called state transitions (Mullineaux & Allen 1990).

As photosynthesis is not shut down completely, fixed carbon which cannot be used for biosynthesis due to a lack of nutrients is either stored intracellularly or excreted (Dubinsky & Berman-Frank 2001).

Organic carbon excretion in the light As mentioned above, phototrophs supply heterotrophic mat members with organic carbon. While carbon used for biomass synthesis is not available to heterotrophs until cell death and lysis, carbon that is excreted can be directly metabolised by heterotrophs. Excretion products include low molecular weight organic carbon compounds and extracellular polymeric substances (EPS). EPS is predominantly composed of polysaccharides some of which contain negatively charged uronic acid or sulphate groups but also proteins can contribute significantly (Decho 1990; Stal 2000). Furthermore, it usually contains varying amounts of lipids and nucleic acids (Flemming & Wingender 2001). Several reasons for EPS excretion by cyanobacteria and diatoms have been suggested. One possible explanation arises from the negative charge of EPS, which allows adhesion to sediment and also scavenging of metals (Decho 1990). Furthermore excretion of EPS was shown to be enhanced under nutrient limitation, or during transition from

exponential to stationary phase and under high light conditions (Myklestad et al. 1989; Staats et al. 2000). In addition, EPS may protect against desiccation and grazing and might be involved in cell motility (Stal 2000). The role it may play in calcification is controversially discussed and will be dealt with in more detail in the section about calcification. Usually, large amounts of EPS are present in microbial mats: Myklestad et al. (1989) found that organic carbon excretion of stationary phase diatoms was dominated by EPS, but 20% of carbon was excreted in the form of amino acids including glutamate, glutamine, alanine and serine. Early studies using simple paper chromatography additionally identified carbohydrates including mannitol and arabinose as excretion products (Hellebust 1965). The photorespiration product glycolate has been shown to be the dominant excretion product in a hot-spring mat (Bateson & Ward 1988) and is therefore considered a suitable organic substrate for mat heterotrophs (Fründ & Cohen 1992; Stal 1995; Stal 2000).

Organic carbon excretion in the dark In the dark oxygenic phototrophs are able to respire intracellular storage compounds but also glucose or fructose (Koike & Satoh 1996) completely to CO_2. Under anoxic conditions most cyanobacteria are able to ferment to sustain basic metabolic needs (Stal 2000). Usually, intracellular storage compounds such as glycogen are fermented, but compatible solutes like trehalose are also used. Fermentation products are excreted and thus become available for heterotrophs. The first report of cyanobacterial fermentation dates from 1979 and described lactate fermentation by *Oscillatoria limnetica* originating from a Solar Lake microbial mat (Oren & Shilo 1979). Since then many different fermentation pathways have been discovered. Fermentation products excreted by cyanobacteria include formate, acetate, ethanol, lactate and also H_2 (Anderson et al. 1987).

Carbon flow in microbial mats The estimation of the relative importance of the above described fates of fixed carbon (biosynthesis vs. storage and excretion) in terms of community carbon flow in microbial mats is hampered by the complex nature of microbial mats. In hot spring mats radiolabelled HCO_3^- was not incorporated in the light into rRNA or protein, but instead into polysaccharides (Nold & Ward 1996). It was therefore suggested that biosynthesis and thus growth of microbial mats might be very low and that the majority of fixed CO_2 might instead be lost from the cell as excretion compounds. However, Bateson & Ward (1988), Paerl et al. (1993), and Teiser (1993) found that in the light around 90% of the fixed CO_2 was incorporated into biomass. How can these findings be reconciled with the low rRNA synthesis? One possible explanation is that in the latter studies the amount of CO_2 used for

phototrophic biosynthesis was overestimated. The labelled biomass might also include heterotrophic cells which incorporated labelled excretion products. A second explanation could be that Nold & Ward (1996) underestimated biosynthesis, as nucleic acids are efficiently recycled within the cells and low incorporation of labelled HCO_3^- does therefore not necessarily mean low rRNA synthesis. The fact that these questions are still unanswered, demonstrates how little the carbon cycle in microbial mats is understood, despite the fact that microbial mats have long been studied.

Anoxygenic phototrophs

Oxygenic photosynthesis dominates primary production in most microbial mats, but usually anoxygenic photosynthetic organisms are also present. As they use e^- donors other than water (incl. Fe^{2+}, H_2, organic carbon, $S_2O_3^{2-}$, S^0) , they do not liberate oxygen. The principle e^- donor for green and purple sulphur bacteria is H_2S, so that these organisms are usually found in the anoxic zone of microbial mats. Due to a higher tolerance towards H_2S and more efficient light harvesting, green sulphur bacteria in mats are usually positioned below purple sulphur bacteria. *Thiocapsa* and *Chromatium* can tolerate high salt concentrations and are representatives of purple sulphur bacteria often found in microbial mats. Mat members of green sulphur bacteria include species of *Chlorobium* and *Prosthecochloris*. *Chloroflexus,* is also an anoxygenic phototroph which belongs to the green non sulphur bacteria. Members of this group usually display a very versatile metabolism. While able to grow photoautotrophically on H_2 or H_2S, they usually prefer photoheterotrophy (using organic carbon, not CO_2 as a carbon source) or even chemoheterotrophy (using organic carbon as e^- donor and carbon source) (Pierson & Castenholz 1992).

Chemolithoautotrophs

Chemolithoautotrophs use inorganic compounds as e^- donor (e.g. H_2S, H_2 or NH_3). A common chemolithoautotroph in mats is *Beggiatoa*, a filamentous colourless sulphur bacterium (CSB) that is typically found at the O_2/H_2S interface where it oxidises H_2S with O_2. As an alternative e^- acceptor NO_3^- can be used. Most *Beggiatoa* species are facultative autotrophs, minimising the expensive autotrophic process by growing mixotrophically, with H_2S as an energy source and organic carbon as carbon source (Grabovich et al. 1998). This versatile metabolism is typical for many bacteria. While the contribution of *Beggiatoa* to autotrophy in microbial mats still remains to be quantified, an important feature is the removal of H_2S, a toxic compound for many mat organisms. Methanotrophs, aerobic chemolithoautotrophs, that consume methane

generated by methanogens were found to be absent from a hypersaline mat (Conrad et al. 1995). Methanogens as well as some sulphate-reducing bacteria are also autotrophic organisms, but because they play an important role in the anaerobic degradation of organic carbon, their ecophysiological role in the carbon cycle will be described in the following section.

Heterotrophy

Organic carbon excreted by autotrophic organisms or released when cells lyse, is an essential substrate for heterotrophic organisms. Organic carbon degradation differs between aerobic and anaerobic conditions. Under aerobic conditions, aerobic heterotrophs usually oxidise organic substrates directly to CO_2 and therefore play an important role in carbon metabolism, but also in the consumption of oxygen in microbial mats. Recently, Jonkers & Abed (2003) found that photosynthetic excretion products were the preferred substrates for numerically important aerobic heterotrophs belonging the genera *Roseobacter* and *Rhodobacter*. In contrast, yeast extract, a mixture of more complex organic carbon compounds, was found to be metabolised by organisms belonging to the genera *Marinobacter* and *Halomonas*. Apart from this study, virtually nothing is know about this important group in microbial mats. Under anaerobic conditions fermentation and anaerobic respiration often co-operate in the degradation of organic substances. Sugars, amino acids and more complex substrates are typically used by fermentative organisms which produce e.g. alcohols or low molecular weight fatty acids (acetate, propionate, butyrate). The energy gained by anaerobic respiration depends on the reduction potential of the e^- acceptor. The suite of alternative e^- acceptors sorted by decreasing energy yield include NO_3^-, Fe^{3+}, SO_4^{2-} and CO_2. While Fe^{3+} is found in microbial mats, it is probably less important for anaerobic respiration, as it is rapidly reduced chemically by H_2S (Zopfi et al. 2002) and kinetically unfavourable due to its solid nature. Denitrification, which only takes place under oxygen exclusion, is thought to be most active in the upper part of the anoxic zone, because it depends on supply of NO_3^- and organic carbon (Joye & Paerl 1993; Paerl & Pinckney 1996; Paerl et al. 2000). The best studied anaerobic respiration process in microbial mats is sulphate reduction by sulphate-reducing bacteria (SRB). These organisms gain energy by oxidising e.g. fermentation products (fatty acids, primary alcohols, H_2) with SO_4^{2-} as e^- acceptor. Sulphate reduction is thought to be the dominant anaerobic respiration process in hypersaline microbial mats, because of high SO_4^{2-} concentrations usually found in mats. In addition, *in situ* evidence for SRB in aerobic habitats are not rare and several authors even reported

sulphate-reducing activity in the presence of oxygen (Canfield & Des Marais 1991; Fründ & Cohen 1992; Jørgensen 1994b). The final steps of anaerobic carbon degradation are acetogenesis and methanogenesis. Both processes, acetogenesis (often performed by *Clostridia*) and methanogenesis (by Archaea), have been demonstrated to occur in microbial mats (Anderson et al. 1987). Methanogenesis converts fermentation products like H_2 and CO_2, but also C1 compounds and acetate to methane. Methanogens gain less energy than sulphate reducers do and in addition have a lower affinity for most substrates than SRBs. However, methanogenesis has been reported to occur in microbial mats with a sulphate concentration of 40 mM and has been attributed to sufficiently high H_2 partial pressures (Hoehler et al. 2001; Hoehler et al. 2002). Acetogenesis, unlike methanogenesis can use complex substrates like sugars and amino acids in addition to H_2, CO_2 and C1 compounds.

Gradients and adaptations to diel changes

The steep gradients that are characteristic for microbial mats, result from the combined action of physical factors (light and mass-transfer resistance) and bacterial metabolism. The steep, small scale gradients hampered the understanding of microbial mat functioning due to the lack of suitable methods. Therefore the application of microsensors in the early 1980´s advanced the understanding of microbial mats considerably. The attenuation of light (Kühl et al. 1994; Kühl et al. 1997) restricts photosynthesis to the top millimetres, where photosynthesis provides a source of organic carbon and acts as a sink of dissolved inorganic carbon (DIC) (Canfield & Des Marais 1993). In addition, oxygenic phototrophs release oxygen, which results in oxygen supersaturation characteristic for microbial mats. The H_2S gradient develops due to the H_2S production by SRBs and the consumption of H_2S by colourless sulphur bacteria and anoxygenic phototrophs (see Fig. 5).

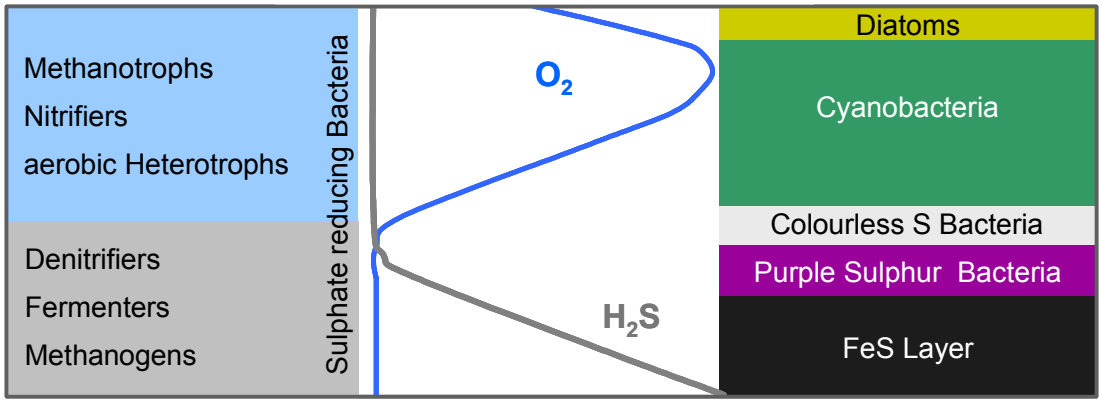

Figure 5 Simplified scheme (not to scale) of the orientation of microbial mat organisms in relation to O_2 and H_2S gradients in the light (modified after Van Germerden (1993) and Karsten & Kühl (1996)). The orientation of layers and organisms that contribute to the visible lamination of the mat is depicted to the right. The H_2S and O_2 gradients often do not overlap, for example when iron serves as a buffer. The orientation of organisms that do not contribute to the visible layering in relation to the O_2 gradient is shown to the left.

In this gradient system, microbial mat organisms need to find a niche, where they are provided with suitable e^- donors, e^- acceptors and energy sources, but also are protected from compounds that inhibit their metabolism or from competition with other microbes. The orientation of phototrophic organisms in the vertical gradient results in a lamination of the mat, which is usually visible to the naked eye due to the different pigmentation of the phototrophic organisms. Diatoms are often found on top, underlain by a cyanobacterial layer, followed by purple and green sulphur bacteria

(Karsten & Kühl 1996). If present, *Chloroflexus* is usually found in the layer where it is best provided with organic compounds for photoheterotrophic growth. Therefore, it is often found below a thin layer of cyanobacteria, probably using their excretion products as carbon source (Pierson & Castenholz 1992). However, as *Chloroflexus* has a high UV tolerance, inverted mats with *Chloroflexus* on top of the mat, thus moderating the amount of light that reaches lower layers, have also been found (Jørgensen & Nelson 1988). Protection against damaging UV-light in cyanobacteria includes the synthesis of UV-screen pigments like scytonemin, carotenoids and mycosporine-like amino acids (MAAs) (Ehlingschulz et al. 1997). Eukaryotes can relocate their chloroplasts towards the inner part of the cell to protect themselves against high light intensities (Demmig-Adams & Adams 2000). Other possible responses to high light intensities are behavioural modifications. Both diatoms and cyanobacteria are known to migrate in order to find optimal light conditions and avoid photodamage. Ramsing et al. (2000) observed that *Synechococcus* reduced the amount of light received by orientating itself upright in a hot spring mat under high light conditions. A similar response of diatoms has been reported by Jönsson et al. (1994).

Colourless sulphur bacteria (CSB) like *Beggiatoa* often form a distinct layer at the oxic/anoxic interface where they oxidise H_2S with O_2 (Van Gemerden 1993). During dark conditions they often migrate together with the O_2/H_2S interface towards the mat surface, forming conspicuous white areas.

Below the oxic zone, the mat often appears black, probably due to presence of iron sulphide (FeS) or pyrite (FeS_2). This layer has often been considered to harbour sulphate-reducing bacteria (Van Gemerden 1993). However, recent research showed, that they are not confined to the anoxic part, but are abundant and active even in the oxygen supersaturated top layers (Canfield & Des Marais 1991; Fründ & Cohen 1992; Stal 2000; Jonkers et al. 2003). Denitrification, fermentation and methanogenesis are still considered to be confined to the anoxic zone of the microbial mats, while aerobic heterotrophs and nitrifiers are active in the oxic zone.

Zones where organisms find optimal conditions are transient in microbial mats, as gradients change dramatically during the diel cycle. An example is the oxygen distribution in the oxic zone, where changes from supersaturation to anoxia can occur within minutes of darkening. Therefore, organisms of microbial mats witness dramatic changes during a diel cycle and are forced to adapt to this dynamic conditions either by

i) being motile and adjusting their position in the mat, a behaviour that has been described for cyanobacteria, diatoms and *Beggiatoa* (Garcia-Pichel & Castenholz 1999).

ii) tolerating unfavourable conditions.

iii) a metabolism that is able to adapt fast. This can be achieved by a constitutive set of enzymes as is the case e.g. with cyanobacterial fermentation (Stal 2000) or storage compounds to average fluctuating conditions. In cyanobacteria glycogen is known to serve as an energy reserve, while in *Beggiatoa* this function is ascribed to the S-granules.

While these diel changes can make life in mats challenging, at the same time these changes open opportunities temporarily (Jørgensen et al. 1979). The anoxic conditions during the night for example enable non-heterocystous cyanobacteria to efficiently fix N_2.

The distribution and concentration of substances inhibitory to some organism also changes during the diel cycle. The inhibitory property of a given compound depends very much on the concentration. H_2S, for example, can inhibit phototrophs, but diatoms and purple non sulphur bacteria are inhibited by lower concentrations than for example purple sulphur bacteria or cyanobacteria. Some cyanobacteria are able to perform anoxygenic photosynthesis as a detoxification mechanisms using H_2S instead of water as e^- donor. Anoxygenic phototrophs and lithotrophs play an important role in protecting oxygenic phototrophs and aerobic heterotrophs against H_2S diffusing upwards from deeper layers. Thus, despite the steep gradients and contrasting metabolic demands of microbial mat organism, the integrated and combined activity of mat organisms, results in a highly productive ecosystem.

Calcification

Calcification is the precipitation of calcium carbonate according to the following equation:

$$Ca^{2+} + CO_3^{2-} \rightarrow CaCO_3 \downarrow \quad (1)$$

In most ecosystems calcification occurs at pH values where HCO_3^- is the dominant carbonate species, thus

$$Ca^{2+} + HCO_3^- \rightarrow CaCO_3 \downarrow + H^+ \quad (2)$$

is the more accurate description. The acidification shifts the carbonate equilibrium towards CO_2.

$$H_2O + CO_2 \leftrightarrow H_2CO_3 \leftrightarrow H^+ + HCO_3^- \leftrightarrow 2\ H^+ + CO_3^{2-} \quad (3)$$

Therefore calcification at circumneutral pH can be described by

$$Ca^{2+} + 2\ HCO_3^- \rightarrow CaCO_3 \downarrow + CO_2 + H_2O \quad (4)$$

Considering the equations, calcification seems to be a simple process, however it can be counterintuitive as for example calcium carbonate solubility increases at lower temperatures. Detailed descriptions of the carbonate equilibrium and its relation to calcification can be found in Stumm & Morgan (1996) and Zeebe & Wolf-Gladrow (2001).

The solubility of a salt is described by the solubility product. The stoichiometric solubility product (K^*_{sp}) for calcium carbonate is

$$K^*_{sp} = [Ca^{2+}]_{sat} \times [CO_3^{2-}]_{sat} \quad (5)$$

with $[]_{sat}$ being the total (free and complexed) equilibrium ion concentration. For thermodynamic considerations, ion activities have to be considered. For the determination of ion activities in salt-containing solutions laborious and uncertain calculations are necessary (Zeebe & Wolf-Gladrow 2001) and therefore stoichiometric constants are often used. Calcification in natural waters is often closely linked to biological activity. Coccolithophores and foraminifers are the largest contributors to the global marine $CaCO_3$ precipitation, other contributors include corals, lime algae and bivalves, making calcium carbonate the most abundant biogenic sediment in the oceans (Press & Siever 1995). Calcification by prokaryotic organisms, e.g. cyanobacteria or sulphate-reducing bacteria, in marine environments is restricted

to a few sites, but is quantitatively more important in hypersaline and alkaline environments.

Whether microbially mediated calcification takes place is influenced by three factors (Arp et al. 2001):

i) the initial supersaturation state of the solution

ii) the increase in supersaturation by microbial activity

iii) the crystal formation e.g. presence of nucleation sites or nucleation inhibitors.

The supersaturation state (Ω) of a solution is described by

$$\Omega = \frac{\left[Ca^{2+}\right]\left[CO_3^{2-}\right]}{K^*_{sp}} \qquad (6)$$

with $[Ca^{2+}]$, $[CO_3^{2-}]$ being the concentrations and K^*_{sp} the stoichiometric solubility product. If Ω is > 1 than the solution is supersaturated with respect to $CaCO_3$. Supersaturation is observed in many environments, e.g. the surface ocean waters are seven-times oversaturated with respect to calcium. Oversaturation can be a consequence of the presence of inorganic or organic molecules that inhibit nucleation or crystal growth. Increasing the supersaturation e.g. by increasing the calcium concentration or by shifting the carbonate equilibrium towards CO_3^{2-} by increasing pH eventually overcomes this barrier. Thus, microbial processes that have the potential to increase the pH or calcium concentration promote calcification (Visscher et al. 1998; Castanier et al. 1999; Arp et al. 2001). Theoretically, a pH increase due to CO_2 fixation can be induced by all autotrophic processes including photosynthesis, but also colourless sulphur bacteria and methanogens (Stal 2000). It has also been suggested that sulphate-reducing bacteria induce calcification by increasing the pH (Castanier et al. 1999; Stal 2000). But also by providing nucleation sites or removing nucleation inhibitors can microbes promote calcification. In microbial mats, negatively charged acidic groups of EPS bind divalent cations such as Ca^{2+}. Whether this binding promotes or inhibits nucleation depends on the spatial configuration, as defined distances between the bound Ca^{2+} corresponding to the crystal lattice promote calcification, but irregular binding of Ca^{2+} to EPS inhibits precipitation (Stal 2000; Arp et al. 2001; Paerl et al. 2001). Other inhibitors of calcification include magnesium, phosphate and sulphate ions, the removal of which has been suggested to induce precipitation in foraminifers.

Principles and applications of microsensors

Microsensors are characterised by a small measuring tip which is typically smaller than 20 µm or alternatively are defined as sensors with a spatial resolution of at least 0.1 mm (Kühl & Revsbech 1998). They record chemical and physical gradients with high spatial resolution and have therefore been extensively used to study microbiogeochemical processes in gradient systems like microbial mats (Revsbech et al. 1983; Wieland & Kühl 2000), sediments (Jørgensen & Revsbech 1985; Stief & de Beer 2002), corals (de Beer et al. 2000; Richardson et al. 2001; Al-Horani et al. 2003), biofilms (Santegoeds et al. 1998; Schramm et al. 1998), and marine snow (Ploug 1997). Due to their small size, they are very fragile and a micromanipulator has to be used to position the sensors. Microsensors used in environmental microbiology are either electrochemical sensors (microelectrodes) or fibre-optic microsensors (optodes). Depending on the measuring principle, three different types of microelectrodes can be distinguished: potentiometric, amperometric and voltammetric sensors (see Fig. 6). For a concise overview of microsensors and applications consult (Kühl & Revsbech 1998; Taillefert et al. 2000).

Voltammetric sensors

Voltammetric sensors scan the current induced by modulating the applied voltage and are able to measure H_2S, O_2, trace metals and Mn^{2+} or Fe. While the advantage is the detection of several analytes in the same potential scan, the chief problem lies in the interpretation of the scans. During the scan, chemical reactions take place that might generate chemicals which are subsequently detected by the measurement. Mercury thin film electrodes and hanging mercury drop electrodes have been used to analyse sediments, but have not been used for the work presented in this thesis (see Taillefert et al. (2000) and references therein for an overview).

Amperometric sensors

Amperometric sensors apply a polarising voltage to reduce the chemical that is to be measured (analyte) and the current resulting from this reaction is linearly proportional to the concentration of the analyte. This primary current is very small and therefore sensitive amplifiers (Picoamperemeters) and well shielded cables are required. Due to the small currents, microsensor set-ups are sensitive to electrical noise and should be well shielded. The two amperometric microsensors most widely used are the oxygen

sensor (see Fig. 6) which is a miniaturised Clark-type oxygen electrode and the H_2S electrode. Clark et al. (1953) equipped the oxygen electrode with a gas-permeable membrane, behind which the reduction of oxygen at the gold cathode takes place, improving signal stability and interference by calcium ions or pH. The oxygen microelectrode (Revsbech & Ward 1983) has been advanced in 1989 by introducing a guard electrode that consumes the oxygen present in the electrolyte and thereby minimising the zero current (Revsbech 1989). The first application of a simple oxygen microelectrode in microbiology was by Whalen et al. (1969) in biofilms from a polluted stream. Based on the oxygen microprofiles, they measured oxygen consumption rates at different substrate concentrations (Bungay et al. 1969).

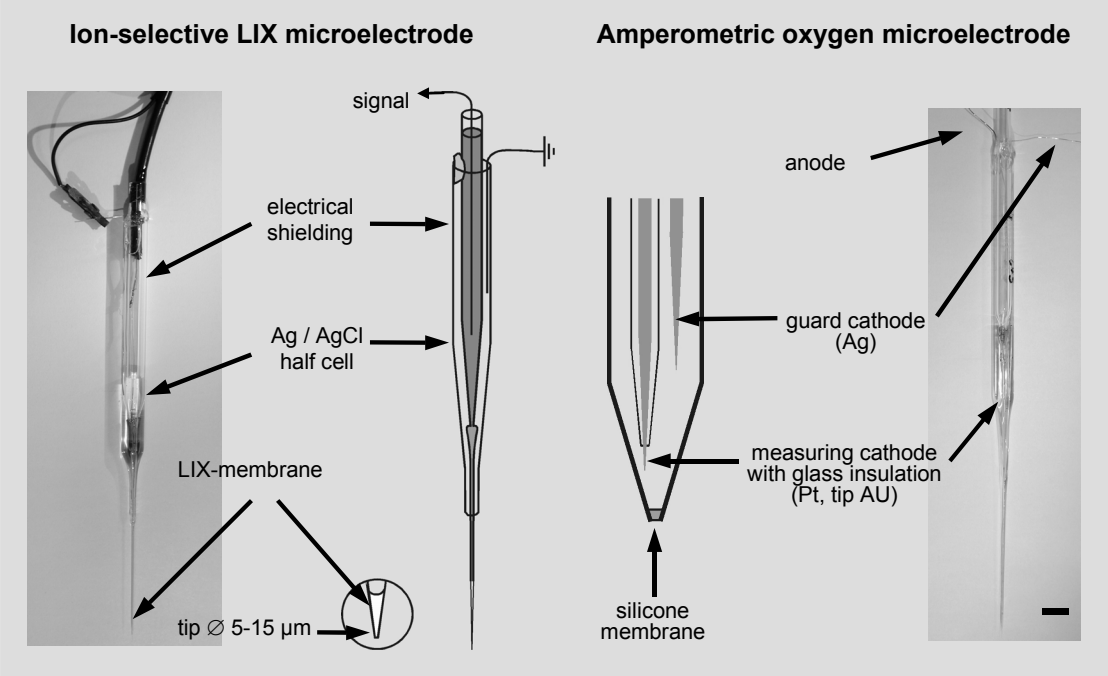

Figure 6 Comparison of a potentiometric LIX microelectrode and an amperometric oxygen electrode (modified with kind permission of A. Gieseke). Scale bar is 1 cm.

The H_2S electrode contains ferricyanide as a redox mediator. Ferricyanide is reduced by H_2S to ferrocyanide, which is reoxidised at a polarising voltage of 0.08V (Jeroschewski et al. 1996; Kühl et al. 1998). As this sensor detects only H_2S, pH has to be recorded simultaneously to allow calculations of the total dissolved sulphide concentration. While this electrode is superior to the potentiometric Ag/Ag_2S electrode in most respects, its biggest disadvantage is that it is sensitive to light in the UV region, hampering *in situ* measurements at high irradiances.

Potentiometric sensors

For potentiometric sensors, concentration differences of ions between the analyte and the electrolyte over an ion-permeable membrane creates a potential difference, which is proportional to the analyte concentration. Membranes used for potentiometric sensors include ion-specific glass, as is the case for the glass pH electrodes, or of a liquid membrane in the case of LIX sensors (LIX = liquid ion exchangeable membrane, see Fig. 6). While LIX microsensor are relatively easy to make (de Beer et al. 1997), their major disadvantage is the short lifetime. In this study LIX-sensors were used to measure pH and Ca^{2+} (see de Beer (2000) for an overview of LIX microsensors used in environmental microbiology). Another barrier type is crystalline as is the case for the Ag/Ag_2S microsensor, which has a silver tip coated with Ag_2S (Revsbech et al. 1983). As the solubility product of Ag_2S is constant, changes in S^{2-} concentration alter the Ag^+ activity and thereby induce a shift of the potential. The S^{2-} sensor can be only applied in anoxic environments, as the electrode depolarises when oxygen is reduced at the negatively charged electrode surface.

Biosensors

While the array of substances that can be directly detected with electrochemical sensor is limited, this spectrum is extended by the introduction of biosensors (Cronenberg et al. 1991). In the sensing tip of biosensors, bacteria or enzymes are embedded, which convert a specific substrate to a substance that can be measured using a conventional microelectrode. The nitrate biosensor contains e.g. *Agrobacterium radiobacter,* which converts nitrate to N_2O (Larsen et al. 1996; Larsen et al. 1997). Alternatively, bacteria change the concentration of a substance that can be measured electrochemically (e.g. O_2) while converting the analyte. The methane biosensor uses this principle and measures the consumption of oxygen by methane-oxidising bacteria in an internal reservoir (Damgaard & Revsbech 1997).

Micro-optodes

Micro-optodes are microsensors that apply a different functional principle: Light in optic fibres induces an evanescent field at the sensor tip, which is altered by the analyte or a reaction caused by the analyte. Either the analyte interacts directly with the light (e.g. by absorption or fluorescence) or it induces changes in luminescence, luminescence life time or absorption of an indicator chemical applied at the sensor tip. The signal (light intensity or spectrum) is conducted from the sensor tip to the detector unit by an optical fibre. In addition, to measure chemical species like O_2,

CO_2, pH, (Liebsch et al. 2000) or pigment distribution, optodes are also able to measure physical parameters like temperature, light intensity and quality, diffusivity and flow (Kühl & Revsbech 1998). Indicator dyes can also be applied to foils, which allows recording two-dimensional "profiles" (Glud et al. 1996). These planar optodes have been applied to measure oxygen in sediments (Glud et al. 1996; Glud et al. 2001), but planar optodes that measure pH and CO_2 do also exist.

Microprofiles and functional information

Between microbial mats and the overlying water a transition occurs from a stationary solid to a moving liquid (see Fig. 7). Free flowing water is thoroughly mixed by turbulence. While approaching the mat surface, turbulence and flow velocity decrease, leaving a layer that is dominated by viscous forces, the so called viscous sublayer (VSL). There, turbulence is still present but no longer effecting momentum exchange. With decreasing distance to the surface turbulence decreases even more until it no longer dominates mass transport processes.

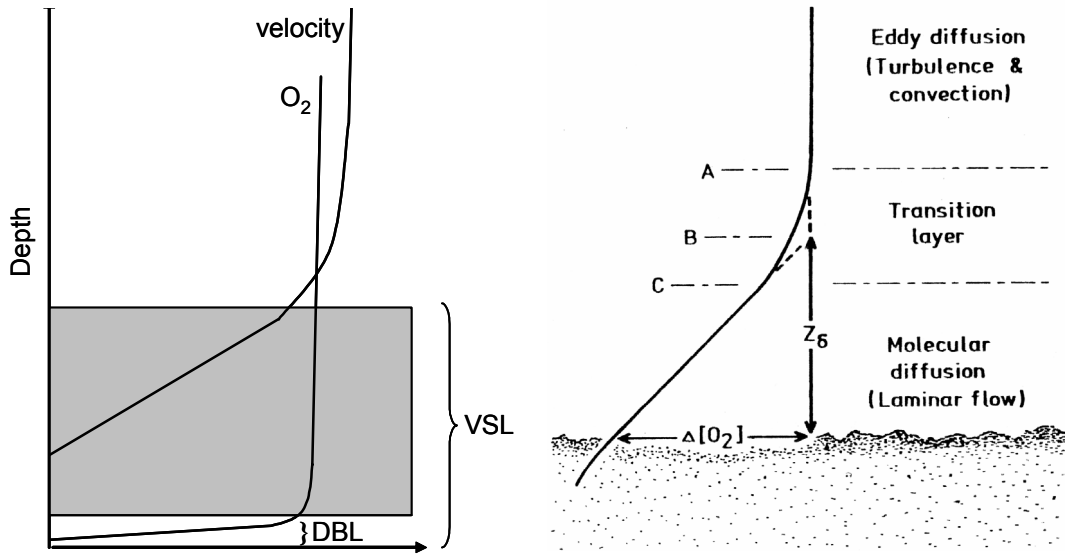

Figure 7 Left: Effect of decreasing eddy diffusion on velocity and transport when approaching a surface (exemplified by an O_2 profile). In the hatched area the decreased eddy diffusion has no effect on diffusive transport but on velocity. **Right:** Cut-out, magnifying the DBL and its effect on the O_2 profile. A gives the outer limit of the DBL, B the effective DBL, C the true DBL. From Jørgensen & Revsbech (1985), copyright by the American Society of Limnology and Oceanography.

The ~10% of the VSL, where molecular diffusion is the most important transport process is called diffusive boundary layer (DBL) (Jørgensen and Revsbech 1985). The true DBL is where only diffusion is driving transport, so that the flux profile is linear. For practicality most often the effective DBL is used, which is determined by extrapolating the linear part of the concentration gradient in the DBL to the

concentration of the mixed water column. The solute flux J (µmol cm^{-2} h^{-1}) resulting from molecular diffusion is described by Fick´s 1st law:

$$J = -D\frac{\delta C}{\delta z} \quad (1)$$

with D being the molecular diffusion coefficient (cm^2 h^{-1}) and $\partial C/\partial z$ the concentration gradient. D is a constant for each chemical species at given environmental conditions like temperature and salinity, so that the gradient resulting from diffusive flux in the DBL is linear.

Compared to turbulence, molecular diffusion is a slow process. In calm sea water mixing via eddy diffusion is about 6 orders of magnitude higher than by molecular diffusion. The restriction of transport and high microbial activity in microbial mats leads to the formation of steep chemical gradients. Bioirrigation in hypersaline microbial mats is not important, as higher organisms are mostly excluded, leaving molecular diffusion as the only effective transport process. The gradients that develop due to the activity of mat organisms therefore witness all exchange processes in the mat and all processes are mirrored in the profiles. Fluxes in the DBL under steady state conditions as calculated by Fick´s 1st law represent the production or consumption rates of a given compound integrated over the depth, the so called areal rates. The oxygen flux out of a photosynthesising mat, for example, represents the areal net photosynthesis rate, that is the amount of oxygen liberated by phototrophic organisms in the mat minus the amount respired within the mat. Production and consumption rates in different mat horizons, the volumetric conversion rates are derived from Fick´s 2nd law:

$$\frac{dC(z,t)}{dt} = -D_{eff}\frac{\delta^2 C(z,t)}{\delta z^2} - R \quad (2)$$

For steady state conditions the left term is zero, which leaves the following equation to calculate volumetric conversion rates at steady state.

$$R = -D_{eff}\frac{\delta^2 C(z,t)}{\delta z^2} \quad (3)$$

R is the volumetric conversion rate (µmol cm^{-3} h^{-1}), D_{eff} the apparent diffusion coefficient in the mat (that is D corrected for porosity and tortuosity, cm^2 h^{-1}), z the distance (cm) and t the time (h). The quotient in equation (2) is the 2nd derivative of the profile, i.e. the curvature.

Gross photosynthesis is measured from the O_2 concentration change ($\mu M\ s^{-1}$) immediately after darkening i.e. the light-dark shift method (Revsbech et al. 1983; Jørgensen et al. 1988; Glud et al. 1992; Kühl et al. 1996): The decrease in oxygen concentration is assumed to equal the amount of oxygen produced by photosynthesis before darkening. In the very short time period after darkening (typically 1-2 s), the gradients and thus the flux have not yet changed. The time period during which the decrease is measured determines the spatial resolution of this method. It is necessary that oxygen does not diffuse from one measuring depth to the next in the time frame of the measurement in order to obtain independent results in adjacent depths. A measurement at a given depth yields the volumetric gross photosynthesis, consecutive repetitions with increasing depth and integration of the obtained volumetric rates over depth gives the areal gross photosynthesis rate.

Sampling/study sites

"La Salada de Chiprana", Spain

In this thesis microbial mats were investigated which originated from "La Salada de Chiprana", a 31 ha large lake located in the Ebro basin in North-eastern Spain in the province of Zaragossa (see Fig. 8). On a geological time scale, "La Salada de Chiprana" is relatively young, being formed during the Quaternary when drainage into the Ebro was blocked by an alluvial fan (Vidondo et al. 1993). The characteristics of this enclosure have changed even more recently (a few centuries ago), when it changed from a shallow playa (non-permanent) lake to a deep (maximum 5.6 m) permanent lake, most likely due to the onset of irrigation agriculture (Valero-Garces et al. 2000). The groundwater that feeds "La Salada de Chiprana" flows through evaporitic rocks which influences the ion composition of the lake. The athalassic (non-marine) "La Salada de Chiprana" is therefore characterised by an ion composition which is markedly distinct from marine hypersaline systems, with magnesium and sulphate being the dominant ions.

Groundwater inflow and evapotranspiration have long been the only factors governing the water regime, but today "La Salada de Chiprana" receives additional water by irrigation runoff and through a channel which connects it to a freshwater lake (Lake Salobrosa). The irrigation runoff did not only greatly reduce salinity, but also led to heavy eutrophication in the early 1990's which negatively affected microbial mats. However, the value of this special ecosystem has been acknowledged and in 1994 "La Salada de Chiprana" was included in the Ramsar convention and a management plan has been developed to protect the lake.

The salinity of "La Salada de Chiprana" during our visits (years 2000-2002) was always found to be around 78‰, but strong fluctuations in salinity have been observed before (Diaz et al. 1998). During periods of meromixis, which do not seem to be a constant feature of the lake, populations of anoxygenic phototrophs (*Chlorobium vibrioforme* and *Prosthecochloris aestuarii*) develop in the anoxic hypolimnion (Vila et al. 2002). Microbial mats cover the sediments of "La Salada de Chiprana" up to a depth of 1.5 m. Chapter 2 contains a detailed description of the microbial community and a general description of the lake biota.

Figure 8 "La Salada de Chiprana", (Spain) which features extensive microbial mats in the shallow parts of the Lake. Characteristic are fingers of land protruding into the lake, so-called paleochannels, sanded up and fossilised former channels of the Ebro. These fossilised riverbeds are less erodible than the adjacent silt deposits between the channels and are consequently exposed. This structure is known as inverted relief (Vidondo et al. 1993; Diaz et al. 1998).

Cuatro Ciénegas, Mexico

In this thesis, recent oncolites from a river in the Cuatro Ciénegas basin were investigated (see Fig. 9). The Cuatro Ciénegas basin is an intermontane valley of 150000 ha located in the Sierra Madre Oriental in the Mexican state of Coahuila, just south of Cuatro Ciénegas de Carranza. It is surrounded by limestone mountains up to 3000 m high. Located in an arid region, it receives large amounts of subterranean water by an aquifer of unknown but probably distant origin. The aquifer dissolves the Cretaceous limestone, gypsum and dolomite formations, resulting in water high in minerals (with $CaSO_4$ being the most abundant) but low in nutrients. Cuatro Ciénegas is a karstic system, a geological term for an area of limestone terrain, characterised by sinks, ravines, dolines, caves and underground streams. The Cuatro Ciénegas valley harbours a large variety of flora and fauna including a high number of endemic species, which have been kept from interbreeding by the mountains surrounding the valley. Cuatro Ciénegas means four marshes, a term referring to times when the water input remained within the valley. Since 1989 canals were built which now transport most of the water out of the valley (Minckley 1969).

The microbialites found in Rio Mesquites, the main river draining the valley are either attached to the ground forming domal stromatolites or detached oncolites (Burne & Moore 1987).

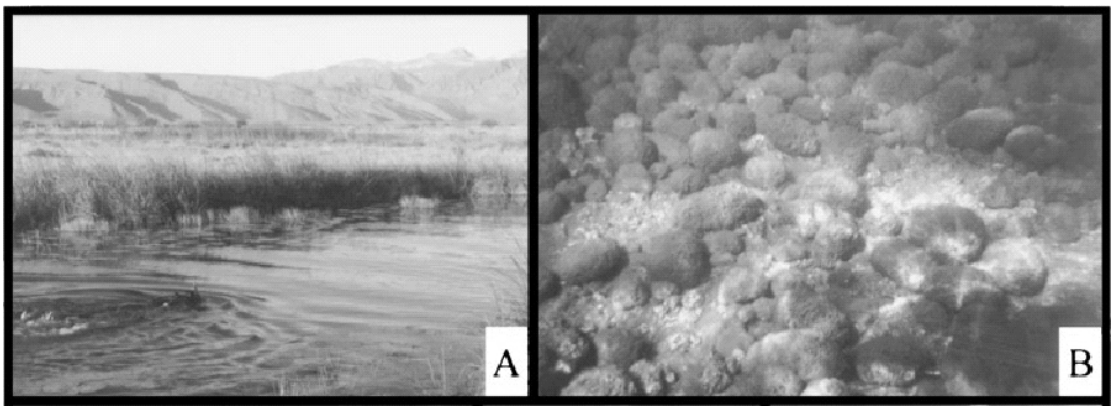

Figure 9 Photo of Rio Mesquites, Cuatro Ciénegas, Mexico **(A)** and stromatolitic oncolites **(B)**.

References

Al-Horani, F. A., Al-Moghrabi, S. M., de Beer, D. (2003) The mechanism of calcification and its relation to photosynthesis and respiration in the scleractinian coral *Galaxea fascicularis*. Mar. Biol. 142: 419-426

Anderson, K. L., Tayne, T. A., Ward, D. M. (1987) Formation and fate of fermentation products in hot-spring cyanobacterial mats. Appl. Environ. Microbiol. 53: 2343-2352

Arp, G., Reimer, A., Reitner, J. (2001) Photosynthesis-induced biofilm calcification and calcium concentrations in Phanerozoic oceans. Science 292: 1701-1704

Awramik, S. M. (1971) Precambrian columnar stromatolite diversity - Reflection of metazoan appearance. Science 174: 825-827

Awramik, S. M. (1984) Ancient stromatolites and microbial mats. In: Cohen, Y., Castenholz, R. W., Halvorson, H. O. (eds.) Microbial mats: Stromatolites, pp 1-22

Bateson, M. M., Ward, D. M. (1988) Photoexcretion and fate of glycolate in a hot spring cyanobacterial mat. Appl. Environ. Microbiol. 54: 1738-1743

Belkin, S., Jannasch, H. (1989) Microbial mats at deep-sea hydrothermal vents: New observations. In: Cohen, Y., Rosenberg, E. (eds.) Microbial mats - Physiological ecology of benthic microbial communities. American Society for Microbiology, Washington, D.C., pp 16-21

Blankenship, R. E., Hartman, H. (1998) The origin and evolution of oxygenic photosynthesis. Trends Biochem. Sci. 23: 94-97

Brocks, J. J., Logan, G. A., Buick, R., Summons, R. E. (1999) Archean molecular fossils and the early rise of Eukaryotes. Science 285: 1033-1036

Bungay, H. R., Whalen, W. J., Sanders, W. M. (1969) Microprobe techniques for determining diffusivities and respiration rates in microbial slime systems. Biotechnol. Bioeng. 11: 765-772

Burne, R. V., Moore, L.S. (1987) Microbialites: Organosedimentary deposits of benthic microbial communities. Palaios 2: 241-254

Canfield, D. E., Des Marais, D. J. (1991) Aerobic sulfate reduction in microbial mats. Science 251: 1471-1473

Canfield, D. E., Des Marais, D. J. (1993) Biogeochemical cycles of carbon, sulfur, and free oxygen in a microbial mat. Geochim. Cosmochim. Acta 57: 3971-3984

Canfield, D. E., Habicht, K. S., Thamdrup, B. (2000) The Archean sulfur cycle and the early history of atmospheric oxygen. Science 288: 658-661

Castanier, S., Le Métayer-Levrel, G., Perthuisot, J. P. (1999) Ca-carbonates precipitation and limestone genesis - the microbiogeologist point of view. Sediment. Geol. 126: 9-23

Clark, L. C., Wolf, R., Granger, D., Taylor, A. (1953) Continuous recording of blood oxygen tension by polarography. J. Appl. Physiol. 6: 189-193

Conrad, R., Frenzel, P., Cohen, Y. (1995) Methane emission from hypersaline microbial mats - Lack of aerobic methane oxidation activity. FEMS Microbiol. Ecol. 16: 297-305

Cronenberg, C., Vangroen, B., de Beer, D., Vandenheuvel, H. (1991) Oxygen-independent glucose microsensor based on glucose-oxidase. Anal. Chim. Acta 242: 275-278

Damgaard, L. A., Revsbech, N. P. (1997) A microscale biosensor for methane containing methanotrophic bacteria and an internal oxygen reservoir. Anal. Chem. 69: 2262-2267

de Beer, D. (2000) Potentiometric microsensors for *in situ* measurements in aquatic environments. In: Buffle, J., Horvai, G. (eds.) *In situ* monitoring of aquatic systems: Chemical analysis and specification. John Wiley and Sons, pp 162-194

de Beer, D., Kühl, M., Stambler, N., Vaki, L. (2000) A microsensor study of light enhanced Ca^{2+} uptake and photosynthesis in the reef-building hermatypic coral *Favia* sp. Mar. Ecol. Prog. Ser. 194: 75-85

de Beer, D., Schramm, A., Santegoeds, C. M., Kühl, M. (1997) A nitrite microsensor for profiling environmental biofilms. Appl. Environ. Microbiol. 63: 973-977

Decho, A. (1990) Microbial exopolymer secretions in ocean environments: Their role(s) in food webs and marine processes. Oceanogr. Mar. Biol. Annu. Rev. 28: 73-153

Demmig-Adams, B., Adams, W. W. (2000) Photosynthesis - Harvesting sunlight safely. Nature 403: 371-374

Diaz, P., Guerrero, M. C., Alcorlo, P., Baltanas, A., Florin, M., Montes, C. (1998) Anthropogenic perturbations to the trophic structure in a permanent hypersaline shallow lake: "La Salada de Chiprana" (north-eastern Spain). Int. J. Salt Lake Res. 7: 187-210

Dubinsky, Z., Berman-Frank, I. (2001) Uncoupling primary production from population growth in photosynthesizing organisms in aquatic ecosystems. Aquat. Sci. 63: 4-17

Ehling-Schulz, M., Bilger, W., Scherer, S. (1997) UV-B-Induced synthesis of photoprotective pigments and extracellular polysaccharides in the terrestrial cyanobacterium *Nostoc commune*. J. Bacteriol. 179: 1940-1945

Falkowski, P. G., Raven, J. A. (1997) Aquatic photosynthesis. Blackwell science

Flemming, H. C., Wingender, J. (2001) Relevance of microbial extracellular polymeric substances (EPSs) - Part I: Structural and ecological aspects. Water Sci. Technol. 43: 1-8

Forterre, P., Philippe, H. (1999) Where is the root or the universal tree of life? Bioassays 21: 871-879

Fründ, C., Cohen, Y. (1992) Diurnal cycles of sulfate reduction under oxic conditions in cyanobacterial mats. Appl. Environ. Microbiol. 58: 70-77

Fuerst, J. A. (1995) The Planctomycetes - Emerging models for microbial ecology, evolution and cell biology. Microbiology-(UK) 141: 1493-1506

Galtier, N., Tourasse, N., Gouy, M. (1999) A nonhyperthermophilic common ancestor to extant life forms. Science 283: 220-221

Garcia-Pichel, F., Castenholz, R.W. (1994) On the significance of solar ultraviolet radiation for the ecology of microbial mats. In: Stal, L., Caumette, P. (eds.) NATO ASI Series. Springer-Verlag, Berlin Heidelberg

Garcia-Pichel, F., Castenholz, R. W. (1999) Photomovements of microorganisms in benthic and soil microenvironments. In: Häder, D. P. (ed.) Photomovements. Elsevier

Glud, R. N., Ramsing, N. B., Revsbech, N. P. (1992) Photosynthesis and photosynthesis-coupled respiration in natural biofilms quantified with oxygen microsensors. J. Phycol. 28: 51-60

Glud, R. N., Ramsing, N. B. Gundersen, J. K., Klimant, I. (1996) Planar optodes - a new tool for fine scale measurements of two-dimensional O_2 distribution in benthic communities. Mar. Ecol. Prog. Ser. 140: 217-226.

Glud, R. N., Tengberg, A., Kühl, M., Hall, P. O. J., Klimant, I., Holst, G. (2001) An *in situ* instrument for planar O_2 optode measurements at benthic interfaces. Limnol. Oceanogr. 46: 2073-2080.

Grabovich, M. Y., Dubinina, G. A., Lebedeva, V. Y., Churikova, V. V. (1998) Mixotrophic and lithoheterotrophic growth of the freshwater filamentous sulfur bacterium *Beggiatoa leptomitiformis* D-402. Microbiology 67: 383-388

Grossman, A. R., Schaefer, M. R., Chiang, G. G., Collier, J. L. (1994) Cyanobacterial acclimation processes. In: Bryant, D. (ed.) The molecular biology of cyanobacteria. Kluwer Academic Publishers, Dordrecht. pp 641-675

Grotzinger, J. P. (1990) Geochemical model for Proterozoic stromatolite decline. Am. J. Sci. 290A: 80-103

Guerrero, R., Mas, J. (1989) Multilayered microbial communities in aquatic ecosystems: Growth and loss factors. In: Cohen, Y., Rosenberg, E. (eds.) Microbial mats - Physiological ecology of benthic microbial communities. American Society for Microbiology, Washington DC, pp 494

Habicht, K. S., Gade, M., Thamdrup, B., Berg, P., Canfield, D. E. (2002) Calibration of sulfate levels in the Archean Ocean. Science 298: 2372-2374

Hellebust, J. (1965) Excretion of some organic compounds by marine phytoplankton. Limnol. Oceanogr. 10: 192-206

Hoehler, T. M., Albert, D. B., Alperin, M. J., Bebout, B. M., Martens, C. S., Des Marais, D. J. (2002) Comparative ecology of H_2 cycling in sedimentary and phototrophic ecosystems. Antonie Van Leeuwenhoek 81: 575-585

Hoehler, T. M., Bebout, B. M., Des Marais, D. J. (2001) The role of microbial mats in the production of reduced gases on the early Earth. Nature 412: 324-327

Jeroschewski, P., Steuckart, C., Kühl, M. (1996) An amperometric microsensor for the determination of H_2S in aquatic environments. Anal. Chem. 68: 4351-4357

Jonkers, H. M., Abed, R. M. M. (2003) Identification of aerobic heterotrophic bacteria from the photic zone of a hypersaline microbial mat. Aquat. Microb. Ecol. 30: 127-133

Jonkers, H. M., Ludwig, R., de Wit, R., Pringault, O., Muyzer, G. Niemann, H., Finke, N., de Beer, D. (2003) Structural and functional analysis of a microbial mat ecosystem from a unique permanent hypersaline inland lake: '"La Salada de Chiprana"' (NE Spain). FEMS Microbiol. Ecol. 44: 175-189

Jönsson, B., Sundbäck, K., Nilsson, C. (1994) An upright life-form of an epipelic motile diatom - On the behavior of *Gyrosigma balticum*. Eur. J. Phycol. 29: 11-15

Jørgensen, B. B.(1994a) Diffusion processes and boundary layers in microbial mats. In: Stal, L.J., Caumette, P. (eds.) Microbial Mats. Springer-Verlag, Berlin Heidelberg, pp 243-253

Jørgensen, B. B. (1994b) Sulfate reduction and thiosulfate transformations in a cyanobacterial mat during a diel oxygen cycle. FEMS Microbiol. Ecol. 13: 303-312

Jørgensen, B. B., Revsbech, N. P. (1985) Diffusive boundary layers and the oxygen uptake of sediments and detritus. Limnol. Oceanogr. 30: 111-122.

Jørgensen, B. B., Cohen, Y., Revsbech, N. P. (1988) Photosynthetic potential and light-dependent oxygen consumption in a benthic cyanobacterial mat. Appl. Environ. Microbiol. 54: 176-182

Jørgensen, B. B., Nelson, D. C. (1988) Bacterial Zonation, Photosynthesis, and spectral light-distribution in hot-spring microbial mats of Iceland. Microbial Ecol. 16: 133-147

Jørgensen, B. B., Revsbech, N. P., Blackburn, T. H., Cohen, Y. (1979) Diurnal cycle of oxygen and sulfide microgradients and microbial photosynthesis in a cyanobacterial mat system. Appl. Environ. Microbiol. 38: 46-58

Joye, S. B., Paerl, H. W. (1993) Contemporaneous nitrogen fixation and denitrification in intertidal microbial mats: Rapid response to runoff events. Mar. Ecol. Prog. Ser.94: 267-274

Kaplan, A., Marcus, Y., Reinhold, L. (1988) Inorganic carbon uptake by cyanobacteria. Methods Enzymol. 167: 534-539

Karsten, U., Kühl, M. (1996) Die Mikrobenmatte - das kleinste Ökosystem der Welt. Biologie in unserer Zeit 26: 16-26

Koike, H., Satoh, K. (1996) Respiration and photosynthetic electron transport system in cyanobacteria - Recent advances. J. Sci. Ind. Res. 55: 564-582

Krüger, M., Meyerdierks, A., Glöckner, F. O., Amann, R., Widdel, F., Kube, M., Reinhardt, R., Kahnt, R., Bocher, R., Thauer, R. K., Shima, S. (2003) A conspicuous nickel protein in microbial mats that oxidize methane anaerobically. Nature 426: 878-881

Kühl, M., Lassen, C., Jørgensen, B. B. (1994) Optical properties of microbial mats: Light measurements with fiber-optic microprobes. In: Stal, L.J. Caumette., P. (eds.) Microbial mats: Structure, development and environmental significance. Springer-Verlag, Berlin, Heidelberg, New York, pp 149-166

Kühl, M., Glud, R. N., Ploug, H., Ramsing, N. B. (1996) Microenvironmental control of photosynthesis and photosynthesis-coupled respiration in an epilithic cyanobacterial biofilm. J.Phycol. 32: 799-812

Kühl, M., Lassen, C., Revsbech, N. P. (1997) A simple light meter for measurements of PAR (400 to 700 nm) with fiber-optic microprobes: Application for P vs E_0 (PAR) measurements in a microbial mat. Aquat. Microb. Ecol. 13: 197-207

Kühl, M., Revsbech, N. P. (1998) Biogeochemical microsensors for boundary layer studies. In: Boudreau, B. P., Jørgensen, B. B. (eds.) The benthic boundary layer. Oxford University Press, Oxford. pp 180-210

Kühl, M., Steuckart, C., Eickert, G., Jeroschewski, P. (1998) A H_2S microsensor for profiling biofilms and sediments: application in an acidic lake sediment. Aquat. Microb. Ecol. 15: 201-209

Larsen, L. H., Kjaer, T., Revsbech, N. P. (1997) A microscale NO_3^- biosensor for environmental applications. Anal. Chem. 69: 3527-3531

Larsen, L. H., Revsbech, N. P., Binnerup, S. J. (1996) A microsensor for nitrate based on immobilized denitrifying bacteria. Appl. Environ. Microbiol. 62: 1248-1251

Laval, B., Cady, S. L., Pollack, J. C., McKay, C. P., Bird, J. S., Grotzinger, J. P., Ford, D. C., Bohm, H. R. (2000) Modern freshwater microbialite analogues for ancient dendritic reef structures. Nature 407: 626-629

Liebsch, G., Klimant, I., Frank, B., Holst, G., Wolfbeis, O. S. (2000) Luminescence lifetime imaging of oxygen, pH, and carbon dioxide distribution using optical sensors. Appl. Spectrosc. 54: 548-559

Lowe, D. R. (1994) Abiological origin of described stromatolites older than 3.2 Ga. Geology 22: 387-390

Martin, W.; Russell, M. J. (2003) On the origins of cells: a hypothesis for the evolutionary transitions from abiotic geochemistry to chemoautotrophic prokaryotes, and from prokaryotes to nucleated cells. Phil. Trans. R. Soc. Lond. B 358: 59-83

Minckley, W. L. (1969) Environments of the Bolson of Cuatro Ciénegas , Coahuila, Mexico, with special reference to the aquatic biota. Univ. Tex. El Paso Stud. Sci. 2: 1-65

Mullineaux, C. W., Allen, J. F. (1990) State 1-State 2 transitions in the cyanobacterium *Synechococcus* 6301 are controlled by the redox state of electron carriers between photosystem I and Photosystem II. Photosynth. Res. 23: 297-311

Myklestad, S., Holm-Hansen, O., Varum, K. M., Volcani, B. E. (1989) Rate of release of extracellular aminoacids and carbohydrates from the marine diatom *Chaetoceros affinis*. J. Plankton Res. 11: 763-773

Nealson, K., Rye, R. (2003) Evolution of metabolism. In: Schlesinger, W. (ed.) Biogeochemistry. Elsevier, Amsterdam, pp 41-61

Nisbet, E. G., Fowler, C. M. R. (2003) The early history of life. In: Schlesinger, W. (ed.) Biogeochemistry. Elsevier, pp 1-39

Nisbet, E. G., Fowler, C. M. R. (1999) Archaean metabolic evolution of microbial mats. Proc. R. Soc. Lond. B. 266: 2375-2382

Nisbet, E. G., Sleep, N. H. (2001) The habitat and nature of early life. Nature 409: 1083-1091

Nold, S. C., Ward, D. M. (1996) Photosynthate partitioning and fermentation in hot spring microbial mat communities. Appl. Environ. Microbiol. 62: 4598-4607

Olson, J. M. (2001) 'Evolution of Photosynthesis' (1970), re-examined thirty years later. Photosynth. Res. 68: 95-112

Oren, A., Shilo, M. (1979) Anaerobic heterotrophic dark metabolism in the cyanobacterium *Oscillatoria limnetica*: Sulfur respiration and lactate fermentation. Arch. Microbiol. 122: 77-84

Pace, N. R. (1997) A molecular view of microbial diversity and the biosphere. Science 276: 734-740

Paerl, H. W., Bebout, B. M., Joye, S. B., Des Marais, D. J. (1993) Microscale characterization of dissolved organic matter production and uptake in marine microbial mat communities. Limnol. Oceanogr. 38: 1150-1161

Paerl, H. W., Pinckney, J. L. (1996) A mini-review of microbial consortia: Their roles in aquatic production and biogeochemical cycling. Microbial Ecol. 31: 225-247

Paerl, H. W., Pinckney, J. L., Steppe, T. F. (2000) Cyanobacterial-bacterial mat consortia: examining the functional unit of microbial survival and growth in extreme environments. Environ. Microbiol. 2: 11-26

Paerl, H. W., Steppe, T. F., Reid, R. P. (2001) Bacterially mediated precipitation in marine stromatolites. Environ. Microbiol. 3: 123-130

Pierson, B. K., Castenholz, R. W. (1992) The Family Chloroflexaceae. In: Balows, A., Trüper, H., Dworkin, M., Harder, W., Schleifer, K. (eds.) The Prokaryotes. 2nd edition. Springer, New York

Ploug, H., Kühl, M., Buchholz-Cleven, B., Jørgensen, B. B. (1997) Anoxic aggregates - an ephemeral phenomenon in the pelagic environment? Aquat. Microb. Ecol. 13: 285-294

Pratt, B. R. (1982) Stromatolite decline - a reconsideration. Geology 10: 512-515

Press, F., Siever, R. (1995) Allgemeine Geologie. Spektrum Akademischer Verlag, Heidelberg

Ramsing, N. B., Ferris, M. J., Ward, D. M. (2000) Highly ordered vertical structure of *Synechococcus* populations within the one-millimeter-thick photic zone of a hot spring cyanobacterial mat. Appl. Environ. Microbiol. 66: 1038-1049

Raven, J. A. (1997) CO_2 -concentrating mechanisms: a direct role for thylakoid lumen acidification. Plant, Cell and Environment 20: 155-166

Reid, R. P., Visscher, P. T., Decho, A. W., Stolz, J. F., Bebout, B. M., Dupraz, C., MacIntyre, I. G., Paerl, H. W., Pinckney, J. L., Prufert-Bebout, L., Steppe, T. F., Des Marais, D. J. (2000) The role of microbes in accretion, lamination and early lithification of modern marine stromatolites. Nature 406: 989-992

Revsbech, N. P., Jørgensen, B. B., Blackburn, T. H., Cohen, Y. (1983) Microelectrode studies of the photosynthesis and O_2, H_2S, and pH profiles of a microbial mat. Limnol. Oceanogr. 28: 1062-1074

Revsbech, N. P., Ward, D. M. (1983) Oxygen microelectrode that is insensitive to medium chemical composition: Use in an acid microbial mat dominated by *Cyanidium caldarium*. Appl. Environ. Microbiol. 45: 755-759

Revsbech, N. P. (1989) An oxygen microsensor with a guard cathode. Limnol. Oceanogr. 34: 474-478

Richardson, L. L., Smith, G. W., Ritchie, K. B., Carlton, R. G. (2001) Integrating microbiological, microsensor, molecular, and physiologic techniques in the study of coral disease pathogenesis. Hydrobiologia 460: 71-89

Riding, R. (2000) Microbial carbonates: the geological record of calcified bacterial-algal mats and biofilms. Sedimentology 47: 179-214

Rost, B., Riebesell, U., Burkhardt, S., Sultemeyer, D. (2003) Carbon acquisition of bloom-forming marine phytoplankton. Limnol. Oceanogr. 48: 55-67

Santegoeds, C. M., Schramm, A., de Beer, D. (1998) Microsensors as a tool to determine chemical microgradients and bacterial activity in wastewater biofilms and flocs. Biodegradation 9: 159-167

Sarbu, S. M., Vlasceanu, L., Popa, R., Sheridan, P., Kinkle, B. K., Kane, T. C. (1994) Microbial mats in a thermomineral sulfurous cave. In: Stal, L., Caumette, P. (eds.) Microbial Mats - Structure, Development and Environmental Significance. Springer, Berlin, pp 45-50

Scherer, S., Almon, H., Böger, P. (1988) Interaction of photosynthesis, respiration and nitrogen fixation in cyanobacteria. Photosynth. Res. 15: 95-114

Schmetterer, G. (1994) Cyanobacterial Respiration. In: Bryant, D. (ed.) The Molecular Biology of Cyanobacteria. 1st edition. Kluwer Academic Publishers, Dordrecht, pp 409-435

Schramm, A., de Beer, D., Wagner, M., Amann, R. (1998) Identification and activities in situ of *Nitrosospira* and *Nitrospira* spp. as dominant populations in a nitrifying fluidized bed reactor. Appl. Environ. Microbiol. 64: 3480-3485

Shen, Y. , Buick, R., Canfield, D. E. (2001) Isotopic evidence for microbial sulphate reduction in the early Archaean era. Nature 410: 77-81

Staats, N., Stal, L. J., Mur, L. R. (2000) Exopolysaccharide production by the epipelic diatom *Cylindrotheca closterium*: effects of nutrient conditions. J. Exp. Mar. Biol. Ecol. 249: 13-27

Stal, L. J. (2000) Cyanobacterial Mats and Stromatolites. In: Whitton, B., Potts, M. (eds.) The Ecology of Cyanobacteria. Kluwer Academic, pp 61-120

Stal, L. J. (1995) Physiological ecology of cyanobacteria in microbial mats and other communities. New Phytol. 131: 1-32

Stief, P., de Beer, D. (2002) Bioturbation effects of *Chironomus riparius* on the benthic N- cycle as measured using microsensors and microbiological assays. Aquat. Microb. Ecol. 27: 175-185

Stumm, W., Morgan, J. J. (1996) Aquatic chemistry. John Wiley & Sons, INC., New York

Summons, R. E., Jahnke, L. L., Hope, J. M., Logan, G. A. (1999) 2-Methylhopanoids as biomarkers for cyanobacterial oxygenic photosynthesis. Nature 400: 554-557

Taillefert, M., Luther, G. W., Nuzzio, D. B. (2000) The application of electrochemical tools for *in situ* measurements in aquatic systems. Electroanal. 12: 401-412

Teiser, M. L. (1993) Extracellular low molecular weight organic compounds produced by *Synechococcus* sp. and their roles in the food web of alkaline hot spring microbial mat communities. Ph.D. Thesis. University of Oregon, Oregon

Valero-Garces, B. L., Navas, A., Machin, J., Stevenson, T., Davis, B. (2000) Responses of a saline lake ecosystem in a semiarid region to irrigation and climate variability - The history of Salada Chiprana, central Ebro basin, Spain. Ambio 29: 344-350

Van Gemerden, H. (1993) Microbial Mats - A joint venture. Mar. Geol. 113: 3-25

Vidondo, B., Martinez, B., Montes, C., Guerrero, M. C. (1993) Physicochemical characteristics of a permanent Spanish hypersaline lake – La Salada de Chiprana (NE Spain). Hydrobiologia 267: 113-125

Vila, X., Guyoneaud, R., Cristina, X. P., Figueras, J. B., Abella, C. A. (2002) Green sulfur bacteria from hypersaline Chiprana Lake (Monegros, Spain): habitat description and phylogenetic relationship of isolated strains. Photosynth. Res. 71: 165-172

Visscher, P. T., Reid, R. P., Bebout, B. M., Hoeft, S. E., MacIntyre, I. G., Thompson Jr., J. A. (1998) Formation of lithified micritic laminae in modern marine stromatolites (Bahamas): The role of sulfur cycling. Am. Mineral. 83: 1482-1493

Wayne, R. (2000) Chemistry of the atmospheres. Oxford University Press, Oxford

Whalen, W. J., Bungay, H. R., Sanders, W. M. (1969) Microelectrode determination of oxygen profiles in microbial slime systems. Environ. Sci. Technol. 3: 1297-1298

Wieland, A., Kühl, M. (2000) Short-term temperature effects on oxygen and sulfide cycling in a hypersaline cyanobacterial mat (Solar Lake, Egypt). Mar. Ecol. Prog. Ser. 196: 87-102

Woese, C. R. (2000) Interpreting the universal phylogenetic tree. P. Natl. Acad. Sci. USA 97: 8392-8396

Zeebe, R., Wolf-Gladrow, D. (2001) CO_2 in seawater: Equilibrium, kinetics, isotopes. Elsevier, Amsterdam

Zopfi, J., Wieland, A., Kühl, M. (2002) Biogeochemical cycling of C, O, and S in an iron rich hypersaline microbial mat. Geochim. Cosmochim. Acta 66: A883-A883

Chapter 2

Structural and functional analysis of a microbial mat ecosystem from a unique permanent hypersaline inland lake: 'La Salada de Chiprana' (NE Spain)

2

Structural and functional analysis of a microbial mat ecosystem from a unique permanent hypersaline inland lake: 'La Salada de Chiprana' (NE Spain)

Henk M. Jonkers, Rebecca Ludwig, Rutger de Wit, Olivier Pringault, Gerard Muyzer, Helge Niemann, Niko Finke, Dirk de Beer

Abstract

The benthic microbial mat community of the only permanent hypersaline natural inland lake of Western Europe, 'La Salada de Chiprana', north-eastern Spain, was structurally and functionally analysed. The ionic composition of the lake water is characterised by high concentrations of magnesium and sulphate, which were 0.35 M and 0.5 M, respectively at the time of sampling while the total salinity was 78 g l^{-1}. Community composition was analysed by microscopy, HPLC pigment analyses and by studying culturable bacteria from different functional groups. Therefore, denaturing gradient gel electrophoresis (DGGE) was applied on most-probable-number (MPN) dilution cultures. Microscopy revealed that a thin layer of *Chloroflexus*-like bacteria overlaid various cyanobacteria-dominated layers each characterised by different morphotypes. DGGE analysis of MPN dilution cultures from distinct mat layers showed that various phylotypes of anoxygenic phototrophic-, aerobic heterotrophic-, colourless sulphur-, and sulphate-reducing bacteria were present. The mats were furthermore functionally studied and attention was focussed on the relationship between oxygenic primary production and the flow of carbon through the microbial community. Microsensor techniques, pore water- and sediment photopigment analysis were applied in order to estimate oxygenic photosynthetic rates, daily dynamics of (in)organic carbon pore water concentration and migration behaviour of phototrophs. Chiprana microbial mats produced dissolved organic carbon (DOC) both during the day and night. It was estimated that 14% of the mats gross photosynthetic production and 49% of the mats net photosynthetic production diffused out of the mat in the form low molecular weight fatty acids, although these compounds made up only 2% of the total DOC pool. The high flux of dissolved fatty acids from the microbial mat to the water column may explain why in this system

Chloroflexus-like bacteria proliferate on top of the cyanobacterial layers since these photoheterotrophic bacteria grow preferably on organic phototrophic exudates. Furthermore it may also explain why high numbers of viable sulphate-reducing bacteria were found in the fully oxygenated sediment surface layers. These organisms apparently do not have to compete with aerobic heterotrophic community members due to the ample availability of organic substrates. Moreover, the high production of DOC strongly indicates that the mat community was nutrient limited in its growth. Photopigment analysis revealed furthermore that chlorophyll *a* (Chl*a*) and three of its allomers had a complementary depth distribution what suggests that the Chl*a* allomers are functional adaptations to differences in light quality and/or quantity and may be species specific.

Introduction

Saline and hypersaline inland lakes occur world-wide, particularly in areas with a semiarid climate (Bauld 1981; Williams 1986). These lakes are extremely interesting from an ecological point of view because many harbour biological communities which are often characterised by the presence of unique species. Biodiversity in such lakes varies due to differences in environmental conditions and specific lake characteristics such as local climate, lake size, depth, and lake water salt composition. The occurrence of natural hypersaline inland lakes in Western Europe is confined to the semiarid endorheic regions of the Iberian Peninsula (Guerrero & DeWit 1992). Here, most lakes are shallow and non-permanent with a wide spectrum of ionic types, ranging from sodium-chloride and sodium-sulphate dominated (Andalucian lakes) to sodium-chloride and magnesium-sulphate dominated ones (Aragón and La Mancha lakes).

The lake, 'La Salada de Chiprana' located in the central Ebro Basin in northern Spain, stands out in being the only permanent hypersaline lake in Western Europe. This unique lake with a maximum depth of 5.6 m and an average salinity of 78 ‰ dominated by magnesium sulphate, is part of a complex of lakes in the Chiprana-Caspe region. A paleolimnological analyses has shown that the current hydrology of the lake is the result of the subtle interaction between human and natural factors. During the last millennium the lake changed from a typical playa lake with temporary water, into a permanent deep lake particularly because of deforestation, introduction of agriculture and irrigation since the seventeenth century (Valero-Garces et al. 2000). Extensive *Microcoleus chthonoplastes* microbial mats and macrophyte prairies were observed in the late 1980's (Vidondo et al. 1993). However, the ecosystem suffered from heavy eutrophication in the early 1990's when the lake received particularly high quantities of nutrient-rich fresh water from the adjacent shallow lake 'Laguna de las Roces' through a small canal (Diaz et al. 1998; Valero-Garces et al. 2000). In concert with a drastic decrease of the water column grazer *Artemia parthenogenetica* this had a very negative impact on water column transparency and therefore on the distribution of macrophytes and on the structural integrity of the microbial mats (Diaz et al. 1998). These observations led the local authorities to develop a management plan, which included a restriction of the nutrient-rich fresh water inputs into the lake. After the particularly dry year 1995, water column transparency quickly recovered (Valero-Garces et al. 2000) and we observed extensive and healthy *M. chthonoplastes*

mats since the summer of 1996. Nowadays, several distinct lacustrine sub-environments are recognised each characterised by specific biological assemblages: 1) littoral areas characterised by reed *Phragmites* spp. beds; 2) a sub-littoral area down to a depth of 1.5 m dominated by benthic microbial mat communities interspersed with charophyte *Lamprothamnium papulosum* and macrophyte *Ruppia maritima* L. var. *maritima* meadows; 3) an anoxic hypolimnion characterised by blooms of the green sulphur bacterium *Chlorobium vibrioforme* (Diaz et al. 1998; Valero-Garces et al. 2000; Vidondo et al. 1993; Vila et al. 2002). 'La Salada de Chiprana' with its unique but fragile ecosystem was included in the Ramsar Convention in 1994 because of its particular ecological value (Diaz et al. 1998) and the regional government (Diputación General de Aragón, Zaragoza) recently developed a management plan in co-operation with local farmers to conserve and protect the lake.

In this study the benthic microbial mat community that dominates the sub-littoral area of lake Chiprana was structurally and functionally analysed. Main goal of this study was to make an ecological analysis of this ecosystem, i.e. relating the community structure to its functioning. The *in situ* primary production of the oxygenic phototrophic community was related to the dynamics and flow of dissolved organic carbon. The community structure was analysed using a combination of microscopic-, culturing- and molecular techniques, while community functioning was studied by application of *in situ* microsensor techniques in combination with (in)organic carbon analyses of pore water and HPLC analysis of photopigments of the microbial mat ecosystem.

Materials and methods

Study area and sampling periods

'La Salada de Chiprana' (41°14'30''N, 0°10'50''W) has a total surface of 31 ha. The lake lies on the Upper Oligocene – Miocene Caspe Formation that is mainly composed of sand- and silt stones. The lake's hydrology is governed by high evapotranspiration (1000-1500 mm yr^{-1}), low rainfall (300-350 mm yr^{-1}), water runoff, irrigation returns and groundwater flow. The latter is thought to be the main source of the lake's solutes due to the dissolution of the carbonate- and evaporite rocks of the area's Tertiary formations, resulting in an ionic composition dominated by magnesium-sulphate (Vidondo et al. 1993; Valero-Garces et al. 2000). The average salinity of the lake water is around 78‰ but was reported to decrease significantly

during occasional periods of heavy rainfall (Diaz et al. 1998; Vidondo et al. 1993). For this study, the lake was visited in successive autumn and spring seasons, October 2000 and May 2001 respectively, during which microsensor *in situ* measurements were performed. Samples taken for further laboratory analyses were directly frozen on site and transported to the laboratory in a liquid nitrogen cooled transportation vessels (CP100, Taylor-Wharton, USA).

Structural community analyses

Macroscopic and microscopic observations

Vertical cuts of freshly collected mats (October 2000 and May 2001) were macroscopically photographed with a digital camera in order to visualise the distinct coloured layers of which the mats consisted. Subsequently, with the aid of binoculars and watchmaker forceps, microscopic slides were prepared from sub samples taken from these distinct depth layers. The volumetric abundance of morphologically clearly distinguishable phototrophic community members in these preparations (cyanobacteria, diatoms and filamentous *Chloroflexus*-like bacteria) were subsequently estimated by bright field, phase contrast and fluorescence microscopy. For the latter, microscopic preparations were excited with blue (450-495 nm) or green (546 nm) light and emitted light was cut-off with filters for wavelengths below 520 and 590 nm respectively, facilitating the distinction between chloroplast-containing algae and phycobiliprotein-containing cyanobacteria respectively.

Numerical estimation of culturable bacteria

The abundance of culturable bacteria belonging to four different functional groups, aerobic heterotrophic bacteria, sulphate-reducing bacteria, anoxygenic phototrophic sulphur bacteria and colourless sulphur bacteria respectively, were estimated in freshly collected mats (October 2000) by the most-probable-number (MPN) methodology. Duplicate microbial mat cores were randomly collected using 25 mm diameter perspex sediment corers. The top 6 mm of these cores were sliced in two 3 mm thick layers representing the photic (top-layer) and equally thick aphotic zone of the microbial community. Slices were fragmented by cutting, suspended in 9 volumes of 0.2 µm filtered and autoclaved Chiprana lake water. Suspensions were further homogenised by three cycles of rigorously vortexing (2 minutes) followed by sonication (10 seconds) in a 50 Watts ultrasonic bath. Microtiter plates (8 * 12 wells, Merck, Germany) were filled with MPN medium amended with functional-group-specific substrates (see below for medium composition). The first row of wells

(representing 8 replicates) was inoculated with 10% (volume) microbial mat suspension (10^{-2} dilution) followed by serial dilution up to the 10^{-12} dilution level, leaving the last row as blanks (abiotic controls). Plates were incubated either aerobically (aerobic heterotrophs and colourless sulphur bacteria) or anaerobically using the Merck anaerocult system (sulphate-reducing and anoxygenic phototrophic sulphur bacteria). All plates were incubated at room temperature for 14 weeks in the dark except for the anoxygenic phototrophic bacterial plates which were incubated under a light/dark cycle of 16 hours light (20 µmol photons m^{-2} s^{-1}) and 8 hours darkness. Growth was followed visually by comparing medium turbidity to abiotic controls. After incubation, MPN-scores representing numbers of culturable bacteria of the respective functional groups present in the original microbial mat, were calculated using the MPN computer program of (Clarke & Owens 1983).

MPN medium was composed of 50% 0.2 µm filtered and autoclaved Chiprana lake water and 50% artificial medium. The latter contained per litre of MilliQ water: NaCl (17.5 g), $MgSO_4 \cdot 7H_2O$ (78.0 g), NH_4Cl (0.2 g), KH_2PO_4 (0.02 g), $CaCl_2 \cdot 2H_2O$ (0.225 g), KCl (0.2 g), Na_2CO_3 (2.0 g) and EDTA-trace element solution of (Widdel & Bak 1992) (1 ml l^{-1}). This medium was amended with growth factors and substrates for the respective functional groups. For sulphate-reducing bacteria: Wo/Se solution and vitamin solution of (Heijthuijsen & Hansen 1986) (1 ml l^{-1}), lactic acid (15 mM) and acetic acid (15 mM). For anoxygenic phototrophic bacteria: cyanocobalamine (vitamin B12, 20 µg/l), hydrogen sulphide (1.6 mM) and acetic acid (0.8 mM). For colourless sulphur bacteria: cyanocobalamine (20 µg/l) and thiosulphate (6.4 mM). For aerobic heterotrophic bacteria: cyanocobalamine (20 µg/l) and either glycolic acid (20 mM) or a mixture of glycolic acid, glucose, lactic acid and acetic acid (5 mM each). The pH of all media was adjusted to 8.2.

Molecular characterisation of MPN dilutions

The within-functional group diversity of bacteria was studied in MPN culture samples by application of the polymerase chain reaction (PCR) followed by separation of DNA products using denaturing gradient gel electrophoresis (DGGE). Culture samples from moderate (10^{-4}) and highest positive (10^{-6}, 10^{-7} or 10^{-8}) MPN dilution levels were analysed. Therefore 0.2 ml culture samples were taken, centrifuged (10 min * 16000 *g*) followed by resuspension of the pellet in 30 µl TE buffer (10 mM Tris-HCl, 1 mM EDTA; pH 8). DNA was extracted by subjecting cell suspensions to 5 cycles of freeze-thawing followed by heating for 10 min at 95°C. Mixtures of 16S rRNA genes in these samples were PCR amplified with GM5 forward (with GC

clamp) and 907 reverse primers resulting in 0.5 Kbase fragment lengths and DGGE was subsequently performed as described by (Muyzer et al. 1995).

Functional community analyses

In situ microsensor measurements

In situ microbial mat profiles of oxygen concentration (October 2000) and *in situ* profiles of oxygen, pH, oxygenic gross photosynthesis and sulphide concentrations (May 2001) were measured during 24 hour cycles. Clark-type amperometric oxygen microsensors (10 µm tip diameter), and potentiometric pH and sulphide (S^{2-}) minisensors (100 µm tip diameter) were applied (for a detailed description of used sensors see Kühl et al. (1998) and Revsbech & Jørgensen (1983)). The latter two sensors were glued in steel needles because unprotected glass pH microsensors broke always on calcium carbonate precipitates in the microbial mats, whereas use of amperometric H_2S sensors was hampered by high UV light intensities during *in situ* measurements. *In situ* profiles were obtained by fixing microsensors in a manual micromanipulator connected to a heavy stand. The set-up was positioned on the sediment surface of a 20 cm deep submerged microbial mat. Gross photosynthesis profiles were obtained by application of the light/dark shift method. For these measurements oxygen microsensors with a response time of less than 0.2 seconds were used (Revsbech & Jørgensen 1983). Darkening was done by rapidly covering the set-up and underlying mat with a black cloth cover for five-second time intervals. The initial decrease in oxygen concentration was registered on a strip chart recorder.

Photopigment quantification

Photopigments were analysed by HPLC. One-mm thick slices of microbial mats sampled in October 2000 were analysed in Arcachon following the procedure described by Buffan-Dubau et al. (2001). In summary, the pigments were extracted with cold acetone and four successive extractions were pooled. Pigment extracts were methylated with diazomethane, subsequently dried by centrifugation under vacuum and dissolved in solvent A. A binary gradient (solvent A= 50 % methanol, 45 % acetonitrile + 5 % aqueous solution of 0.05 M ammonium acetate; solvent B: 80 % ethyl acetate, 19 % methanol and 1 % acetonitrile) was applied, pigments were separated on a Lichrospher 100RP (250 x 4 mm, 5 µm) column, and a Thermo-Separation Products (Les Ulis, France) TSP UV6000 diode array spectrophotometer was used as a detector. The TSP UV6000 was programmed to obtain the on-line absorption spectra from 320 to 800 nm, and chromatograms were plotted at 440 nm

(detection of carotenoids and chlorophylls) and at 664 nm (specific detection of chlorophylls and degradation products (Buffan-Dubau et al. 2001). Pigments were identified by comparison with authentic standards if available. An extract of a culture of *Chlorobium tepidum* ATCC was used as source for Bacteriochlorophyll *c* homologues.

A higher depth resolution of the photopigments was achieved on samples from May 2001 using HPLC equipment in Bremen. The vertical distribution of photopigments in the microbial mats was determined in sediment cores taken at 5 a.m. and 5 p.m. in order to study diel migration phenomena. These cores were immediately frozen on site in liquid nitrogen and transported to the laboratory. The top 6 mm of the frozen cores were sliced in 200 µm thick layers with the aid of a Cryomicrotom (Microm HM 505E) at –30°C. Individual slices were weighed and immediately extracted in 1.2 ml 100 % methanol. For the quantification of Zeaxanthine slices were washed in 2 ml saline water (80 g NaCl per litre MilliQ water) prior to extraction. This washing step was necessary because during direct extraction Zeaxanthine was degraded by an unknown compound present in the sediment pore water in deeper sediment layers. Photopigments in methanol extracts were subsequently separated on a Waters HPLC (2690 Separation Module) equipped with a Eurospher-100 C18, 5µm Vertex column (Knauer Berlin, Germany) according to the method of Wright et al. (1991). Absorption spectra of separated compounds were measured on a Waters 996 Photo Diode Array (PDA) detector and pigment quantity and purity were checked by comparing peak areas, peak retention times, and absorption spectra to pigment standards. The following pigment standards were used (in brackets retention time in minutes on our HPLC system): Peridinin (11.5), Fucoxanthin (12.4), Chlorophyll *b* (Chl*b*) (16.8), Zeaxanthin (17.0), Lutein (17.2), Chlorophyll *a* (Chl*a*) (17.7) and ß-carotene (20.4). Standards were purchased from Sigma, USA or DHI Water and Environment, Denmark. Three allomers of Chl*a* were detected in field samples. These allomers had identical absorption spectra but different retention times as Chl*a*. Retention times were 15.1, 17.4 and 18.1 minutes and these allomers are annotated in the following as Chla_1, Chla_2 and Chla_3 respectively. Allomers were quantified using Chl*a* as standard.

Chemical analyses of pore water

The daily dynamic of dissolved organic carbon (DOC) and dissolved inorganic carbon (DIC) concentrations in the microbial mats pore water was analysed in order to relate this to the mats photosynthetic activity. In May 2001 water column samples and

triplicate mat cores were taken at 5 a.m. and 5 p.m. The sediment cores were immediately sliced on site in distinct layers (0-2 mm, 2-4 mm and 4-8 mm) followed by centrifugation of the sediment slices (10 min * 6000 *g*). Supernatant (pore water) aliquots were immediately frozen in liquid nitrogen. The concentration of dissolved organic and inorganic carbon of these samples was measured with a Shimadzu TOC-5050A Total Organic Carbon Analyser in connection with a Shimadzu ASI-5000A autosampler. The samples were 5-fold diluted with MilliQ water prior to analysis.

Pore water and water column samples were additionally analysed for low-molecular-weight fatty acids (formic-, glycolic-, acetic-, lactic-, propionic-, butyric-, iso-butyric–, valeric- and iso-valeric acid). Fatty acids were derivatised prior to analysis with phenylhydrazine and quantified by HPLC according to the method described by Albert & Martens (1997).

The ionic composition of Chiprana lake water (October 2000 and May 2001) was determined in 0.2 µm filtered water samples by ion chromatography on a Dionex DX 500 Chromatograph according to the method of Schippers & Jørgensen (2001). Calcium concentrations were checked and confirmed by atomic absorption spectrometry (AAS).

Results

Ionic composition of Chiprana lake water

The salt composition of Chiprana lake water did not vary much during the autumn and spring season of the years 2000 and 2001, but differed markedly from 'average' seawater, not only in terms of total salinity but also in ratio of the respective ions (Table 1). Chiprana water appeared to be particularly rich in calcium, magnesium and sulphate, with respective concentrations being 2, 7 and 17 times higher as seawater.

Table 1 Salt composition of Chiprana lake water and seawater. Chiprana water appeared to be particularly rich in magnesium, calcium and sulphate.

	Seawater: *	Chiprana water: October 2000	Chiprana water: May 2001
Ions:	mM	mM	mM
K^+	10	5	6
Mg^{2+}	53	322	375
Na^+	468	497	515
Ca^{2+}	10	18	20
Cl^-	545	309	356
SO_4^{2-}	28	500	446
Cations	604	1182	1311
Anions	601	1309	1248
Ions:	g/l	g/l	g/l
K^+	0.4	0.2	0.2
Mg^{2+}	1.3	7.8	9.1
Na^+	10.8	11.4	11.8
Ca^{2+}	0.4	0.7	0.8
Cl^-	19.5	11	12.7
SO_4^{2-}	2.7	48.1	42.9
Total	35.1	79.2	77.5

* Seawater values taken from Stumm and Morgan (1996)

Structural analyses of the microbial mat community

Macroscopic and microscopic analysis

The macroscopically clearly visible vertical layering of the Chiprana lake microbial mat is shown in Figure 1. Microscopic observations revealed a high diversity of morphologically distinct autofluorescent organisms. These are in the following described according to morphology, i.e. unicellular or filamentous, and cell size (individual cells, width * length). Biomass of morphotypes in the microscopic preparations was estimated in terms of volumetric percentage. The orange-brown 0.5 mm thick top layer (layer 1, see Figure 2) was mainly composed of *Chloroflexus*-like thin (0.5-1 * >100 µm) filamentous bacteria. These were only weakly autofluorescent in the near infrared light range and their biomass was estimated to make up 90% of the total biomass in this layer. Other conspicuous autofluorescent organisms in this layer were two types of diatoms (*Nitzschia* sp.: 4 * 70 µm, 5-10%; and *Navicula* sp.: 20 * 80 µm, 1 %), and three types of cyanobacteria, one Halothece-like unicellular (1 * 1-2 µm; 1 %), and one *Microcoleus*-like (2 * 5 µm, 1 %, annotated as

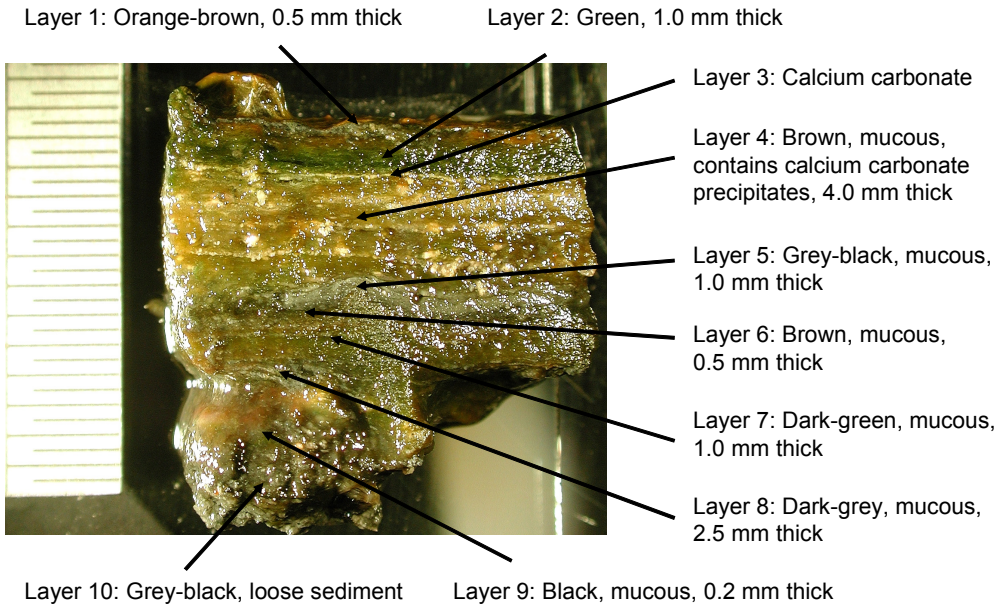

Figure 1 Photograph of a vertical cut of a Chiprana lake microbial mat. Distinct layers are clearly visible. See results section for a microscopic description of cyanobacterial and algal morphotypes present in the respective layers.

filamentous cyanobacterium type 2) and one *Pseudoanabaena*-like (1.5-2 * 4-5 µm; 2-5 %, annotated as type 5) filamentous bacteria. The underlying layer (layer 2) had a thickness of about 1 mm and was brightly green. This layer consisted predominantly of four types of filamentous cyanobacteria: three *Microcoleus*-like (1 * 4 µm, 80 %,

annotated as type 3; 2 * 5 µm, 2-5 %, type 2 and 5 * 10 µm, 5-10 %, annotated as type 1 respectively) and one *Pseudoanabaena*-like (1.5-2 * 4-5 µm, 2-5 %, type 5) bacterium. Layer 2 and 4 were separated by a clearly visible calcium carbonate layer (layer 3). Layer four was a 4 mm thick brown gelatinous layer, interspersed with calcium carbonate crystals, and was dominated, like layer 2, by a *Microcoleus*-like filamentous cyanobacterium (80 %, type 3) with type 1 (2 %), and a Halothece-like unicellular (1 * 1µm; 1 %) and two types of *Gloeocapsa*-like (2 * 2 µm, 2 % and 5 * 7 µm, 2 %) cyanobacteria also being present. The underlying 1 mm thick layer 5 was greyish-black and had a cyanobacterial composition similar to layer 4. Below layer 5 the mat layering seemed to repeat itself with layers 6,7,8 and 9 corresponding to layers 1, 2, 4 and 5. However, the autofluorescence of the cyanobacteria in the layers 6 to 9 was much weaker and present diatom frustules were predominantly empty. In layer 6 a low abundant (< 1%) morphologically different type of filamentous bacterium with clearly separated individual cells was detected (1 * 2 µm, annotated as type 4). In the whole mat, 11 different morphotypes of autofluorescent organisms could microscopically be detected, 2 diatoms, 1 *Chloroflexus*-like filamentous bacterium, 2 *Gloeocapsa*-like cyanobacteria, 1 Halothece-like unicellular cyanobacterium and 5 filamentous cyanobacteria.

Pigment analyses of the mat's top mm

Pigment chromatograms of the top mm of the mat are shown in Fig 2. Fucoxanthin and chlorophyll c reflect the presence of diatoms, while myxoxanthophyll and zeaxanthin reflect the presence of the cyanobacteria. The latter compound is also present in some green algae, but because the green algal pigments chlorophyll b and lutein were below the limit of detection, we can safely assume that the bulk of zeaxanthin originated from cyanobacteria. Other major carotenoids comprised γ carotene and β carotene. Chlorophyll *a* (Chl*a*) was the major peak. Two chlorophyll a-like pigments were detected that likely correspond to a chlorophyll *a*-allomer and a chlorophyll *a* epimer (Jeffrey et al. 1997). Chlorophyllide *a* and Phaeophytin *a*, but no phaeophorbides, were detected as degradation products arising from Chl*a*.

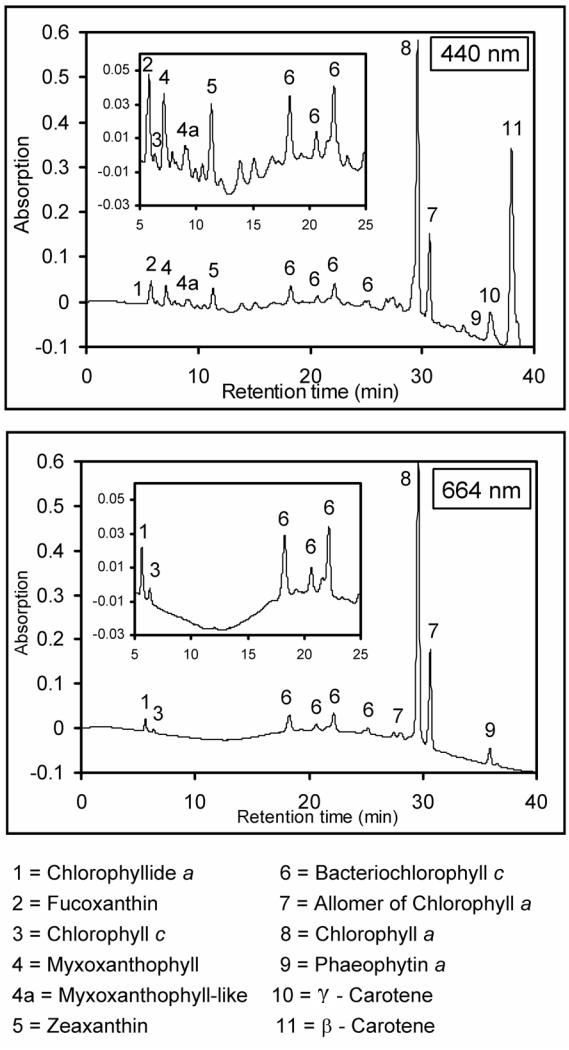

Figure 2 HPLC chromatograms of a pigment extract of the top mm of the mat sampled in October 2000. *Chloroflexus*-like filamentous bacteria dominate the mats surface layer what is reflected by the presence of BChl*c*.

A group of peaks eluting between 18 and 26 min were identified as Bacteriochlorophyl *c* (BChl*c*). The absorption spectrum and the retention time of these compounds corresponded to the secondary BChl*c*-homologues of *Chlorobium tepidum.* The retention times were longer than for the farnesol-esterified BChl*c*-homologues (BChlc_F), which are the main homologues in *Chlorobium tepidum*. This indicates that the BChl*c*-homologues were more hydrophobic than the BChlc_F homologues and therefore esterified with another alcohol (Airs et al. 2001; Borrego & Garcia-Gil 1994). HPLC-MS analyses is requested for identification of the esterifying alcohol (Airs et al. 2001; Villanueva et al. 1994). The BChl*c*-homologues most likely originated from *Chloroflexus*-like filamentous bacteria, they were most abundant in the top layer and decreased strongly with depth (data not shown).

Estimation of diversity and number of culturable bacteria

In addition to the autofluorescent microbial mat inhabitants, the diversity and number of culturable microorganisms of four different functional groups (aerobic heterotrophic bacteria, sulphate-reducing bacteria, anoxygenic phototrophic bacteria and colourless sulphur bacteria) was estimated by a combination of the MPN methodology and PCR-DGGE.

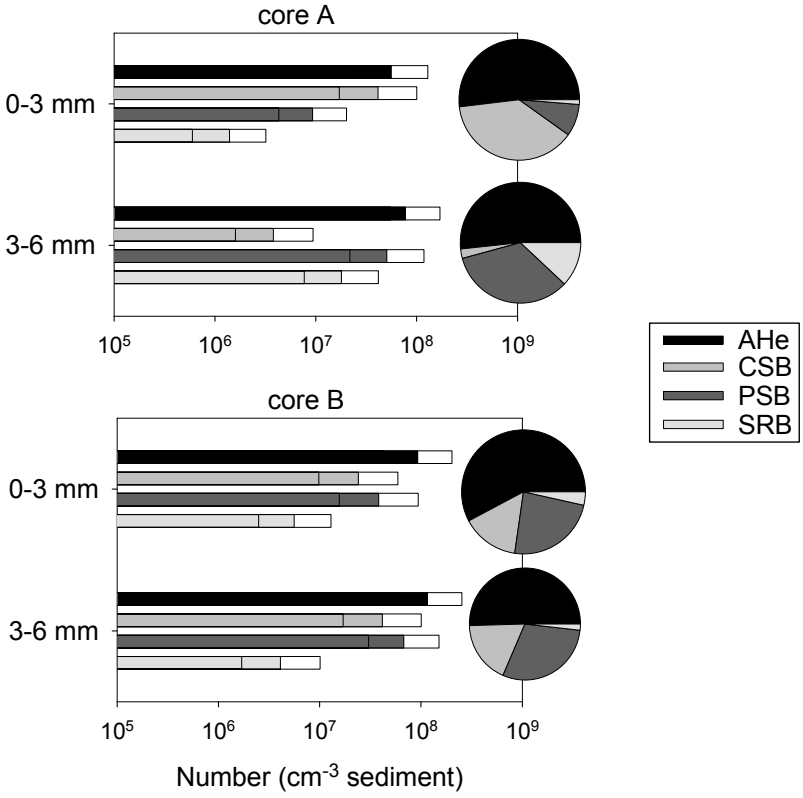

Figure 3 Most-probable-number estimates in duplicate cores of aerobic heterotrophic-, sulphate reducing-, anoxygenic phototrophic- and colourless sulphur bacteria in the photic (0-3 mm) and aphotic (3-6 mm) layers of the Chiprana lake microbial mat. Pie charts show relative abundance of estimated groups.

The functional group of anoxygenic phototrophic bacteria was dominated by purple sulphur bacteria. Figure 3 depicts the numerical (MPN) estimates of bacteria of the four functional groups in the photic (0-3 mm) and aphotic (3-6 mm) layers of the mat. Numbers of culturable bacteria of these four functional groups appeared to be hardly different between the two layers. Aerobic heterotrophic bacteria were numerically dominant in both layers followed by smaller population sizes of colourless- and purple sulphur bacteria with the sulphate-reducing bacteria being numerically the smallest population. The latter group, however, was still present in significant numbers both in the photic and the aphotic zone. Not shown in Figure 3 are the

numbers of the aerobic heterotrophs cultured on glycolic acid only, because this group represents a sub population of the aerobic heterotrophs cultured on a mixture of organic substrates (glycolic acid, glucose, acetic acid and lactic acid).

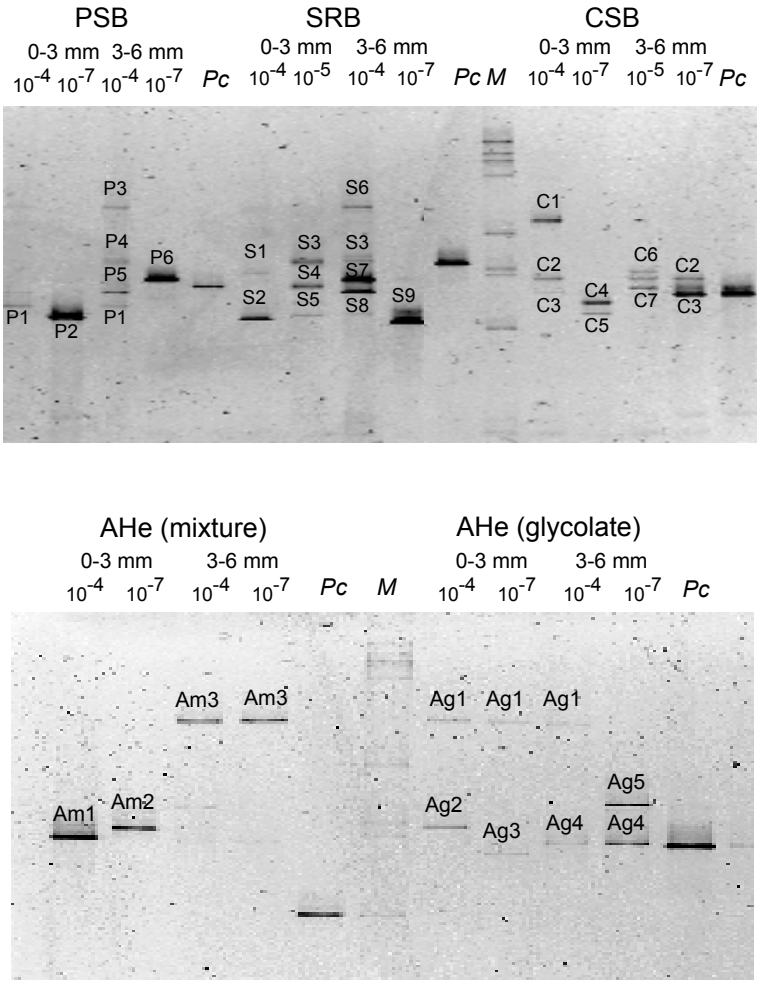

Figure 4. Negative images of DGGE separation patterns of PCR-amplified 16S rRNA gene fragments from MPN enrichment cultures. Functional group, depths layer (0-3 or 3-6 mm) and MPN dilution levels are shown above the lanes. *Pc* and *M* refer to positive controls and mass standards respectively. Distinct band (phylotypes) numbers refer to the specific functional group (P, purple sulphur bacteria; S, sulphate-reducing bacteria; C, colourless sulphur bacteria; Am, aerobic heterotrophs enriched on mixed organic substrates; Ag, aerobic heterotrophs enriched on glycolic acid) and to the distinct migration position in the gel.

The MPN estimate of the former group was 25 % lower than of the latter group. This means that 75 % of the aerobic heterotrophic bacteria that grew on the substrate mixture can grow on glycolic acid as sole carbon source.

An estimate of the within-functional group diversity was made by application of PCR-DGGE on the MPN series. Figure 4 shows the obtained DGGE patterns of the intermediate (10^{-4}) and highest positive (10^{-5}-10^{-8}) MPN dilution levels.

Assuming that the individual distinguishable bands (phylotypes) represent distinct species, it can be concluded that the within group diversity is considerable. However, these results should be interpreted with some care because the possible occurrence of multiple copies of 16S rRNA genes in individual species, which may result in an increased number of phylotypes and therefore, in an overestimation of the microbial biodiversity. Generally, different phylotypes were found in the photic and aphotic mat layers indicating that different species dominated the respective layers. Furthermore, phylotypes from the highest positive dilution levels were generally different from those that appeared in the lower (10^{-4}) dilution level. An interesting phenomenon occurred in the aerobic heterotrophic cultures. Here, growth on glycolic acid as sole substrate resulted in the appearance of a higher number of phylotypes than with growth on a mixture of substrates. The apparent diversity of (micro)organisms of different functional groups of Chiprana lake microbial mats is summarised in Table 2.

Table 2 Apparent diversity of functional groups of (micro)organisms in Lake Chiprana microbial mats. Number of phylotypes correspond to the number of distinguishable DGGE bands (see also Figure 4). Individual cell sizes of the different morphotypes and estimated biomass in the microbial mat layer (see Figure 1) where they appeared most prominently are given.

Functional Group:				Number of morphotypes (m) or phylotypes (p)*:
Oxygenic phototrophs				
Diatoms:				2 (m)
Nitzschia sp. layer 1	(4 × 70 µm)	5%	layer 1	
Navicula sp. layer 1	(20 × 80 µm)	1%	layer 1	
Cyanobacteria:				8 (m)
Halothece-like unicellular	(1 × 1-2 µm)	1%	layer 1,4	
Gloeocapsa-like	(2 × 2 µm)	2%	layer 4	
Gloeocapsa-like	(5 × 7 µm)	2%	layer 4	
Microcoleus-like type 1	(5 × 10 µm)	5-10%	layer 2	
Microcoleus-like type 2	(2 × 5 µm)	2-5%	layer 2	
Microcoleus-like type 3	(1 × 4 µm)	80%	layer 2,4	
Microcoleus-like type 4	(1 × 2 µm)	1%	layer 6	
Pseudoanabaena-like type 5	(1.5 × 4 µm)	2-5%	layer 2	
Anoxygenic phototrophic bacteria				
Chloroflexus-like bacteria	(1 × > 100 µm)	90%	layer 1	1 (m)
Purple sulphur bacteria				6 (p)
Aerobic heterotrophic bacteria				5 (p)
Colourless sulphur bacteria				7 (p)
Sulphate-reducing bacteria				9 (p)

Morphotypes determined by microscopy and phylotypes by PCR-DGGE (see material & methods)

Functional analyses

Photosynthesis rates and daily dynamics of oxygen, sulphide and pH

The *in situ* measurements of oxygen dynamics during a daily cycle are presented in Fig. 5. The oxygen concentration rapidly built up directly after sunrise and reached over 5 times air saturation (1 mM oxygen) already at 10 a.m. at a light intensity of 800 µmol photons m^{-2} s^{-1}. Subsequently, at increased light intensities, oxygen penetrated deeper in the mat and multiple concentration maxima became visible in the profiles (Figure 5b; 1400 and 2400 µmol photons m^{-2} s^{-1}). At higher light intensities, another interesting phenomenon occurred. Oxygen not only penetrated deeper in the mat but concentrations of oxygen also decreased near the top of the mat, indicating that either downward migration of oxygenic phototrophs or photo-inhibition occurred. In the early evening the situation reversed: a decrease in light intensity resulted in higher oxygen concentrations in the mat surface layer (Figure 5C; 2100 and 845 µmol photons m^{-2} s^{-1}), indicating upward migration or a decrease in photo-inhibition. Another indication for vertical migration of photosynthetic activity is that oxygen concentration maxima moved from 0.5 mm depth in the morning (Figure 5A; 09:15h and 09:45h) to 1.5 mm depth in the evening (Figure 5C; 18:15h and 18:43h) while light intensities at these times were comparable (between 100 and 300 µmol photons m^{-2} s^{-1}).

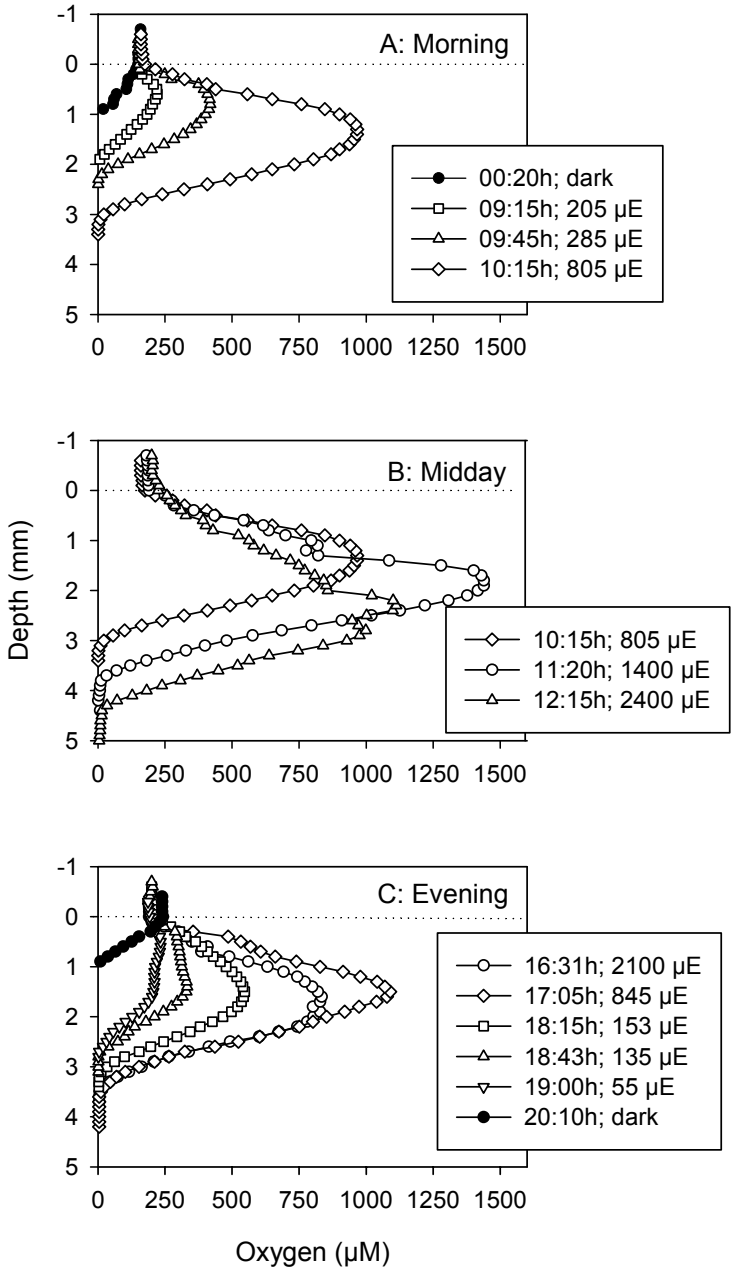

Figure 5 *In situ* daily dynamics of oxygen concentration in a Chiprana Lake microbial mat (October 2000). Midday profiles (B) show that at higher light intensities (1400 and 2400 µmol photons m^{-2} s^{-1}) multiple oxygen concentration maxima occur but that the oxygen concentration in the surface layer (0-2 mm) simultaneously decreases.

Gross photosynthesis profiles (Figure 6) measured in May 2001 showed double peaks at higher light intensities (870, 1240 and 1450 µmol photons m^{-2} s^{-1}), with peak maxima around 1 and 2.5 mm depth, corresponding to the double peaks in the oxygen profiles. Calculated areal gross photosynthetic rates (sum of depth-integrated gross volumetric values) amounted to 0.05, 0.21, 0.44 and 0.29 nmol O_2 cm^{-2} s^{-1} at light intensities of 125, 870, 1240 and 1450 µmol photons m^{-2} s^{-1} respectively. The latter value indicates that at high light intensities photo-inhibition occurred.

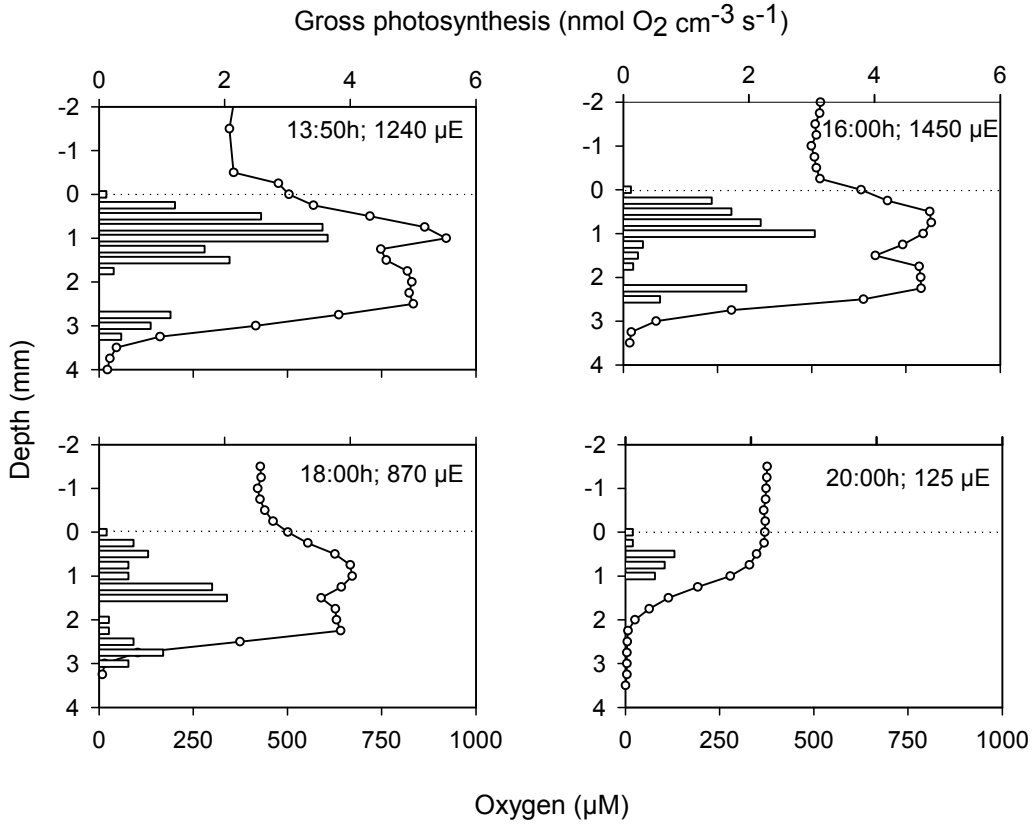

Figure 6 *In situ* oxygen and photosynthesis depth profiles (May 2001). Oxygen concentration maxima at higher light intensities coincide with photosynthesis maxima.

A comparison between oxygen dynamics in May and October revealed little seasonal variation. While the oxygen penetration depths were similar (3-4 mm depth), the oxygen concentration maximum was highest in October, i.e. 1400 µM and 900 µM in October and May, respectively. Sulphide (S^{2-}), measured with a needle mini-sensor, could be detected near the sediment surface during the night (at 1 mm depth) but only in deeper mat layers during the day (> 4 mm depth; results not shown). Maximal total sulphide concentrations (H_2S, $HS^-$and S^{2-}) in the dark, calculated using the S^{2-} and depth corresponding pH values according to Revsbech et al. (1983), amounted to 2 mM. The pH of Chiprana lake water was 8.5 but increased in the photosynthetically

active layer of the mat during the day to values above 9. The pH decreased in deeper mat layers during the day as well as in the whole mat during the night to values around 7.5. The water temperature was measured directly above the microbial mat sediment surface. The temperature increased from lowest night-time values (15 and 25ºC in October and May, respectively) to highest midday time values (19 and 28ºC in October and May, respectively). The higher water temperatures in May resulted in lower peak values of oxygen concentration in the photic zone possibly by a combination of lower solubility of oxygen in warmer water and increased respiration.

Depth distribution of photopigments

In order to determine diurnal vertical migration behaviour of phototrophic organisms, the photopigment distribution in microbial mat cores taken at 5 a.m. and 5 p.m. were compared. Photopigment profiles of Chl*a* and three of its allomers, fucoxanthine, zeaxanthine and ß-carotene, diagnostic pigments for oxygenic phototrophs (diatoms, cyanobacteria) and general phototrophs respectively, are shown in Figure 7 and 8. Lutein, Chl*b* and peridinin, signature pigments for green algae (lutein and Chl*b*) and dinoflagellates (peridinin), were below detection limit (0.1 µg/g sediment). The vertical distribution of Chl*a* and its allomers (Figure 7) show that the individual compounds have distinct distributions and, moreover, that their depth maxima during the day are complementary with respective maxima at 1, 3 and 6 mm (Chl*a*), 4 mm (Chla_1), 2-3 and 6 mm (Chla_2), and 1.5 and 5.5 mm (Chla_3). Comparison of day and night profiles shows that maxima or part the maxima of the night profiles are shifted upwards with one to two millimetres. The profiles of the carotenoids fucoxanthine, zeaxanthine and ß-carotene, however, do not show clear differences between day and night depth distributions (Figure 8).

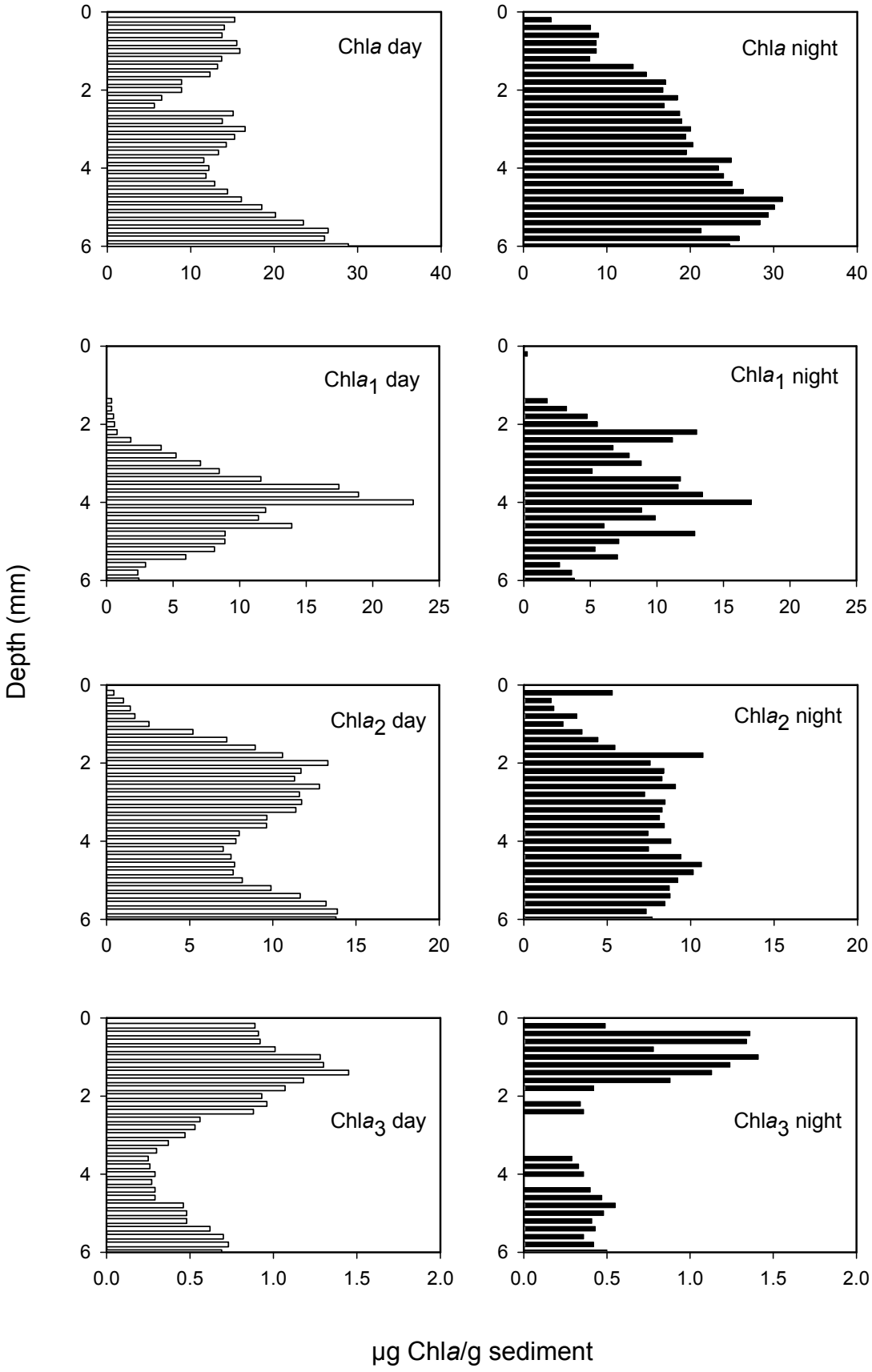

Figure 7 Day and night depth distribution of Chl*a* and Chl*a* allomers (Chla_1, Chla_2 and Chla_3) in Chiprana lake microbial mats showing an upward shift of photopigment distribution at night.

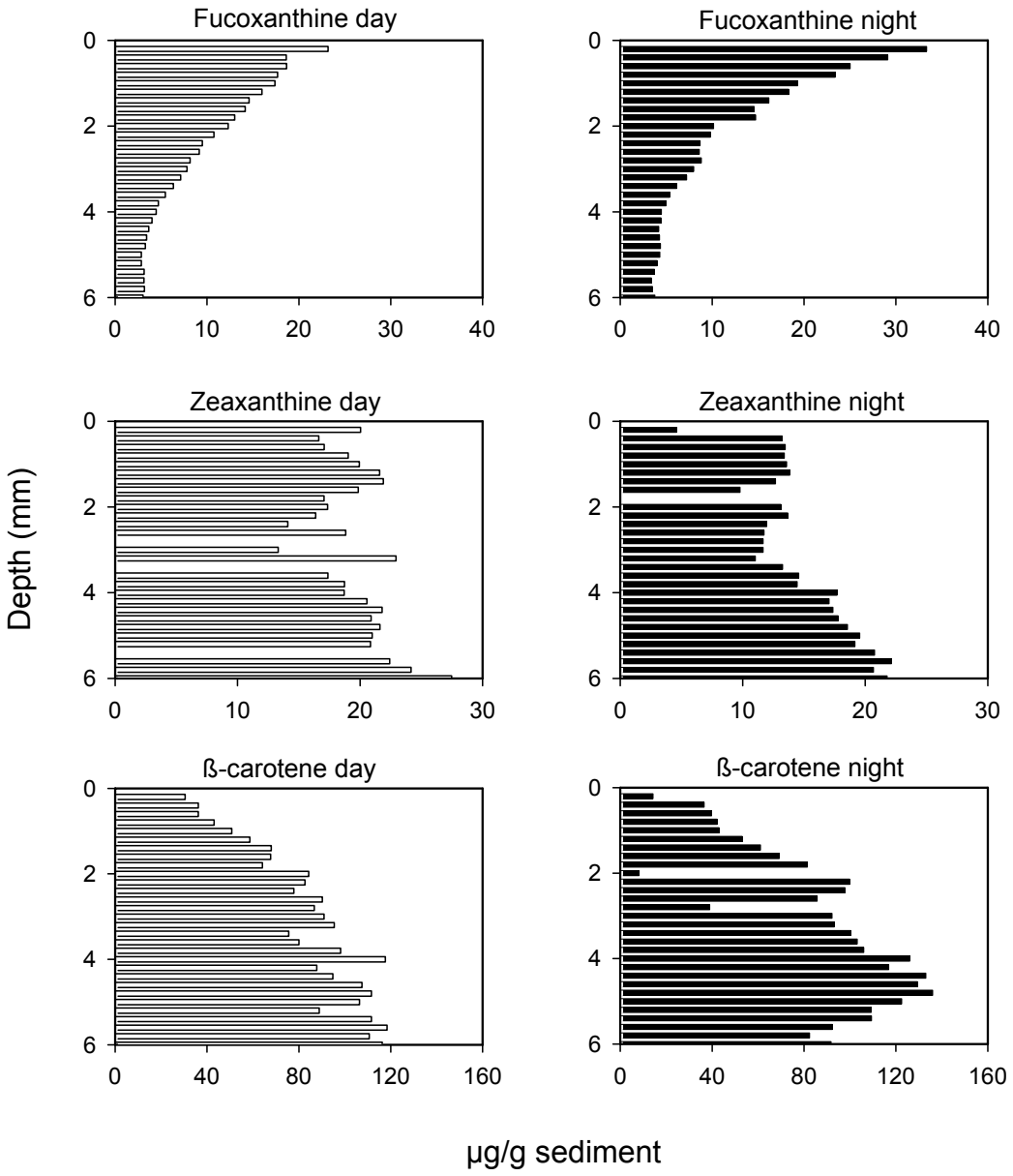

Figure 8 Day and night depth distribution of Fucoxanthine, Zeaxanthine and ß-carotene in Chiprana Lake microbial mats, respective marker pigments for diatoms, cyanobacteria and phototrophic organisms.

Daily dynamics in pore water DIC, DOC and fatty acids: flux calculations

Dynamics in microbial mat pore water concentrations of dissolved organic (DOC) and inorganic carbon (DIC) were studied because these may reflect autotrophic and heterotrophic activities. The 0-2 mm depth layer showed the highest concentration differences between day and night (Figure 9). The lowest DIC and highest DOC concentrations were measured in this layer during the day, indicating a respective flux of DIC into and flux of DOC out of this layer. The DOC concentration difference between the 0-2 mm depth layer and the water column was much higher than between

the 0-2 mm and 2-4 mm depth layer. This indicates that the main flow of DOC was primarily towards the water column. The chemical composition of the DOC pool remains largely unknown since in this study only short-chain fatty acids were measured. Significant concentrations of formic-, acetic-, lactic- and propionic acid

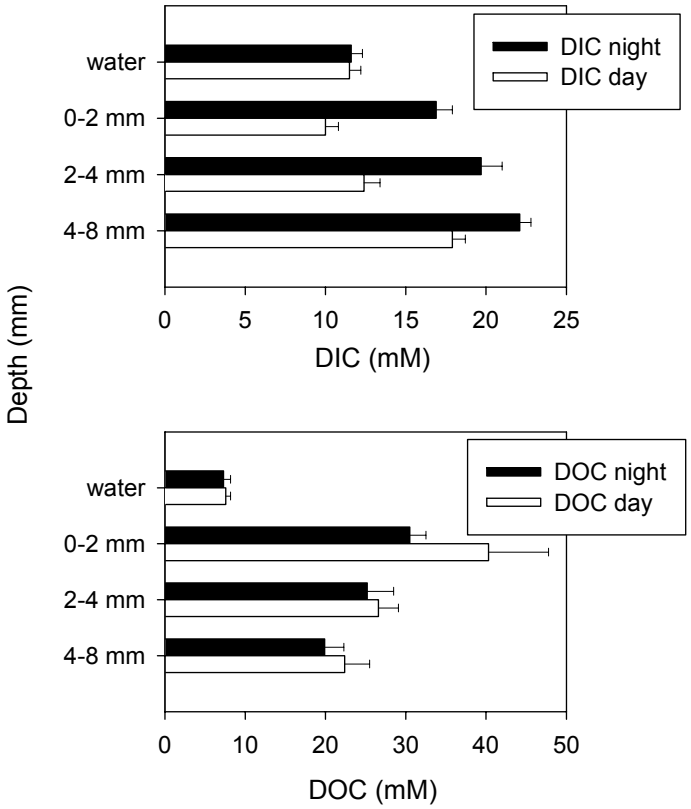

Figure 9 Day and night pore water concentrations of dissolved organic carbon (DOC) and dissolved inorganic carbon (DIC) in Chiprana Lake microbial mats. Profiles show that the 0-2 mm depth layer is reduced in DIC during the day while DOC concentrations in the mat are significantly higher then in the water column both during day and night.

could be detected. Concentration profiles of these compounds, except for formic acid, were similar to the DOC profiles. Low concentrations of fatty acids were found in the water column, while higher concentrations were found in the mat with maximum concentrations in the 0-2 mm depth layer. Concentrations were higher during the day, except for formic acid what was only detected in the 0-2 mm depth layer in night samples (Figure 10). Glycolic-, butyric-, iso-butyric-, valeric- and iso-valeric acid could all be detected, but concentrations were always below 5 µM in both during day and night. The total pore water concentration of fatty acids in terms of organic carbon in the 0-2 mm depth layer was 0.87 mM and 0.56 mM during day and night, respectively. These values amount to 2.2% and 1.8% of the DOC pool in this layer.

An estimate of the daily fatty acid flux out of the mat can be made based on the measured concentration profiles. The flux (F) is denoted by:

$$F = D * (\Delta C/\Delta z)$$

where D is the molecular diffusion coefficient and ($\Delta C/\Delta z$) the difference in concentration between the 0-2 mm sediment layer and the overlying water. Diffusion coefficients for formic acid, acetic acid, propionic acid and lactic acid were estimated by the Wilke-Chang technique (Perry & Green 1984) and were $1.59*10^{-5}$, $1.24*10^{-5}$, $1.06*10^{-5}$ and $1.06*10^{-5}$ cm^2 s^{-1} respectively. The day light period was 16 hours and oxygenic gross photosynthesis during this period amounted to 25.3 µmol O_2 cm^{-2} assuming an average light intensity of 1240 µmol photons m^{-2} s^{-1}. Net photosynthesis rates at 1240 µmol photons m^{-2} s^{-1} and 0 µmol photons m^{-2} s^{-1} were calculated to be 0.140 and –0.025 nmol cm^{-2} s^{-1} respectively from which we calculated a daily net oxygen production rate of 7.3 µmol O_2 cm^{-2}. The calculated flux of fatty acids out of the mat during the day (16 hours) and night (8 hours) period amounted respectively to –0.02 and 0.15 µmol cm^{-2} for formic acid, 0.55 and 0.26 µmol cm^{-2} for acetic acid, 0.06 and 0.02 µmol cm^{-2} for propionic acid and 0.46 and 0.07 µmol cm^{-2} for lactic acid. The total daily flux of fatty acids was 3.58 µmol organic carbon cm^{-2} what corresponds to 14 % of the daily gross photosynthesis and 49 % of the daily net photosynthesis.

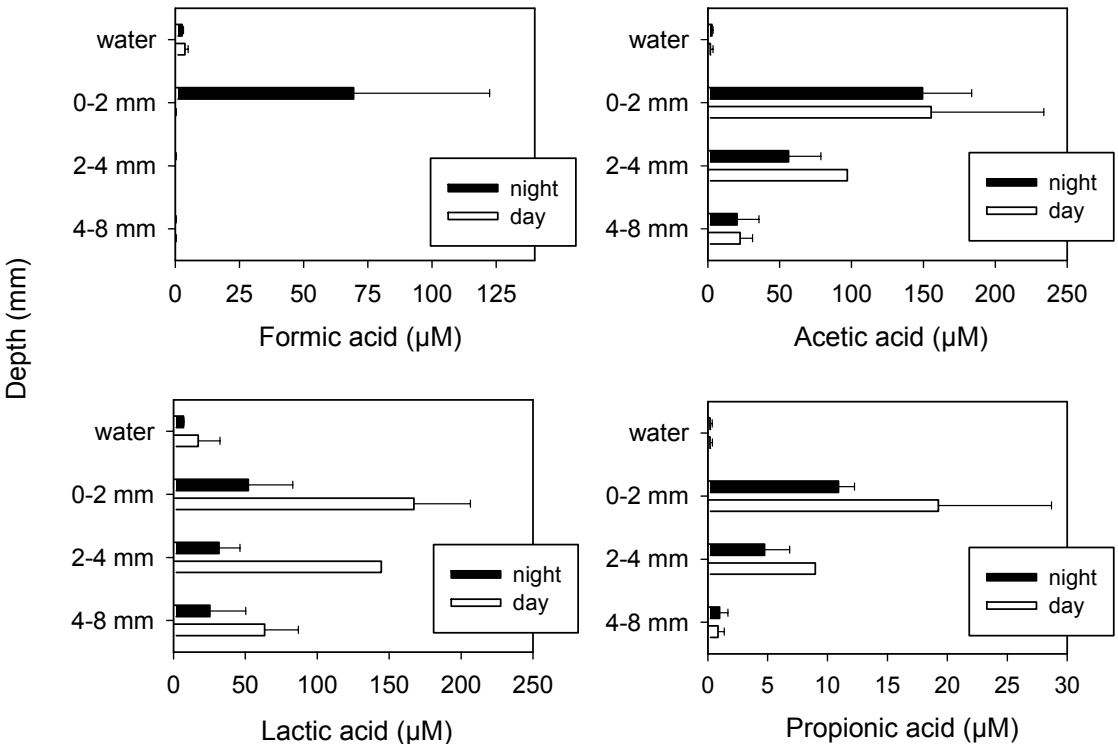

Figure 10 Day and night pore water concentrations of formic-, acetic-, lactic-, and propionic acid. Except for formic acid, day time concentrations are higher then night time concentrations in all mat layers.

Discussion

Chiprana lake microbial mats are apparently rich in species. DGGE patterns of MPN dilution series revealed that specific enrichment cultures harboured a variety of numerically important species. Direct microscopic observations furthermore disclosed a high diversity of phototrophic organisms since 11 morphotypes could be distinguished. It should be realised, however, that the biodiversity estimation in our study was based for the majority on culture based techniques. Since many organisms resist culturing in standard media, the actual biodiversity may have been much higher. The high concentration of magnesium in Chiprana lake water, 7 times higher than seawater, apparently did not restrict microbial diversity to a major extend. Whether the high magnesium concentration, that is thought to be inhibitory for many microorganisms (Guerrero & DeWit 1992), resulted in a genetically different community composition compared to other hypersaline mats remains to be investigated. We are presently constructing a clone library of 16S rDNA genes amplified from environmental DNA extracted from the Chiprana microbial mat to further investigate this matter. The structural community analysis of the Chiprana microbial mat, however, revealed conspicuous characteristics. Firstly, different morphotypes of cyanobacteria had a different depth distribution. Secondly, in Chiprana microbial mats a *Chloroflexus*-like bacteria-dominated layer was situated on top instead of below cyanobacteria-dominated layers as was reported for other *Chloroflexus*-harbouring mats (Pierson & Castenholz 1992). The *Chloroflexus*-like bacteria were the most likely source of the Bacteriochlorophyll *c* homologues detected in highest concentrations in the top mm of the mat. Similar BChl*c* homologues were also observed in thalassic hypersaline microbial mats in coastal salterns (Villanueva et al. 1994). *Chloroflexus aurantiacus* contains γ-carotene and β-carotene as the major carotenoid pigments (Schmidt 1978). The latter, but not the former, is also synthesised by cyanobacteria. The top layer of the mat contained both γ-carotene and β-carotene, a phenomenon that was also observed in the mats of the coastal solar salterns (Villanueva et al. 1994). Thirdly, equal numbers of culturable sulphate-reducing bacteria were found in the photic, during the day fully oxic, top layer and underlying aphotic, permanently anoxic layer. These structural community characteristics can be explained by the functional analysis as will be discussed in the following.

The vertical distribution of photopigments in Chiprana microbial mats revealed that Chl*a* and three of its allomers had a complementary depth distribution. Moreover,

differences in day and night depth distributions, particularly of the allomers Chla_1, Chla_2 and Chla_3, indicate that oxygenic phototrophs showed daily vertical migration behaviour. Although Chl*a* allomers are known to occur in microbial mats (Buffan-Dubau et al. 2001) specific depth distributions have not been reported before. Comparison with the microscopically observed depth distribution of different phototrophic morphotypes does not show a clear correlation with Chl*a* and Chl*a* allomere depth distributions. Whether the Chl*a* allomers are species specific photopigments or rather species unspecific adaptations to changes in depth related light quantity or quality remains therefore to be investigated. Alternatively, some of these Chl*a* allomers may represent diagenetic conversion products, because oxygen radicals and other compounds induce allomerisation of free Chl*a* (Jeffrey et al. 1999). However, diagenetic conversion products are very unlikely subjected to vertical migration, unless they are carried by living organisms. Diatoms apparently did not migrate in Chiprana mats since the depth distribution of fucoxanthine, specific carotenoid for diatoms, did not show differences between day and night. The carotenoid zeaxanthine is known to occur both in cyanobacteria and chlorophytes (Jeffrey et al. 1999) but since the latter group also produces Chl*b* and this compound was not detected in significant amounts in Chiprana mats, it can be concluded that zeaxanthine in Chiprana mats originated from cyanobacteria. Although Chl*a* and its allomers did show clear differences in day and night depth distributions, zeaxanthine and ß-carotene did not. This can be explained by the fact that all cyanobacterial species produce zeaxanthine and most phototrophic organisms ß-carotene while apparently only some of the present cyanobacterial species showed migration behaviour. The amount of zeaxanthine and ß-carotene translocated by the migrating cyanobacteria may thus have been obscured by the total amount of zeaxanthine and ß-carotene present in the microbial mat. BChl*c* could only be detected in the top millimetre of the mat an observation that is congruent with the microscopically observed depth distribution of *Chloroflexus*-like bacteria. However, concentrations were near the detection limit what hampered the determination of a more detailed depth distribution in thinner mat slices. The downward migration during the day of at least a part of the actively photosynthesising community explains the decrease in oxygen concentration in the mat surface layer during the day at increasing light intensities. Also it explains the appearance of multiple oxygen concentration maxima in deeper parts of the microbial mat. Light-induced downward migration of cyanobacteria was also reported to occur in hypersaline mats from Guerrero Negro, Mexico, and here also only a few members of the phototrophic community actively

migrated (Garcia-Pichel et al. 1994; Kruschel & Castenholz 1998). In these studies it was concluded that vertical migration predominantly occurred in order to escape ultra-violet light-induced damage and photoinhibition at high levels of visible light radiation. Diatoms and *Chloroflexus*-like filamentous bacteria, which dominated the surface layer of the Chiprana Lake mats, are known to be UV-light resistant as they produce specific high-light intensity and UV screen pigments, mycosporine-like amino acids (Jeffrey et al. 1999) and hydroxy-γ-carotene-glucoside (Pierson & Castenholz 1992; Pierson et al. 1993) respectively. These organisms do not only protect themselves but also to a certain extend the underlying microorganisms from overexposure to UV and high light intensities. In turn, as discussed below, *Chloroflexus*-like bacteria also benefit from the underlying cyanobacteria.

Both photosynthesis profiles and dissolved (in)organic carbon profiles reflect that the highest primary production rates occurred in the 0-2 mm surface layer of the mat. Here, inorganic carbon concentration was low during the day while in the overlaying water and in deeper sediment layers concentrations were higher. This means that during the day a flux of dissolved inorganic carbon occurred both from above and from below towards this layer. At night however, inorganic carbon concentration increased with increasing sediment depth meaning that a flux of inorganic carbon from the mat to the overlaying water occurred, a phenomenon that was expected because at night mineralization generally exceeds carbon dioxide fixation. Interestingly, dissolved organic carbon profiles show that Chiprana mats produced organic carbon both during the day and at night because concentrations in pore water were always higher than in the overlaying water. Although some organic carbon that is produced in the 0-2 mm depth layer diffuses towards deeper layers in the mat, the main flow of dissolved organic carbon will be towards the overlaying water since the difference in concentration is much higher between these two. In this study it was estimated that although low molecular weight fatty acids make up only 2% of the pore water DOC pool, the daily flux of these compounds from the mat to the water column amounts to 14% of the daily gross photosynthesis and 49% of the daily net photosynthesis. The as yet unidentified fraction of the DOC pool probably consists for the major part of polymeric compounds such as polysaccharides and proteins. These larger molecules have typically much smaller diffusion coefficients and are therefore less mobile. Although the contribution of the latter compounds to the DOC pool may be much higher the flux out of the mat may be much smaller than that of low molecular weight fatty acids. The main flow direction of the DOC compounds explains why in Chiprana mats the *Chloroflexus*-like bacteria grow on top instead of

below the cyanobacterial layers. Here they can maximally benefit from the flow of organic photosynthates excreted by oxygenic primary producers which are the preferred substrates of these photoheterotrophic organisms (Bateson & Ward 1988). The DOC profiles furthermore strongly suggest that primary production in Chiprana mats is nutrient limited. Oxygenic primary producers are known to direct the flow of reduced photosynthetic carbon towards the production of extracellular polymeric substances and low molecular weight organic compounds instead to structural cell components under nutrient-limiting conditions (Hoagland et al. 1993; Stal 1995). Significant concentrations of acetic-, lactic- and propionic acid, typical substrates for sulphate-reducing bacteria, were detected both in day and night pore water samples. This may explain why sulphate-reducing bacteria occur in relatively high numbers in the oxic surface layer because they apparently do not have to compete with aerobic heterotrophic bacteria for substrates. Moreover, as recent findings indicate, sulphate-reducing bacteria can tolerate high oxygen concentrations but need occasional periods of anoxia for good growth (Cypionka 2000), conditions that occur in the major part of the photic zone during the night. Although future analyses have to clarify what the nature and identity of the compounds are that make up the major fraction of the dissolved organic carbon pool, it can be concluded that a large fraction of the oxygenic primary production in Chiprana microbial mats leaves the system as dissolved organic carbon and is not used for biomass synthesis.

This study showed that the benthic microbial mats of Chiprana Lake not only represent an excellent model ecosystem for the study of biogeochemical processes but is also an original and diverse benthic microbial ecosystem, the study of which may contribute to a better understanding of ecological, physiological and genetic questions. Efforts should therefore be undertaken to protect the unique Chiprana Lake ecosystem in order to conserve its still largely unexplored biodiversity.

Acknowledgements

We are indebted to the local authorities in Chiprana for granting permission to access the lake and take microbial mat samples and we are particularly grateful to Alfredo Legaz (Guard) for support during field work. Axel Schippers and Kirsten Neumann are thanked for their help with sample analysis and Gerhard Holst for photographing microbial mat samples.

References

Airs, R. L., Atkinson, J. E., Keely, B. J. (2001) Development and application of a high resolution liquid chromatographic method for the analysis of complex pigment distributions. J. Chromatography A 917: 167-177

Albert, D. B., Martens, C. S. (1997) Determination of low molecular weight organic acid concentrations in seawater and pore water samples via HPLC. Mar. Chem. 56: 27-37

Bateson, M. M., Ward, D. M. (1988) Photoexcretion and fate of glycolate in a hot spring cyanobacterial mat. Appl. Environ. Microbiol. 54: 1738-1743

Bauld, J. (1981) Occurrence of benthic microbial mats in saline lakes. Hydrobiologia 81: 87-111

Borrego, C., Garcia-Gil, L. (1994) Separation of bacteriochlorophyll homologues from green photosynthetic bacteria by reversed-phase HPLC. Photosynth. Res. 41: 157-163

Buffan-Dubau, E., Pringault, O., de Wit, R. (2001) Artificial cold-adapted microbial mats cultured from Antarctic lake samples. 1. Formation and structure. Aquat. Microb. Ecol.. 26: 115-125

Clarke, T., Owens, N. (1983) A simple and versatile micro-computer program for the determination of ‘’'most probable number’. J. Microbiol. Meth. 1: 133-137

Cypionka, H. (2000) Oxygen respiration by Desulfovibrio species. Annu. Rev. Microbiol. 54: 827-848

Diaz, P., Guerrero, M. C., Alcorlo, P., Baltanas, A., Florin, M., Montes, C. (1998) Anthropogenic perturbations to the trophic structure in a permanent hypersaline shallow lake: La Salada de Chiprana (North-eastern Spain). Int. J. Salt Lake Res. 7: 187-210

Garcia-Pichel, F., Mechling, M., Castenholz, R. W. (1994) Diel migrations of microorganisms within a benthic, hypersaline mat community. Appl. Environ. Microbiol. 60: 1500-1511

Guerrero, M. C., de Wit, R. (1992) Microbial mats in the inland saline lakes of Spain. Limnetica 8: 197-204

Heijthuijsen, J. H. F. G., Hansen, T. A. (1986) Interspecies hydrogen transfer in co-cultures of methanol- utilizing acidogens and sulfate-reducing or methanogenic bacteria. FEMS Microbiol. Lett. 38: 57-64

Hoagland, K. D., Rosowski, J. R., Gretz, M. R., Roemer, S. C. (1993) Diatom extracellular polymeric substances: Function, fine structure, chemistry, and physiology. J. Phycol. 29: 537-566

Jeffrey, S., Mantoura, R., Björnland, T. (1997) Phytoplankton pigments in oceanography: Guidelines to modern methods. UNESCO Publishing, Paris

Jeffrey, S. W., MacTavish, H. S., Dunlap, W. C., Vesk, M., Groenewoud, K. (1999) Occurrence of UVA- and UVB-absorbing compounds in 152 species (206 strains) of marine microalgae. Mar. Ecol. Prog. Ser. 189: 35-51

Kruschel, C., Castenholz, R. (1998) The effect of solar UV and visible irradiance on the vertical movements of cyanobacteria in microbial mats of hypersaline waters. FEMS Microbiol. Ecol. 27: 53-72

Kühl, M., Steuckart, C., Eickert, G., Jeroschewski, P. (1998) A H_2S microsensor for profiling biofilms and sediments: application in an acidic lake sediment. Aquat. Microb. Ecol. 15: 201-209

Muyzer, G., Teske, A., Wirsen, C. O., Jannasch, H. W. (1995) Phylogenetic relationships of *Thiomicrospira* species and their identification in deep-sea hydrothermal vent samples by denaturing gradient gel electrophoresis of 16S rDNA fragments. Arch. Microbiol.164: 165-172

Perry, R., Green, D. (1984) Diffusion coefficients. In: Crawford, H., Eckes, B. (eds) Perry's chemical engineers' handbook. 6th edn. McGraw-Hill Inc, Singapore, pp 3/285-3/287

Pierson, B., Castenholz, R. (1992) The Family *Chloroflexaceae*. In: Balows, A., Trüper, H., Dworkin, M., Harder, W., Schleifer, K. (eds) The Prokaryotes. 2nd edn. Springer-Verlag, New York

Pierson, B., Mitchell, H. K., Ruffroberts, A. L. (1993) *Chloroflexus aurantiacus* and ultraviolet-radiation: Implications for Archean shallow-water stromatolites. Origins Life Evol. B. 23: 243-260

Revsbech, N. P., Jørgensen, B. B. (1983) Photosynthesis of benthic microflora measured with high spatial resolution by the oxygen microprofile method: Capabilities and limitations of the method. Limnol. Oceanogr. 28: 749-756

Revsbech, N. P., Jørgensen, B. B., Blackburn, T. H., Cohen, Y. (1983) Microelectrode studies of the photosynthesis and O_2, H_2S, and pH profiles of a microbial mat. Limnol. Oceanogr. 28: 1062-1074

Schippers, A., Jørgensen, B. B. (2001) Oxidation of pyrite and iron sulfide by manganese dioxide in marine sediments. Geochim. Cosmochim. Acta 65: 915-922

Schmidt, K. (1978) Biosynthesis of carotenoids. In: Clayton, R.K., Sistrom, W.R. (eds) The photosynthetic bacteria. Plenum Press, New York, pp 729-750

Stal, L. J. (1995) Physiological ecology of cyanobacteria in microbial mats and other communities. New Phytol. 131: 1-32

Stumm, W., Morgan, J. J. (1996) Aquatic Chemistry. John Wiley & Sons, Inc, New York

Valero-Garcés, B. L., Navas, A., Machin, J., Stevenson, T., Davis, B. (2000) Responses of a saline lake ecosystem in a semiarid region to irrigation and climate variability - The history of Salada Chiprana, central Ebro basin, Spain. Ambio 29: 344-350

Vidondo, B., Martinez, B., Montes, C., Guerrero, M. C. (1993) Physico-chemical characteristics of a permanent Spanish hypersaline lake: La Salada de Chiprana (NE Spain). Hydrobiologia 267: 113-125

Vila, X., Guyoneaud, R., Cristina, X., Figueras, J.B., Abella, C.A. (2002) Green sulfur bacteria from hypersaline Chiprana Lake (Monegros, Spain): Habitat description and phylogenetic relationships of isolated strains. Photosynth. Res. 71: 165-172

Villanueva, J., Grimbalt, J. O., De Wit, R., Keely, B. J., Maxwell, J. R. (1994) Chlorophyll and carotenoid pigments in solar saltern microbial mats. Geochim. Cosmochim. Acta 58: 4703-4715

Widdel, F., Bak, F. (1992) Gram-negative mesophilic sulfate-reducing bacteria. In A. Balows, A., Trüper, H. G., Dworkin, M., W., Harder, W., Schleifer, K.-H. (eds.), The prokaryotes, 2nd ed. Springer-Verlag, New York, pp 3353-3378

Williams, W. D. (1986) Limnology, the study of inland waters: A comment on perceptions of studies on salt lakes, past and present. In: De Deckker, P., Williams, W.D. (eds) Limnology in Australia. Dr. W. Junk Publisher, Dordrecht, pp 471-496

Wright, S. W., Jeffrey, S. W., Mantoura, R. F. C., Llewellyn, C. A., Bjørnland, T., Repeta, D., Welschmeyer, N. (1991) An improved HPLC method for the analysis of chlorophylls and carotenoids from marine phytoplankton. Mar. Ecol. Prog. Ser. 77: 183-196

Chapter 3

Limitation of oxygenic photosynthesis and respiration by phosphate and organic nitrogen in a hypersaline microbial mat: A microsensor study

3

Limitation of oxygenic photosynthesis and respiration by phosphate and organic nitrogen in a hypersaline microbial mat: A microsensor study

Rebecca Ludwig, Olivier Pringault, Rutger de Wit, Dirk de Beer, Henk M. Jonkers

Abstract

Microbial mats are characterised by high primary production but low growth rates, pointing to a limitation of growth by the lack of nutrients or substrates. We identified compounds that instantaneously stimulated photosynthesis- and respiration rates in a hypersaline microbial mat by following the short-term response (~6 h) of these processes to addition of nutrients, organic- and inorganic carbon compounds, using microsensors. Net photosynthesis rates were not stimulated by compound additions. However, both gross photosynthesis and respiration were substantially stimulated (by a minimum of 25 %) by alanine (1 mM) and glutamate (3.5 mM) as well as by phosphate (0.1 mM), as rates significantly increased after compound addition. A low concentration of ammonium (0.1 mM) did not affect photosynthesis and respiration, while a higher concentration (3.5 mM) reduced both process rates. High concentrations of glycolate (5 mM) and phosphate (1 mM) inhibited gross photosynthesis but not respiration leading to a decrease of net photosynthesis. Gross photosynthesis was not stimulated by addition of inorganic carbon, nor was respiration stimulated by organic compounds like glycolate (5 mM) or glucose (5 mM), indicating that carbon was efficiently cycled within the mat. Photosynthesis and respiration were apparently tightly coupled, as both processes, if stimulated, in all cases increased proportionally, resulting in unchanged net photosynthesis rates.

Introduction

Phototrophic microbial mats are dense microbial communities typically containing metabolically diverse microorganisms like phototrophs (cyanobacteria, diatoms, purple and green (non) sulphur bacteria), anaerobic (sulphate-reducing bacteria, methanogens, fermentative bacteria) and aerobic bacteria (heterotrophs and chemolithoautotrophs). Due to the diverse metabolic activities of community members, steep vertical gradients of metabolites develop, in which the mat building organisms orientate themselves to find optimal conditions. This often results in a clearly visible vertical lamination (Van Gemerden 1993; Stal 2000). Oxygenic phototrophs are by far the dominant primary producers and primary production rates in microbial mats are high, with highest rates reaching values of tropical rain forests (Guerrero & Mas 1989). However, several studies revealed that in mature mats net growth is much lower than potentially possible when compared to the high rates of primary production (Krumbein et al. 1977; Canfield & Des Marais 1993; Nold & Ward 1996). Low growth rates, despite high primary production, points to a high internal cycling of photosynthetically fixed carbon. If not used for biomass production, reduced carbon may instead be partitioned between intracellular storage compounds and excretion products (Myklestad et al. 1989; Alcoverro et al. 2000; Dubinsky & Berman-Frank 2001). These organic excretion products are typically a major energy source for heterotrophic community members**,** which in turn remineralise it to CO_2 (Canfield & Des Marais 1993; Van Gemerden 1993; Pinckney & Paerl 1997). Part of the excretion products, however, may also be lost from microbial mats by diffusion to the overlying water (Jonkers et al. 2003). Reasons for limited growth of autotrophic and heterotrophic microbial mat organisms may be insufficient supply of nutrients, organic or inorganic carbon. Long-term nutrient enrichment studies (days to weeks) have been widely used to identify nutrient limitation in phytoplankton communities (see Beardall et al. (2001) and Elser et al. (1990) for reviews on this topic). However, far less studies concerned microbial mats (Paerl et al. 1993; Pinckney et al. 1995a; Pinckney et al. 1995b; Pinckney et al. 1995c; Camacho & de Wit 2003). A major draw-back of long-term incubation studies however is that, due to unavoidable community changes, uncertainties remain about the nutrient status of the original community (Paerl et al. 1993).

In this study we tested the hypothesis that addition of growth-limiting compounds to a mature microbial mat will result in an instantaneous increase of the net productivity of

the oxygen producing- and consuming community. Net productivity, measured as net oxygenic photosynthesis (NP), is the difference between areal gross oxygenic photosynthesis (AGP) and aerobic respiration (R). Microsensor techniques were applied in this study for quantification of the instantaneous (≤ 6 h) effect of compound additions on community net- and gross oxygenic photosynthesis as well as on respiration, as the latter process rate can be estimated from the difference of the former two.

Material and Methods

Sampling

Mat samples were collected in Lake Chiprana ('La Salada de Chiprana'), North-eastern Spain. See Jonkers et al. (2003) for a detailed description of the study site, sampling and mat composition, and Table 1 for pore water nutrient concentrations. Prior to experiments, mats were maintained in a laboratory mesocosm under natural light in aerated water of the same ion composition as natural lake water. Experiments were completed within 19 days of sampling. Routine microsensor measurements of oxygen concentration profiles in these mats showed no significant changes during the maintenance period.

Microsensor measurements

For experimental short-term incubations, mat pieces of approximately 20 cm^2 were incubated in a flow-through incubation chamber containing 0.5 l of natural Lake Chiprana water. The mat was illuminated with a fibre optic halogen lamp (300 µmol photons m^{-2} s^{-1}, Li-Cor, Model LI-250). Light intensity corresponded to late morning irradiation at the sampling site, ensuring that mats experienced no photoinhibition. Net oxygenic photosynthesis (NP) and volumetric oxygenic gross photosynthesis (VGP) rates of mats were measured before and after addition of potentially rate-limiting compounds using custom built Clark-type oxygen microsensors (Revsbech 1989). Before the start of actual photosynthesis measurements, time series of oxygen concentration profiles were measured until a steady state situation was reached, (typically within 6 h after start of the incubation and subsequently again within 6 h after compound addition). The diffusive oxygen flux out of illuminated mats was used to calculate net oxygenic photosynthesis rates, i.e. oxygen produced minus oxygen consumed in the mat. Subsequently, volumetric gross oxygenic photosynthetic rates at

100-150 µm depth intervals were measured with the light-dark-shift method as described by Revsbech & Jørgensen (1983). Depth integration of respective VGP rates yields the gross oxygenic photosynthesis rate under a given surface area, called areal gross photosynthesis (AGP). The rate of aerobic respiration (R) was finally calculated as the difference between AGP and NP. See Kühl et al. (1996) for a detailed description of calculation procedures. Within a single addition experiment all profiles were measured at the same spot to allow direct comparison between rates before and after addition. Finally, in addition to the oxygen profiles, sulphide (H_2S) profiles were measured, using an amperometric H_2S microsensor (Kühl et al. 1998) to check whether additions affected sulphide dynamics.

Added compounds

The compounds added represented one of the following classes a) inorganic carbon, b) organic carbon and c) macro- and micronutrients. All solutions were adjusted to the pH of the water (8.3) in which the mats were incubated. Concentrations added (given in brackets as final concentration) were high to allow a fast diffusional supply into the mat. $NaHCO_3$ (20 mM) was added as inorganic carbon source. As representatives for organic carbon, those compounds were chosen that are known to be produced in microbial mats and may represent respiration-limiting compounds. Glucose (5mM) is abundant in mat extracellular polymeric substances (EPS) in form of polyglucose, and glycolate (5mM) is a photorespiration product that was previously found in microbial mats (Bateson & Ward 1988). Alanine (1mM) and glutamate (3.5mM) were chosen as representatives of amino acids. Ammonium (0.1 and 3.5 mM NH_4Cl), phosphate (0.1 and 1 mM $NaHPO_4$) and trace metal solution SL12B (1 ml/l) (Widdel & Bak 1992) were added to check for (micro) nutrient limitation. Trace element solution contained per litre of MilliQ water: Na_2-EDTA (3000 mg), $FeSO_4 \cdot 7H_2O$ (1100 mg), H_3BO_3 (300 mg), $CoCl_2 \cdot 6H_2O$ (190 mg), $MnCl_2 \cdot 4H_2O$ (50 mg), $ZnCl_2$ (42 mg), $NiCl_2 \cdot 6H_2O$ (24 mg), $Na_2MoO_4 \cdot 2H_2O$ (8 mg), $CuCl_2 \cdot 2H_2O$ (2 mg). As a control measurement both NP and VGP were measured twice during a 6 hour period without compound addition.

Statistics

The difference in AGP, NP and R before and after compound addition was calculated. The difference was then compared with the difference in the control using an unpaired, two-tailed t-test ($\alpha = 0.1$). Degrees of freedom were adapted, using a Welch correction, as variances might not have been homogeneous.

Results

Effect of compound addition on photosynthesis and respiration

The effect of addition of inorganic carbon, organic carbon and (micro)nutrients on oxygenic net-, volumetric- and areal gross photosynthesis (NP, VGP and AGP) were tested. The response of the O_2 concentration profiles, AGP, NP and R to some selected compound additions is given in Fig. 1, and an overview of the response of AGP, NP and R to all compounds added is given in Fig. 2. The addition of inorganic carbon did not change the oxygen concentration profile and volumetric gross photosynthesis profiles (Fig. 1A). Also, the parameters derived from these profiles, AGP and R, did not change significantly. To investigate possible effects of inorganic nutrients, ammonium, phosphate or trace metals were added. The addition of ammonium in high concentration (3.5 mM) led to a significant decrease in oxygen concentration, NP, VGP and AGP as well as to the deduced aerobic respiration rate (R) (Fig. 1B). The oxygen concentration after addition decreased because photosynthesis decreased substantially more than respiration. The inhibition of gross photosynthesis was noticeable within five minutes after addition, proving that diffusion of added compounds into the mat was a fast process. Addition of ammonium in lower concentration (0.1 mM), however, had no effect on either the oxygen concentration profile, NP, VGP, AGP nor R. Addition of a relatively high phosphate concentration (1 mM) led to a decrease in both NP and AGP, while the calculated respiration rate (R) did not change significantly.

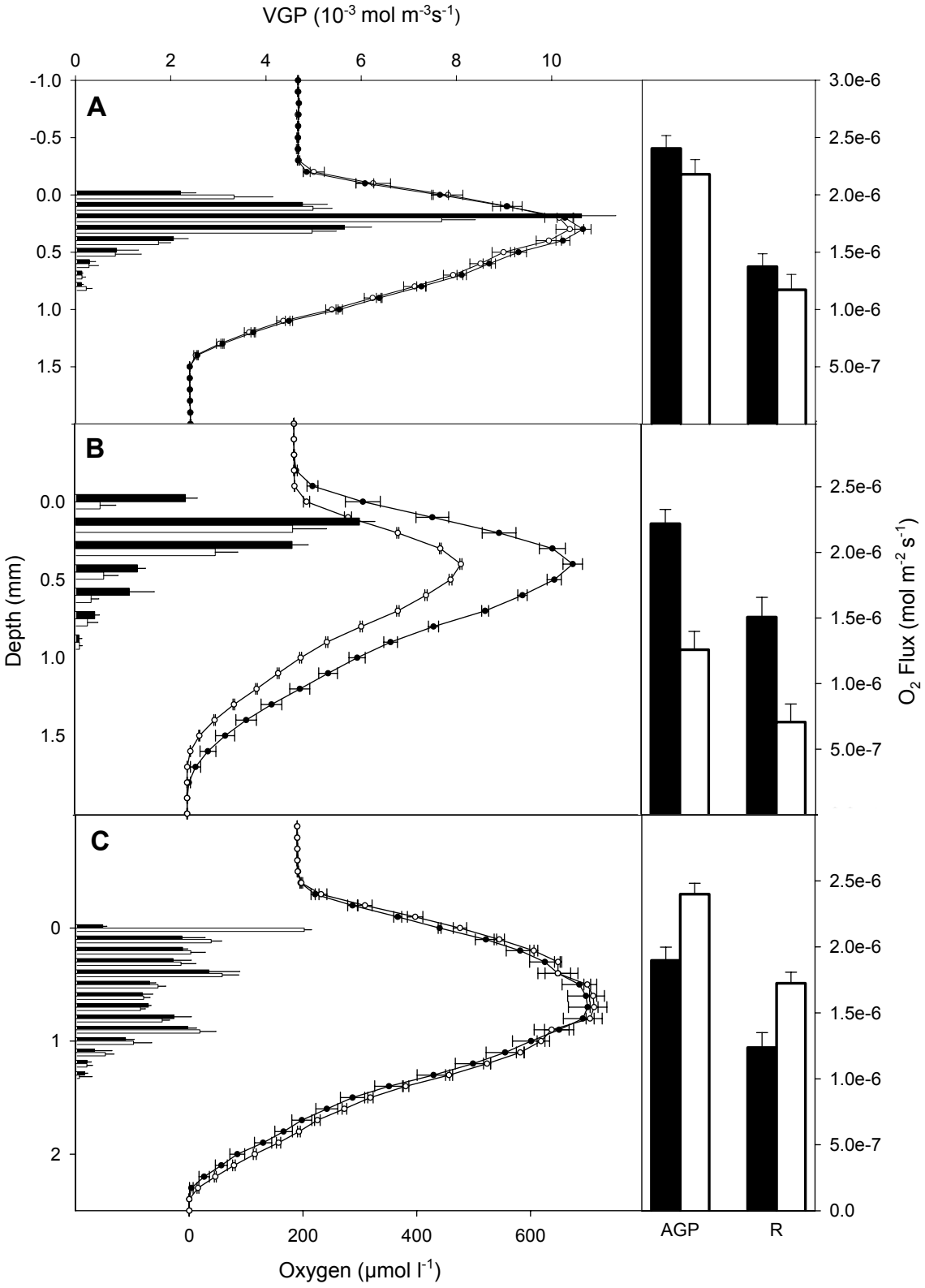

Figure 1: Responses to the addition of selected substances (A: 20 mM Bicarbonate B: 3.5 mM Ammonium C: 0.1 mM Phosphate). **Left panel:** volumetric gross photosynthesis (VGP, horizontal bars) and oxygen profiles. **Right panel:** areal gross photosynthesis (AGP) and respiration (R). Black before addition, white after addition.

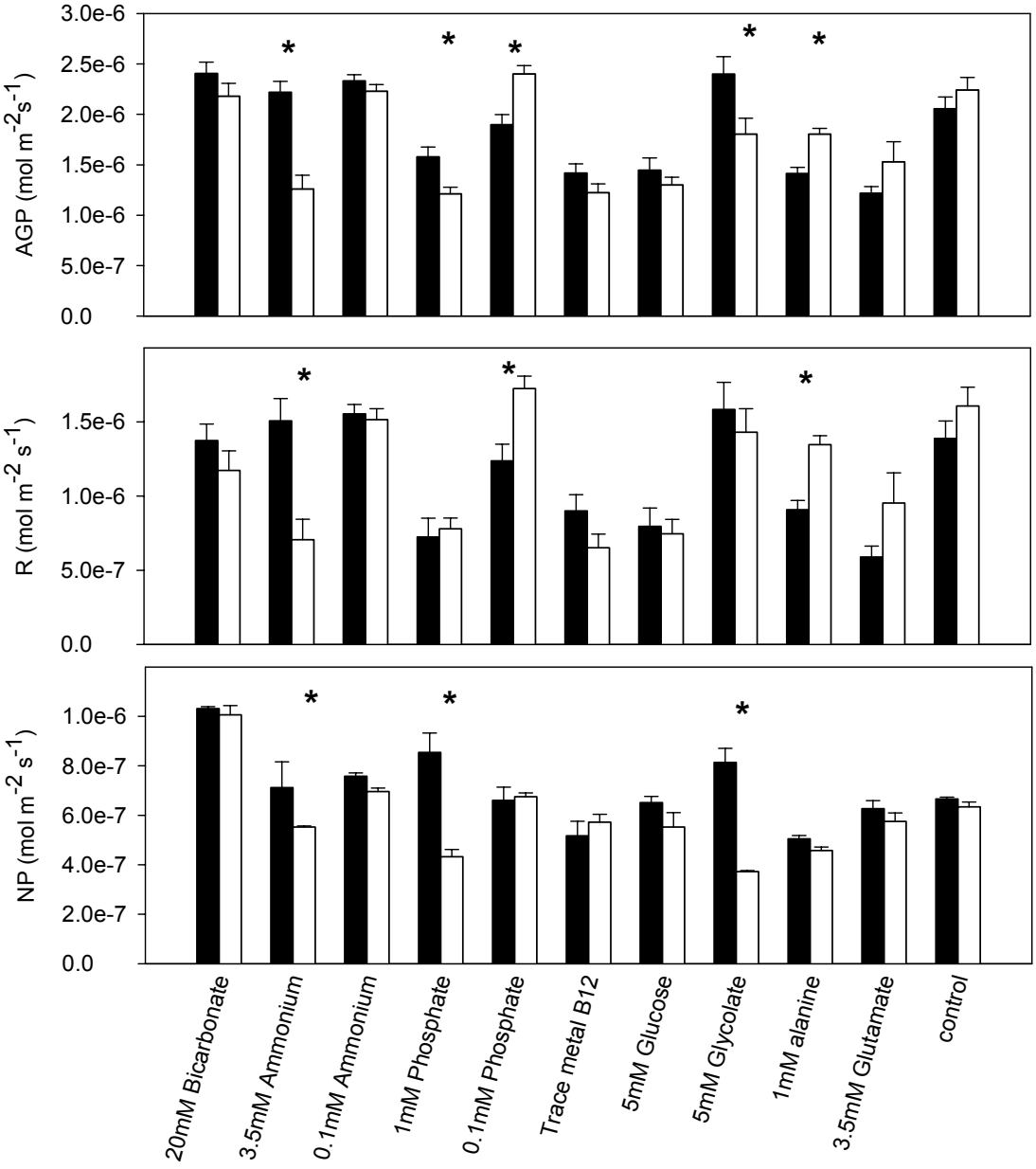

Figure 2: NP, R and AGP before (black) and after addition (white). An asterisk denotes significant difference to the control at the alpha 10% level.

However, addition of a lower phosphate concentration (0.1 mM), but still corresponding to a 10-times higher concentration than present in the mat pore water, had no effect on NP while AGP was significantly enhanced (Fig. 1C). Interestingly in this case, as AGP was increased while NP remained unchanged, R must have increased proportional to AGP, what thus resulted in an unchanged oxygen concentration profile. Addition of trace metal mixture SL12B (1ml/l) did not result in significant changes of NP, VGP or AGP.

Table 1: Nutrient concentrations of lake water and pore water sampled *in situ*. Nutrients were measured in a continuous flow analyser (CFA) according to Clesceri et al. (1989).

Concentration (µM)	Silicate	Phosphate	Ammonium	Nitrate
Water column	85.4	0.4	85.5	20.9
Pore water 0-4 mm	49.7	11.1	208.4	0.6
Pore water 4-8 mm	69.3	5.7	329.7	0.0

Of the added organic compounds, neither glucose (5 mM) nor glycolate (5 mM) significantly affected calculated respiration rates. However, while glucose addition did not affect any process, glycolate addition led to a strong and proportional decrease in both NP and AGP. In contrast to the purely organic compounds glucose and glycolate, the added nitrogen-containing organics alanine (1 mM) and glutamate (3.5 mM) substantially stimulated AGP (by 28% and 25 %, respectively) while NP remained unchanged. As a consequence, aerobic respiration must have increased proportionally to the increased AGP rates, as was observed in the case of phosphate (0.1 mM) addition.

Table 2: Effect of compound addition on the H_2S concentration in illuminated mats. 0 = no change within 7 h after addition, + increase in H_2S after addition.

Final Conc. (mM)	Compound	Effect
20.0	Bicarbonate	0
3.5	Ammonium	0
0.1	Ammonium	0
1.0	Phosphate	0
0.1	Phosphate	0
1.0	Trace metal	0
5.0	Glucose	+
5.0	Glycolate	+
1.0	Alanine	0
3.5	Glutamate	+

Effect of addition on H_2S profiles

As an example of the effect of additions on sulphide (H_2S) concentration in the mat, the influence of glucose addition on the H_2S profiles is shown in Fig. 3. H_2S concentration increased after the addition of glucose. The H_2S front that is the shallowest depth at which H_2S was detectable, moved upwards, but did not, within the duration of the experiment, reach parts of the mat where oxygenic photosynthesis took place. Table 2 shows the effects of the additions of various compounds on H_2S dynamics. The organics glutamate, glycolate and glucose caused an increase in H_2S concentration, but in none of the cases did the H_2S front reach the zone of oxygenic photosynthesis. Increased concentrations of H_2S, therefore, did not inhibit oxygenic photosynthesis and oxygen consumption in the photic zone of the mat.

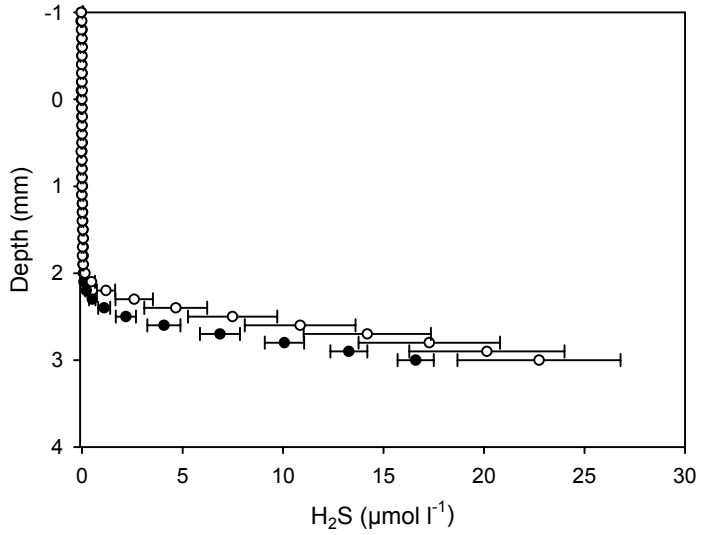

Figure 3: Effect of Glucose addition on H_2S profiles. Black before addition, white after addition.

Discussion

In this study, selected nutrients and carbon compounds were tested for their potential to instantaneously (≤ 6h) stimulate net productivity of the oxygenic microbial community of mature Lake Chiprana microbial mats. We hypothesised that net productivity, i.e. oxygenic net photosynthesis (NP), would increase upon addition of a growth-limiting compound. Unexpectedly, none of the added compounds stimulated NP during the short-term incubation period. In contrast, however, gross photosynthesis and respiration, two processes that underlie net productivity, appeared to be substantially stimulated by certain additions. The respective compounds stimulated both processes by the same molar amount (0.1 mM phosphate stimulated AGP by 3.9×10^{-7} and R by 4.4×10^{-7} mol m^{-2} s^{-1}; alanine + 3.1×10^{-7}/ + 3.6×10^{-7} and glutamate + 5.0×10^{-7}/ + 4.9×10^{-7}), resulting in an virtually unchanged net photosynthesis. These observations are highly interesting as the proportionality of the stimulations indicates that both processes were tightly coupled. Only in the case of inhibition seemed the two processes more loosely coupled. For example, addition of higher concentrations of phosphate (1.0 mM) and the organic compound glycolate resulted in a significant inhibition of gross photosynthesis while respiration apparently remained unchanged, as in these cases measured net photosynthesis rates decreased to the same extent as gross photosynthesis rates.

Stimulation of gross photosynthesis

Gross photosynthesis was only substantially stimulated by phosphate and amino acids (Fig. 2), implying that the process of oxygenic photosynthesis may have been limited by phosphorus and/or amino acids. When biosynthesis is limited due to limited nutrient supply (e.g. N, P), photosynthetic oxygen evolution by PS II is decreased as continuous renewal of the D1 protein is necessary to ensure the functioning of the oxygen evolving complex of PS II. Therefore, increases in photochemical efficiency upon re-supply of a limiting nutrient have been used as a basis for bioassays to identify nutrient limitation of phytoplankton (Beardall et al. 2001). However, as amino acids and phosphate stimulated the process of gross- but not net photosynthesis it is questionable whether these components were also growth-limiting. Documented long-term (days to weeks) addition studies concerning microbial mat communities reported preferential growth of cyanobacteria over diatoms after phosphate addition (Pinckney et al. 1995b; Camacho & de Wit 2003), suggesting that the cyanobacteria

profited from P additions, as they are inferior P-competitors to diatoms (Tilman 1982; Smith 1983).

The observation that amino acids but not inorganic nitrogen stimulated gross photosynthesis may indicate that nitrogen was in fact not limiting growth of the phototrophic community, what is further substantiated by high ammonium concentrations present in the mat pore water. The stimulatory effect of amino acids on gross photosynthesis may instead have been due to the fact, that its uptake and incorporation in structural cell components is energetically more favourable than that of ammonium.

Inhibition of gross photosynthesis

The inhibition of photosynthesis by higher concentrations of phosphate (1 mM) and ammonium (3.5 mM) may have been due to toxic effects. Ammonium becomes deprotonated at high pH and enters cells as uncharged NH_3. As a weak base the flux of NH_3 is directed to the most acidic compartment, e.g. the thylakoid lumen, where it uncouples the H^+ gradient (Belkin & Boussiba 1991; Britto et al. 2001). High phosphate concentrations are known to negatively affect culture growth (Friedlander & Ben-Amotz 1991). High phosphate concentrations have also been suggested to result in iron limitation due to chlorosis by complexation of both compounds (Chalker-Scott, personal communication).

The observed inhibitory effect of glycolate on oxygenic photosynthesis is interesting as glycolate is a known photorespiration product in microbial mats (Bateson & Ward 1988) and may therefore inhibit photosynthesis due to a feedback mechanism. However, the inhibitory effect of glycolate as observed in this study are in contradiction with the observation of Grötzschel et al. (2002) in a different mat system. In that study it was found that photosynthesis and respiration were stimulated by glycolate addition after incubation for 6 days. The observed differences may have been due to differences in community composition or to adaptation of community members to high glycolate concentrations in the latter long term study.

Effect of additions on respiration

Respiration rates were apparently not stimulated by addition of the purely organic components glycolate and glucose but by amino acids, suggesting that this process was nitrogen rather than carbon limited or that a combination of organic carbon and nitrogen is needed. The observation that a substantial increase in gross photosynthesis was in all cases accompanied by a commensurate increase in respiration, while a

decrease in the former was apparently not always accompanied by a decrease of the latter, points to a certain coupling between the two processes. The response of respiration to addition of rate limiting compounds is integrated over a diverse community and includes O_2 consumed by aerobic heterotrophs, but also by oxidation of reduced substances produced by anaerobic respiration. However, as respiration rates were not directly measured but instead derived from quantified net- and gross photosynthesis rates, interpretations should be carefully considered.

Effect of additions on carbon partitioning and growth

An increased gross photosynthesis rate that is not accompanied by an increase in net photosynthesis means that the net community productivity remained unchanged. How can this mechanistically be explained in terms of community carbon flow? Net photosynthesis is the amount of carbon fixed by phototrophs that is not respired within the mat. This can either be organic carbon that is fixed in cell biomass (thus supporting growth), intracellular storage compounds or excretion products that are not respired, e.g. a recalcitrant fraction of EPS or DOC that is lost from the mat to the overlying water (Jonkers et al. 2003). While the oxygen microsensor technique allows calculation of CO_2 fixation rates, this technique does not provide information about the repartition of reduced C among structural cell material, storage compounds, EPS and low molecular weight excretion products. We think that addition of growth limiting nutrients may shift this repartition in favour of structural cell material thus allowing growth without a concomitant increase of net productivity. Documented studies have indeed shown that the fraction of carbon that is excreted by phototrophs is high under nutrient limitation and decreases upon relieve of limitations (Myklestad et al. 1989; Staats et al. 2000).

Close coupling between photosynthesis and respiration

The close coupling between photosynthesis and respiration when stimulated by compound addition is highly interesting and may indicate that heterotrophs depend on phototrophs for carbon supply. Assuming that addition of growth-limiting nutrients for oxygenic phototrophs results in increased channeling of fixed C into structural cell material, implies that the sum of storage compounds and excretion products decreases, if net photosynthesis does not increase. An simultaneous increase in community respiration is then only possible if either the absolute amount or the quality (non-recalcitrant or N- or P-containing compounds) of biodegradable excretion products simultaneously increases. Observations of the present study support the latter

possibility as amino acids but not glucose or glycolate apparently stimulated respiration. On the other hand, the tight coupling between oxygenic photosynthesis and aerobic respiration may also be due to the dependance of phototrophs on heterotrophic CO_2 production. However, this was probably not important in the mat, because the supply of inorganic carbon did not enhance gross photosynthesis. Alternatively, heterotrophs stimulate oxygenic photosynthesis by lowering oxygen partial pressure and thereby also reducing the amount of reactive oxygen species. Increased oxygen partial pressure has indeed been found to inhibit gross photosynthesis in mat communities (Garcia-Pichel et al. 1999).

Conclusions

Using microsensors to monitor responses of photosynthesis and respiration to addition of potentially rate-limiting compounds proved a valuable method to look directly at the nutrient status of the dominant microbial mat organisms. We found evidence that in microbial mats of Lake Chiprana respiration and oxygenic photosynthesis are tightly coupled as both were stimulated by the same compounds. The close coupling between photosynthesis and respiration stresses the importance of a method that distinguishes between gross and net photosynthesis in order to be able to interpret results of addition experiments in communities where photosynthesis and respiration rates might be closely coupled.

Acknowledgements

We thank Ines Schröder, Gaby Eickert, Ingrid Dohrmann and Karin Hohmann for microsensor construction. For statistical advice we are grateful to Werner Wosniok (University Bremen).

References

Alcoverro, T., Conte, E., Mazzella, L. (2000) Production of mucilage by the Adriatic epipelic diatom *Cylindrotheca closterium* (Bacillariophyceae) under nutrient limitation. J. Phycol. 36: 1087-1095

Bateson, M. M., Ward, D. M. (1988) Photoexcretion and fate of glycolate in a hot spring cyanobacterial mat. Appl. Environ. Microbiol. 54: 1738-1743

Beardall, J., Young, E., Roberts, S. (2001) Approaches for determining phytoplankton nutrient limitation. Aquat. Sci. 63: 44-69

Belkin, S., Boussiba, S. (1991) Resistance of *Spirulina platensis* to ammonia at high pH values. Plant Cell Physiol. 32: 953-958

Britto, D. T., Siddiqi, M. Y., Glass, A. D. M., Kronzucker, H. J. (2001) Futile transmembrane NH_4^+ cycling: A cellular hypothesis to explain ammonium toxicity in plants. P. Natl. Acad. Sci. USA 98: 4255-4258

Camacho, A., de Wit, R. (2003) Effect of nitrogen and phosphorus additions on a benthic microbial mat from a hypersaline lake. Aquat. Microb. Ecol. 32: 261-273

Canfield, D. E., Des Marais, D. J. (1993) Biogeochemical cycles of carbon, sulfur, and free oxygen in a microbial mat. Geochim. Cosmochim. Acta 57: 3971-3984

Clesceri, L., Greenberg, A., Trusall, R. (1989) Standard methods for the examination of water and wastewater. 17th edition. American Public Health Association, Washington, D.C., 1200 pages

Dubinsky, Z., Berman-Frank, I. (2001) Uncoupling primary production from population growth in photosynthesizing organisms in aquatic ecosystems. Aquat. Sci. 63: 4-17

Elser, J. J., Marzolf, E. R., Goldman, C. R. (1990) Phosphorus and nitrogen limitation of phytoplankton growth in the freshwaters of North America: A review and critique of experimental enrichments. Can. J. Fish. Aquat. Sci. 47: 1468-1477

Friedlander, M., Ben-Amotz, A. (1991) The effect of outdoor culture conditions on growth and epiphytes of *Gracilaria conferta*. Aquat. Bot. 39: 315-333

Garcia-Pichel, F., Kühl, M., Nübel, U., Muyzer, G. (1999) Salinity-dependent limitation of photosynthesis and oxygen exchange in microbial mats. J. Phycol. 35: 227-238

Grötzschel, S., Abed, R. M. M., de Beer, D. (2002) Metabolic shifts in hypersaline microbial mats upon addition of organic substrates. Environ. Microbiol. 4: 683-695

Guerrero, R., Mas, J. (1989) Multilayered microbial communities in aquatic ecosystems: Growth and loss factors. In: Cohen, Y., Rosenberg, E. (eds.) Microbial mats - Physiological ecology of benthic microbial communities. American Society for Microbiology, Washington DC, pp 37-51

Jonkers, H. M., Ludwig, R., de Wit, R., Pringault, O., Muyzer, G. Niemann, H., Finke, N., de Beer, D. (2003) Structural and functional analysis of a microbial mat ecosystem from a unique permanent hypersaline inland lake: 'La Salada de Chiprana' (NE Spain). FEMS Microbiol. Ecol. 44: 175-189

Krumbein, W. E., Cohen, Y., Shilo, M. (1977) Solar Lake (Sinai). 4. Stromatolitic cyanobacterial mats. Limnol. Oceanogr. 22: 635-656

Kühl, M., Glud, R. N., Ploug, H., Ramsing, N. B. (1996) Microenvironmental control of photosynthesis and photosynthesis-coupled respiration in an epilithic cyanobacterial biofilm. J. Phycol. 32: 799-812

Kühl, M., Steuckart, C., Eickert, G., Jeroschewski, P. (1998) A H_2S microsensor for profiling biofilms and sediments: Application in an acidic lake sediment. Aquat. Microb. Ecol. 15: 201-209

Myklestad, S., Holm-Hansen, O., Varum, K. M., Volcani, B. E. (1989) Rate of release of extracellular aminoacids and carbohydrates from the marine diatom *Chaetoceros affinis*. J. Plankton Res. 11: 763-773

Nold, S. C., Ward, D. M. (1996) Photosynthate partitioning and fermentation in hot spring microbial mat communities. Appl. Environ. Microbiol. 62: 4598-4607

Paerl, H. W., Joye, S. B., Fitzpatrick, M. (1993) Evaluation of nutrient limitation of CO_2 and N_2 fixation in marine microbial mats. Mar. Ecol. Prog. Ser. 101: 297-306

Pinckney, J., Paerl, H. W., Bebout, B. M. (1995a) Salinity control of benthic microbial mat community production in a Bahamian hypersaline lagoon. J. Exp. Mar. Biol. Ecol. 187: 223-237

Pinckney, J., Paerl, H. W., Fitzpatrick, M. (1995b) Impacts of seasonality and nutrients on microbial mat community structure and function. Mar. Ecol. Prog. Ser. 123: 207-216

Pinckney, J., Paerl, H. W., Reid, R. P., Bebout, B. M. (1995c) Ecophysiology of stromatolitic microbial mats, Stocking-Island, Exuma Cays, Bahamas. Microbial Ecol. 29: 19-37

Pinckney, J. L., Paerl, H. W. (1997) Anoxygenic photosynthesis and nitrogen fixation by a microbial mat community in a Bahamian hypersaline lagoon. Appl. Environ. Microbiol. 63: 420-426

Revsbech, N. P. (1989) An oxygen microsensor with a guard cathode. Limnol. Oceanogr. 34: 474-478

Revsbech, N. P., Jørgensen, B. B. (1983) Photosynthesis of benthic microflora measured with high spatial resolution by the oxygen microprofile method: Capabilities and limitations of the method. Limnol. Oceanogr. 28: 749-756

Smith, V. H. (1983) Low nitrogen to phosphorus ratios favor dominance by blue-green algae in lake phytoplankton. Science 221: 669-671

Staats, N., Stal, L. J., Mur, L. R. (2000) Exopolysaccharide production by the epipelic diatom *Cylindrotheca closterium*: effects of nutrient conditions. J. Exp. Mar. Biol. Ecol. 249: 13-27

Stal, L. J. (2000) Cyanobacterial mats and stromatolites. In: Whitton, B., Potts, M. (eds.) The ecology of cyanobacteria. Kluwer Academic, pp 61-120

Tilman, D. (1982) Resource competition and community structure. Princeton University Press, Princeton, New Jersey

Van Gemerden, H. (1993) Microbial mats: A joint venture. Mar. Geol. 113: 3-25

Widdel, F., Bak, F. (1992) Gram-negative mesophilic sulfate-reducing bacteria. In: Balows, A., Trüper, H. G., Dworkin, M. W., Harder, W., Schleifer, K.-H. (eds.) The Prokaryotes. 2nd edition. Springer, New York, pp 3353-3378

Chapter 4

Reduced gas diffusivity and solubility limit metabolic rates in benthic phototrophs at high salinities

4

Reduced gas diffusivity and solubility limit metabolic rates in benthic phototrophs at high salinities

Rebecca Ludwig, Ferran Garcia-Pichel

Abstract

Hypersaline cyanobacterial mats have been shown to suffer from a salt-dependent limitation of photosynthesis and respiration rates. This effect can be caused directly by elevated salt concentrations or indirectly by parameters changing together with salinity (e.g. oxygen solubility and diffusivity). We measured biomass specific respiration rates and photosynthesis rates at different salinities in the halotolerant cyanobacterium PCC 7418, a strain belonging to the Halothece cluster and growing at a wide range of salinities. Rates of photosynthesis and respiration in suspension cultures (a model for planktonic growth conditions) were compared to agar-immobilised cultures (a model for benthic growth conditions). All cultures were pre-adapted to the test salinity and photophysiologically comparable. Photosynthesis and respiration of benthic cultures decreased with increasing salinity, thus reproducing the results of field studies of mixed communities. In contrast, photosynthesis and respiration of suspension cultures remained constant within a wide salinity range (70-200‰) demonstrating that a high salt concentration *per se* was not the limiting factor. The cause must have been a factor that co-varies with salinity only under benthic conditions. We provide evidence that reduced photosynthesis in benthic systems at high salinity was caused by elevated oxygen partial pressure (pO_2). Salt-dependent limitation of respiration also took place in benthic cultures and not in suspension culture, but diffusion limitation could not account for this effect.

Introduction

The phenomenon of salinity dependent decrease of photosynthesis and respiration rates in microbial mats was described by Des Marais et al. (1989) and Pinckney et al. (1995). However, the cause of this limitation was not identified. Garcia-Pichel et al. (1999) provided evidence that this limitation was not due to increased salt concentration *per se* but caused by an indirect effect of salinity. This indirect effect could be due to a decrease in diffusional gas exchange, since elevated salt concentrations decrease the diffusion coefficient (D) of gases. Another factor indirectly influenced by salinity is oxygen solubility, which is reduced at high salinities. At constant molar concentrations a lower solubility causes a higher partial pressure, thereby increasing oxidative stress. Photosynthesis leads to a significant accumulation of oxygen in microbial mats, because the oxygen produced must be transported out of the oxygen producing layers by diffusion. Such an accumulation does not occur around cells in suspension, as the thickness of the diffusive boundary layer around individual cells is only in the order of the cell diameter. Thus, for all practicality, the concentration at the cell surface is the same as in the water column. Reduced diffusivity should therefore affect photosynthesis in benthic systems, but not the same cells in suspension. The effect of reduced gas solubility will also not affect planktonic cells, as the oxygen partial pressure in the water column is in equilibrium with the atmosphere and thus unaffected by salinity. To elucidate whether the decrease of photosynthetic and respiratory rates with increasing salinity is related to decreased gas diffusivity and solubility, we compared photosynthesis and respiration of planktonic and benthic model systems over a range of salinities. If high salt concentration *per se* decreases photosynthesis and respiration by imposing a metabolic burden, both planktonic and benthic model systems should be affected. If high salinity has an indirect effect i.e. via reduced diffusion or gas solubility it should only affect benthic cells that depend on transport from the overlying water by molecular diffusion.

Material and Methods

Liquid culturing of model organism

The hypersaline unicellular cyanobacterial strain PCC 7418 (catalogued presently under *Cyanothece* sp., previously under *Aphanothece halophytica*) belonging to the Halothece cluster of extremely halotolerant cyanobacteria, was used as model organism. Unialgal cultures were grown at 28°C in 50 ml tissue-culture or Fernbach flasks. ½ PES medium (Garcia-Pichel et al. 1998) was adjusted to a range of salinities (40; 70; 100; 120; 160 and 200‰ salt) by addition of Sea salt (Meersalz Professional, hw, Germany). ½ PES medium contains 15 times the amount of N as artificial hw seawater and 31 times more P, ensuring that cultures at all salinities had adequate levels of nutrients. Cultures were grown in a 12h light/12h dark cycle at a light intensity of 32 µmol photons m^{-2} s^{-1}, scalar irradiance (Biospherical Instruments, QSL-100). Salinity was controlled regularly using an Atago S-28E refractometer and sterile MilliQ water was added to account for evaporative losses. Only cultures in exponential phase were used for experiments.

DIC and oxygen concentration in ½ PES medium at air saturation

Samples for both DIC (dissolved inorganic carbon) and oxygen measurements were taken from medium in equilibrium with air at 25°C and 35°C respectively. DIC was measured coulometrically (UIC Inc., ASTM D-513 Method G, coulometric titration method). Winkler titration was used to determine oxygen concentration (Grasshoff et al. 1983).

Cellular photopigment composition

To check whether cells were photobiologically comparable over the salinity range, carotenoids and chlorophyll *a* amounts of cultures were measured by HPLC. Cells of suspension cultures were disrupted by freezing in liquid N_2 and use of a tissue homogenizer. Carotenoids and chlorophyll *a* were extracted in acetone, separated by HPLC and detected with a PDA (photodiode array) detector after Garcia-Pichel et al. (1998). Retention time and spectrum analysis were used to identify chlorophyll *a* and the three most abundant carotenoids. Amounts were calculated as peak area relative to chlorophyll *a* peak area.

Preparation of benthic cultures

Benthic conditions were simulated by concentrating suspension cultures by centrifugation at 2100 g for 15 minutes and then immobilising them in an agarose layer. The agarose-immobilised culture (hereafter called benthic culture) contained ~15 more biomass than planktonic cultures. They were prepared in a Petri dish under sterile conditions as follows. Dishes were filled with a layer of sterile 1% agarose in ½ PES medium. This layer was covered by a sterile vinyliden polymer film (cling film). The agarose layer protected measuring electrodes from breakage and the vinyliden film strongly reduced gas exchange between the sterile agarose layer and the culture poured above it. A concentrated cell suspension was mixed in a ratio of 1:2 (vol/vol) with a 45° C, sterile, 0.5% (w/v) agarose solution in medium and over-lain on the vinyliden to a thickness of 2 mm. The culture used had been preincubated at 38°C for an hour to allow acclimation. Benthic cultures were then transferred into a larger dish, which contained liquid medium. They were incubated for a minimum of three days under sterile conditions to allow acclimation of cultures to the new conditions. Incubation conditions regarding salinity, light and temperature were the same as used for liquid culturing.

Measurement of oxygen partial pressure

Oxygen partial pressure (pO_2) was measured with Clark-type microelectrodes (Revsbech 1989). Tip diameter was <10µm, maximal 90% response time was below 3 s and stirring sensitivity <2%. A two point calibration was performed between culture-media in equilibrium with air and media in equilibrium with N_2. The measured pO_2 was converted into oxygen concentration using a calibration factor acquired from Winkler titration. Benthic cultures were incubated in a benthic flow chamber (Lorenzen et al. 1995) containing fully aerated medium. Incubation temperature was 28°C ± 1.7°C. The benthic culture was illuminated at two light intensities using a halogen fiber optic illuminator (Schott KL 1500). Scalar irradiance at the benthic culture surface was 60 and 250 µmol photons m^{-2} s^{-1}, respectively. Irradiance in the microbial mat is attenuated to 50% of incident light within the top 0.25 – 1mm (Kühl et al. 1997; Kühl & Fenchel 2000). Consequently, the average irradiance in 2 mm thick cultures was close to 22 and 100 µmol photons m^{-2} s^{-1}. Benthic cultures were allowed to equilibrate after changing of light condition by following transient changes in oxygen flux until a new steady state was reached. A minimum of 4 vertical O_2 profiles at different positions were recorded at each salinity to account for spatial

heterogeneity. Measurements were completed within 24 hours to reduce possible external contamination.

Oxygen measurements in suspension cultures were carried out in a 50 ml round-bottom flask, sealed by a silicon rubber stopper through which an oxygen microelectrode was inserted. Air bubbles were excluded and the set-up kept under stirring and at 28°C. The concentration change over time was measured at 25 or 50 µmol photons m^{-2} s^{-1} (scalar irradiance) and in darkness at pO_2 not deviating more than 25% from air saturation.

Creation of elevated oxygen partial pressure in suspension culture

Suspension cultures were illuminated for a prolonged time in order to create elevated oxygen partial pressure in planktonic cultures. Photosynthesis rate was monitored as oxygen increase over time. If photosynthesis decreased and eventually halted, bicarbonate was added to a final concentration of 24 mmol l^{-1} in order to relieve a putative DIC limitation. This procedure was repeated until the incident halt of photosynthesis could not be relieved by bicarbonate addition.

Biomass determination

After experiments, samples for biomass analysis were taken (chlorophyll *a* and cell counts). For chlorophyll *a* content, the suspension culture was harvested on a filter (Millipore, Isopore Membrane Filter 1.2µm RTTP) and chlorophyll was extracted with 100% acetone for 1 hour at 4°C in the dark. The suspension was centrifuged at 9000 g for 5 minutes and the absorption of the supernatant at 663 nm was measured. Chlorophyll *a* concentrations were calculated using an absorption coefficient of 92 l g^{-1} (Vernon 1960). The benthic culture was frozen in liquid N_2 and crushed. Acetone was added to a final concentration of approximately 90%. Further proceedings were the same as described above. For cell counts of suspension culture, three replicate samples were fixed with glutaraldehyde (final concentration 1-2%) and were counted using a counting chamber (Neubauer Improved, Neubauer, Germany). In the case of benthic cultures, cell numbers were counted with the help of an inverse microscope equipped with an ocular grid. Only cells in a focal plane were counted. Depth of focus was interpolated, using values given by James (1976).

Rates of net photosynthesis and respiration in benthic cultures

At steady state, the oxygen flux (J) through the diffusive boundary layer (DBL) represents area-based net production or consumption of benthic cultures. Areal respiration (J_{dark}) was thus calculated from the concentration gradient in the DBL in the darkness using Fick's first law and a salinity corrected diffusion coefficient (Li & Gregory 1974). Net photosynthesis, ($J_{light,}$) was calculated from the gradient in the light. Biomass specific rates (P' and R') were calculated by dividing the areal rates with the areal cell density or chlorophyll *a* content (see Table 1 for overview of parameters).

Where the profile quality allowed, the distribution of volumetric oxygen production rate in the benthic cultures were modelled from the profile curvature using the model of Berg et al. (1998). The profiles were modelled from the mat surface and to the point where the gradient was zero. Boundary conditions in the modelling were zero flux in the bottom of the modelled depth and a forced concentration in this point. No constrains was placed on the calculated rates, and up to 7 distinct zones were allowed. The model routine suggests number of distinct zones in the end result based on F-statistics, and this recommendation was followed (P=0.02). The model is described in detail by Berg et al. (1998).

Table 1 Parameters measured and derived.

Parameter	Definition	Applies to
R	O_2 consumption in the dark	Planktonic cultures
P	O_2 production in the light	Planktonic cultures
J_{light}	O_2 Flux of oxygen between mat and medium in the light	Benthic cultures
J_{dark}	O_2 Flux of oxygen between mat and medium in the dark	Benthic cultures
R'	R or J_{dark} normalised to biomass	Both cultures
P'	P or J_{light} normalised to biomass	Both cultures
R'_{cell}	R or J_{dark} normalised to cell density	Both cultures
R'_{chla}	R or J_{dark} normalised to amount of chlorophyll *a*	Both cultures
P'_{cell}	P or J_{light} normalised to cell density	Both cultures
P'_{chla}	P or J_{light} normalised to amount of chlorophyll *a*	Both cultures

Rates of net photosynthesis in suspension cultures

Respiration is the only oxygen consuming process in suspension cultures in the dark. Thus the oxygen decrease per unit time (dC/dt) directly equals the volumetric respiration rate of the culture. Likewise, net photosynthesis equals (dC/dt) in illuminated cultures. Measurements of volumetric rates in suspension cultures were started at equilibrium with the atmosphere and the maximum deviation from this saturation was 25%. Biomass specific rates were calculated as described for benthic conditions.

Because P' and R' values are a ratio between two measured variables, both coefficients of variation were calculated, added, and the sum multiplied by the mean of the ratio, to calculate the standard deviation for each estimate.

Results

Characteristics of growth media as a function of salinity

Salinity dependent oxygen and DIC concentrations of aerated liquid medium measured at 25°C and 35°C are shown in Figure 1. At both temperatures there was a linear decrease in oxygen solubility with increasing salinity, regression coefficients were high: (25°C: $r^2 = 0.991$; n = 6 and 35°C: $r^2 = 0.994$; n =6). Based on these data a decrease in oxygen solubility of 53% between 70‰ and 160‰ salinity at 28°C (the temperature used for experiments) was calculated.

In contrast, DIC concentration (Fig. 1) showed no clear trend with salinity. The concentration varied between 300 µmol l^{-1} and 800 µmol l^{-1}, being much lower than in typical seawater or marine brines (Des Marais et al. 1989).

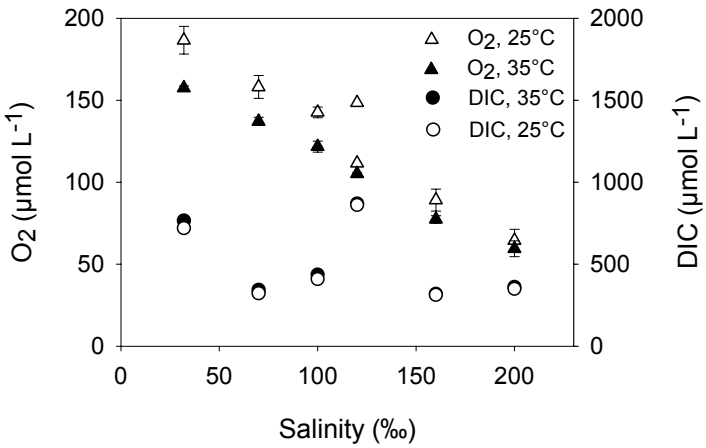

Figure 1 DIC and oxygen concentration at 25°C and 35°C in ½ PES medium in equilibrium with air as function of salinity. Bars indicate +/- SD of three oxygen concentration measurements at 120‰ only two measurements were performed, both shown).

Influence of salinity on cellular pigment content

The cellular chlorophyll *a* content at different salinities and incubation conditions measured after completion of each experiment is shown in Table 2. Chlorophyll *a* content in suspension cultures varied from 0.16 to 0.3 pg Chl*a* $cell^{-1}$ and between 0.19 and 0.24 pg Chl*a* $cell^{-1}$ in benthic cultures. Cell chlorophyll *a* content did not change significantly with salinity. Suspended and benthic cultures were thus photobiologically comparable based on chlorophyll *a* content.

Table 2 Mean Chlorophyll *a* content of PCC 7418 cells grown at different growth conditions. n.a. not analysed.

Growth condition	Salinity (‰)	Chl*a* content (pg Chl*a* cell^{-1})	SD
suspension			
	70	0.20	0.07
	100	0.17	0.04
	120	0.16	0.07
	200	0.30	n.a.
benthic			
	40	0.24	0.04
	70	0.22	0.15
	100	0.21	0.05
	120	0.19	0.05
	160	0.22	n.a.

Table 3 shows carotenoid content relative to chlorophyll *a* of cells grown in liquid culture. A measurable influence of salinity on the photophysiological status of the cells (i.e. chlorophyll *a* and pigments) growing exponentially between 70‰ and 160‰ of salt was not evident, in contrast to reports in other species López-Cortés & Tovar 1992). The only exception were cells grown at 40‰ salt, where myxoxanthophylls were more abundant relative to chlorophyll *a* compared to cells grown at higher salinity. This is typically considered an indicator of physiological stress (Oren et al. 1995; Ehling-Schulz et al. 1997). Indeed 40‰ is close to the minimum salt requirement for growth in this strain, and growth rate is severely reduced (Garcia-Pichel et al. 1998). Evidence then suggests that cells grown at 40‰ salinity might experience stress due to low ionic strength. Data measured in cultures grown at 40‰ of salt were therefore not included in this data set.

Table 3 Cellular content of the three most abundant carotenoids relative to chlorophyll *a* (%) in cells of PCC 7418 grown in suspension culture.

Salinity (‰)	Myxoxanthophylls	Echinenone	ß-Carotene
40	0.444	0.436	0.558
70	0.087	0.235	0.296
100	0.206	0.251	0.267
120	0.055	0.164	0.127
160	0.111	0.385	0.370

Effect of salinity on average biomass specific photosynthesis and respiration rates in benthic cultures

Figure 2 presents biomass specific rates, (P' and R') of benthic cultures over a range of salinities, measured at two light intensities. P' was maximal at 70‰ salinity and decreased constantly at higher salinities. As the full extent of salt-dependent limitation is best gauged by consideration of cultures that were not light limited (250 µmol m^{-2} s^{-1}), only the measurements at 250 µmol m^{-2} s^{-1} were used to analyse the relationship between P' and salinity. Figure 2 B shows that P'_{cell} at 250 µmol m^{-2} s^{-1} dropped from 44 fmol $h^{-1}cell^{-1}$ at 70‰ of salt to 14 fmol h^{-1} $cell^{-1}$at 160‰ of salt, a reduction of 68%. When looking at respiration, R'_{cell} decreased from -16 to -4 fmol h^{-1} $cell^{-1}$ within the same salinity range, a decrease of 75%.

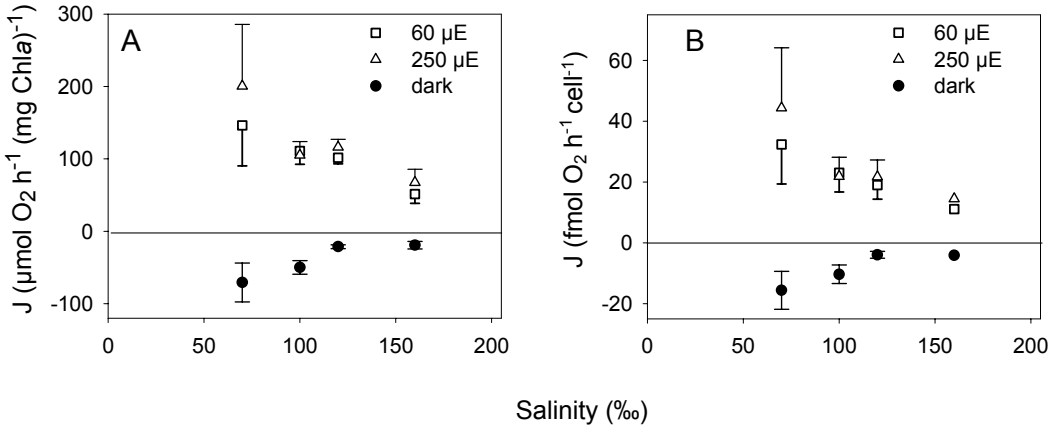

Figure 2 P' (positive J values) and R' (negative J values) of benthic cultures as a function of salinity. P' measured at two different light intensities (60 and 250 µmol m^{-2} s^{-1}) and R' measured in the dark. Bar indicates +/-SD. **A**: R'_{chla} and P'_{chla}. **B**: P'_{cell} and R'_{cell}.

Distribution of oxygen and photosynthesis in benthic cultures

Figure 3 shows examples of oxygen profiles at 70‰ and at 160‰. The vertical lines in the panels for 70‰ in light show the vertical distribution of oxygen production within the mat. The cultures prepared at 100‰ and 120‰ were less dense than the 70‰ and at 160‰ cultures, but still build up a pO_2 to around 300% atm pressure. Curvature throughout those profiles indicated oxygen production throughout but the low curvature did not allow rigid modelling of differences in volumetric rates.

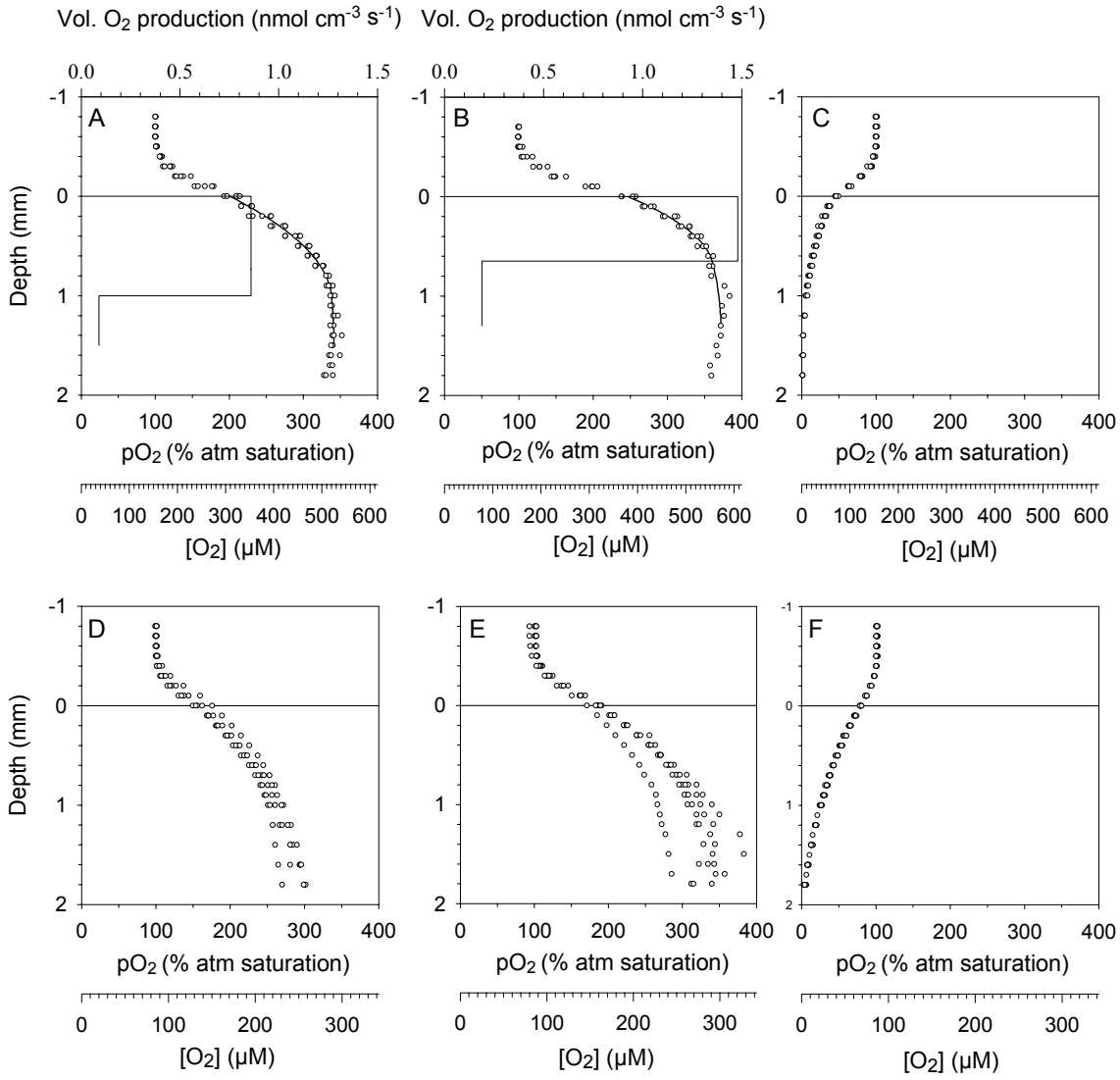

Figure 3 Oxygen profiles (open circles) of benthic cultures of PCC 7418 grown at various salinities (**A – C**: 70‰ , **D – F**: 160‰ salinity) and measured at the following light intensities:
A, D: 60µmol m^{-2} s^{-1}; **B, E**: 250 µmol m^{-2} s^{-1}; **C, F**: dark. The curved lines represent modelled oxygen concentration and the step functions modelled volumetric production rates.

Effect of salinity on biomass specific photosynthesis and respiration in suspension culture

P' and R' of suspension cultures were measured at 25 and 50 µmol photons m^{-2} s^{-1} (Fig. 4). Over the complete salinity range in which the cultures grow well, increasing salt concentration show little or no decrease of photosynthesis and respiration of suspension cultures.

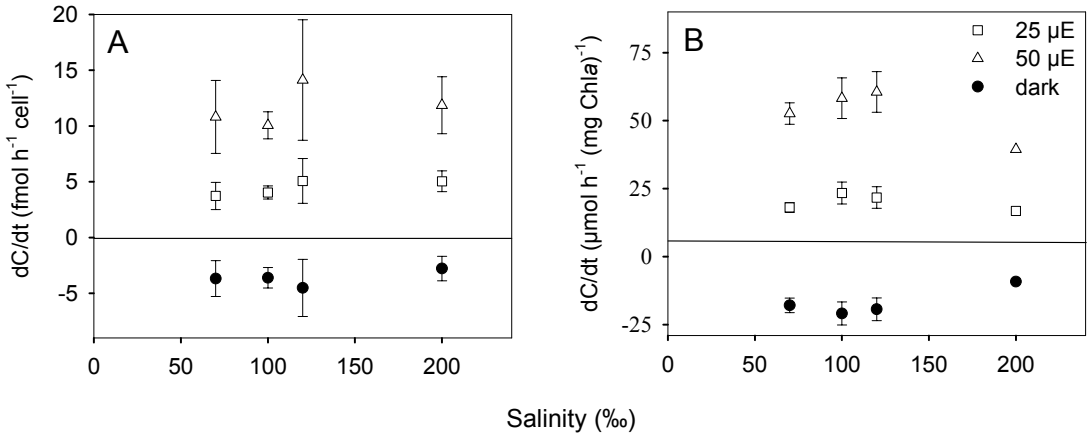

Figure 4 R' and P' in suspension cultures as a function of salinity. P' was measured at 25 and 50 µmol m^{-2} s^{-1}, respectively. R' in the dark. Bar indicates +/-SD. **A**: P'_{cell} and R'_{cell}. **B**: $R'_{chl\,a}$ and $P'_{chl\,a}$.

Effect of elevated pO_2 on photosynthesis in suspension cultures

When exposed to continuous light, oxygen concentration in suspension cultures increased constantly, indicating a constant rate of net photosynthesis. After a doubling in oxygen concentration, the rate decreased due to depletion of bicarbonate. Upon addition of bicarbonate to a final concentration of 0.24 mmol l^{-1}, photosynthesis was resumed at the same rate as before. This procedure was repeated, until addition of DIC could no longer induce photosynthesis. The stop of photosynthesis happened at different molar oxygen concentration (depending on salinity), but invariably at a pO_2 between 375% and 392% atmospheric saturation (Table 4).

Table 4 Minimal pO_2 (% air saturation) causing a total inhibition of O_2 evolution, that could not be relieved on addition of bicarbonate.

Salinity (‰)	maximal pO_2 (% air saturation)
70	375
120	392
160	387

Discussion

When comparing the influence of salt on photosynthesis and respiration it is evident that benthic cultures suffer from a salinity dependent limitation, whereas in planktonic cultures no such effect is traceable over the complete salinity range in which the cultures grow well. This clearly excludes that high salt concentration limits photosynthesis and respiration directly by putting a strain on metabolism or by containing toxic ions. The salinity dependent decrease of photosynthesis and respiration under benthic conditions must therefore be caused by a factor that co-varies with salinity and only comes in effect under benthic conditions.

Cause of salinity effect on photosynthesis

Steady state pO_2 profiles in dense benthic cultures reached values of close to 400% atmospheric saturation regardless of salinity (Fig. 3). This is the same pO_2 where suspension cultures stopped net photosynthesis when pO_2 was experimentally increased, indicating that the controlling factor might be elevation of pO_2 around cells under benthic growth conditions. The inhibitory effect of such high pO_2 is indeed suggested by the modelled volumetric production rates (Fig. 3). The best fit to the measured concentrations divide the cultures into two strata: One stratum with a high volumetric oxygen production rate from the mat surface down to the layer where a pO_2 of 340 - 360% atm saturation was reached. The second stratum with a much lower oxygen production rate was located below this depth. The pO_2 at which the modelled rates decrease agrees with the maximal pO_2 that sustained photosynthesis in suspension cultures. Note that a change in light intensity from 60 to 250 µmol photons m^{-2} s^{-1} increased the oxygen production rate in the upper stratum. The increased production caused pO_2 to build up faster with depth, so that the inhibition of photosynthesis set in closer to the mat surface but at a comparable pO_2. The high oxygen production rates measured at 70‰ could potentially also induce a strong pH increase, which might inhibit oxygen production. But this effect should not apply to high salinity cultures, where photosynthesis rates are low. Therefore an effect of high pH fails to explain the decreased rates at higher salinity (Fig. 3, lower panels).

At higher salinities the pO_2 maximum of 400% atmospheric saturation is related to a smaller increase in molar oxygen concentrations due to the reduced solubility (Fig 3., lower axis). Thus steady state profiles at high salinity exhibit a smaller molar concentration gradient between the oxygen source in the artificial mat and the sink in

the mixed water column. The steady state oxygen flux (which represents NP) is therefore lower at high salinity. The flux is further attenuated by the decrease in oxygen diffusivity with increasing salinity. An increase in salinity from 70‰ to 160‰ reduces the diffusivity of oxygen in seawater by 15% (Li & Gregory 1974), and the solubility by 53% (Fig. 1). Together, the two effects can account for the 68% decrease in benthic photosynthesis.

A mechanistic explanation for the inhibitory effect of high pO_2 could be sought in thermodynamics. The reaction equation for the photolysis of water:

$$2\ H_2O \rightarrow 2\ H_2 + O_2$$

predicts that ΔG would increase with higher pO_2 thus perhaps limiting photosynthesis. However, increasing pO_2 from 0.21 to 0.84 atm, ΔG changes by less then 1%. Thus we can exclude that the effect of high partial pressure is only of thermodynamic nature. More plausible explanations can be found in effects of high pO_2 on of the photosynthetic process (He & Harder 2002). Torzillo et al. (1998) observed that cultures of *Dunaliella* exposed to high pO_2 had lower photochemical yields of PS II in the light relative to cultures grown at moderate oxygen concentration. A similar effect was observed in *Spirulina* cultures by Vonshak (1988) which reported a strong decrease in photon yield upon exposure to high pO_2. Processes which are known to be enhanced at high pO_2 include the Mehler reaction and oxygenase activity of RuBisCO (photorespiration). Both lead to reduced oxygen evolution. Changes in photosynthesis rate which take place during adaptation to changed salinity, cannot account for the phenomena observed in our study as all cultures have been grown at the respective salinity for several generations.

Cause of salinity effects on respiration

Our results demonstrate that salt-dependent limitation of respiration occurs only under benthic conditions. This could potentially be explained by restricted oxygen supply (Garcia-Pichel et al. 1999) due to lower molar oxygen concentration in the water column at saturation and due to reduced diffusivity. However, dark incubated benthic cultures did not get anoxic, except cultures at the lowest salinity (70‰). This anoxia was therefore the effect of a high respiration rate and not the cause for a low rate. Natural mats with large number of heterotrophic bacteria have high respiration rates and are probably restricted by oxygen availability (Garcia-Pichel et al. 1999). But our results point to an additional factor that comes into play when respiration is not limited by oxygen availability.

It should be noted that photosynthesis and respiration decreased to the same extent, which indicates a connection of limitation of respiration to the limitation of photosynthesis. Respiration may in fact have been limited by insufficient supply of photosynthate due photosynthesis limitation. An alternative explanation could be damage to proteins of the respiratory electron transport chain due high oxygen partial pressure, which would explain that both photosynthesis and respiration are limited to the same extent since both respiratory and photosynthetic membrane electron transport share components in cyanobacteria (Scherer et al. 1988).

Comparison to field studies

In benthic cultures, photosynthetic activity in combination with restriction of transport led to an oxygen accumulation of up to 4-times air saturation, a value typical for natural systems. The extent of the salinity dependent limitation of photosynthesis in our model system was identical to the limitation found in a natural system in Baja California. There, photosynthesis decreased exponentially by 70% between 70 and 160‰ of salt, in our model system photosynthesis in the same salinity range decreased by 68%. Thus, we were able to reproduce the phenomenon of salinity dependent decrease of photosynthesis with a model system. Salinity dependant limitation of respiration was also comparable between natural and model systems. Between 70‰ and 160‰ of salt respiration decreased by 75% in the model system and 85% in the natural environment. The benthic model systems we used in order to work under controlled conditions in the laboratory proved to perform in key processes like the natural counterparts.

Conclusions

In conclusion, we presented strong evidence that the salt dependent limitation of photosynthesis and respiration observed in the field is caused indirectly by lowered oxygen solubility and diffusivity. Oxygen concentration under benthic conditions builds up until a pO_2 close to 400% atmospheric saturation regardless of salinity. At high salinity this partial pressure is related to a smaller concentration gradient between the oxygen producing layer and the overlying water, because 400% saturation is reached at a lower molar concentration then at low salinity. As the diffusion coefficient is also reduced, both terms of Fick´s first law are affected, leading to a lower steady state flux at high salinities. This implies that a salinity dependant reduction of photosynthesis and respiration is a general feature of hypersaline mats.

Acknowledgements

We thank Anja Eggers, Gaby Eickert and Vera Hübner for construction of the microelectrodes. Nyree West and Hans Røy for helpful discussions of the manuscript.

References

Berg, P., Risgaard-Petersen, N., Rysgaard, S. (1998). Interpretation of measured concentration profiles in sediment pore water. Limnol. Oceanogr. 43: 1500-1510

Des Marais, D. J., Cohen, Y., Nguyen, H., Cheatham, M., Munoz, E. (1989) Carbon isotopic trends in the hypersaline ponds and microbial mats at Guerrero Negro, Baja California Sur, Mexico: Implications for Precambrian stromatolites. In: Cohen, Y., Rosenberg, E. (eds) Microbial mats: Physiological ecology of benthic microbial communities. American Society for Microbiology, Washington, D.C., pp 191-203

Ehling-Schulz, M., Bilger, W., Scherer, S. (1997) UV-B-Induced synthesis of photoprotective pigments and extracellular polysaccharides in the terrestrial cyanobacterium *Nostoc commune*. J. Bacteriol. 179: 1940-1945

Garcia-Pichel, F., Kühl, M., Nübel, U., Muyzer, G. (1999) Salinity-dependent limitation of photosynthesis and oxygen exchange in microbial mats. J. Phycol. 35: 227-238

Garcia-Pichel, F., Nübel, U., Muyzer, G. (1998) The phylogeny of unicellular, extremely halotolerant cyanobacteria. Arch. Microbiol. 169: 469-482

Grasshoff, K. (1983) Determination of oxygen. In: Grasshoff, K., Ehrhardt, M., Kremling, K. (eds) Methods of seawater analysis. Verlag Chemie, Weinheim, pp 61-72

He, Y. Y., Hader, D - P. (2002) Reactive oxygen species and UV-B: Effect on cyanobacteria. Photochem. Photobiol. Sci. 1: 729-736

James, J. (1976) Light microscopy techniques in biology and medicine. Martinus Nijhoff, The Hague. 336 pages

Kühl, M., Fenchel, T. (2000) Bio-optical characteristics and the vertical distribution of photosynthetic pigments and photosynthesis in an artificial cyanobacterial mat. Microb. Ecol. 40: 94-103

Kühl, M., Lassen, C., Revsbech, N. P. (1997) A simple light meter for measurements of PAR (400 to 700 nm) with fiber-optic microprobes: application for P vs E_0 (PAR) measurements in a microbial mat. Aquat. Microb. Ecol. 13: 197-207

Li, Y.-H., Gregory, S. (1974) Diffusion of ions in sea water and in deep-sea sediments. Geochim. Cosmochim. Acta 38: 703-714

López-Cortés, A., Tovar, D. (1992) Population changes in cyanobacterial mats and the role of NaCl on ß-carotene production in *Microcoleus* strain SC7B9002-1. Geomicrobial. J. 10: 115-123

Lorenzen, J., Glud, R. N., Revsbech, N. P. (1995) Impact of microsensor-caused changes in diffusive boundary layer thickness on O_2 profiles and photosynthetic rates in benthic communities of microorganisms. Mar. Ecol. Prog. Ser. 119: 237-241

Oren, A., Kühl, M., Karsten, U. (1995) An endoevaporitic microbial mat within a gypsum crust: Zonation of phototrophs, photopigments, and light penetration. Mar. Ecol. Prog. Ser. 128: 151-159

Pinckney, J. L., Paerl, H. W., Bebout, B. M. (1995) Salinity control of benthic microbial mat community production in a Bahamian hypersaline lagoon. J. Exp. Mar. Biol. Ecol. 187: 223-237

Revsbech, N. P. (1989) An oxygen microsensor with a guard cathode. Limnol. Oceanogr. 34: 474-478

Scherer, S., Almon, H., Böger, P. (1988) Interaction of photosynthesis, respiration and nitrogen fixation in cyanobacteria. Photosynth. Res. 15: 95-114

Torzillo, G., Bernardini, P., Masojídek, J. (1998) On-line monitoring of chlorophyll fluorescence to assess the extent of photoinhibition of photosynthesis induced by high oxygen concentration and low temperature and its effect on the productivity of outdoor cultures of *Spirulina platensis* (Cyanobacteria). J. Phycol. 34: 504-510

Vernon, L. P. (1960) Spectrophotometric determination of chlorophylls and phaeophytins in plant extracts. Anal. Chem. 32: 1144-1150

Vonshak, A., Guy, R., Guy, M. (1988). The response of the filamentous cyanobacterium *Spirulina platensis* to salt stress. Arch. Microbiol. 150: 417-420

Chapter 5

Photosynthesis controlled calcification in a hypersaline microbial mat

5

Photosynthesis controlled calcification in a hypersaline microbial mat

Rebecca Ludwig, Fuad A. Al-Horani, Dirk de Beer and Henk M. Jonkers

Abstract

Calcification in microbial mats is thought to be directly influenced by diel changes of biological and physicochemical parameters that alter Ca^{2+} and CO_3^{2-} activities. In this study we investigated the hypothesis that sulphate reduction rather than oxygenic photosynthesis controls calcification in such microbial ecosystems. We present for the first time Ca^{2+} microsensor data of diel pore water concentrations in the photic zone of a calcifying hypersaline microbial mat. Calcium concentration in the photic zone decreased in illuminated but not in dark incubated mats. Incubation experiments with ^{45}Ca radioisotopes performed under light and dark conditions confirmed that calcium binding took place predominantly in the photic zone of the mat during illumination. The decrease in calcium concentration in illuminated mats coincided with increased pH and oxygen concentration. The ion concentration product (ICP) of calcium carbonate, derived from pore water pH, DIC and Ca^{2+} concentration, was higher in light than in dark incubated mats. The high pH during light incubation was shown to be the main factor influencing the ICP by increasing CO_3^{2-} concentration, while diel changes in Ca^{2+} concentration played a subsidiary role. Measurements of light and dark sulphate reduction rates and gross photosynthesis rates revealed that the pH increase in illuminated mats was chiefly caused by photosynthetic activity. We therefore conclude that photosynthesis but not sulphate reduction drives calcification in these hypersaline mats.

Introduction

Microbial mats are laminated benthic structures that are regarded as homologues of stromatolites due to their similar physiognomy (Des Marais 1990; Margulis et al. 1980). The present day distribution of microbial mats by far exceeds that of recent stromatolites. While the former occur world wide in fresh, marine and hypersaline waters (Van Gemerden 1993), the distribution of true microbial stromatolites is confined to a few marine coastal (Reid et al. 2000; Visscher et al. 2000) and freshwater (Laval et al. 2000, Garcia-Pichel et al. 2004) locations. Calcification occurs in all living stromatolites but only in some, mainly hypersaline, microbial mats (Krumbein et al. 1977). Ancient stromatolites were widely distributed in the Precambrian world and became preserved just because they were calcifying. Calcification is the process in which Ca^{2+} and CO_3^{2-} combine to form calcium carbonate. This process is in a first approximation described by the stoichiometric solubility product:

$$K_{sp}^{*} = [Ca^{2+}][CO_3^{2-}]$$

Thus all microbial processes that induce changes in either of the components will influence the saturation state. Increases in the ion concentration product (ICP) of calcium carbonate ($[Ca^{2+}][CO_3^{2-}]$) therefore indicate that calcification is more likely to take place. Calcification in stromatolites or microbial mats has been attributed to either photosynthetic or heterotrophic bacteria. The former group is thought to change the carbonate equilibrium by increasing pH and concomitantly the carbonate concentration during high rates of CO_2 fixation (Arp et al. 2001; Riding 2000). Heterotrophs, and particularly sulphate-reducing bacteria, are thought to increase local calcium concentrations through the mineralization of calcium-binding extracellular polymeric substances (EPS) (Paerl et al. 2001; Visscher et al. 2000). Furthermore sulphate reduction might also increase pH and thereby shift the carbonate equilibrium towards the CO_3^{2-} ion (Visscher et al. 1998). Although both mechanisms may account for calcification in microbial mats and stromatolites, direct evidence for either hypothesis proved difficult to obtain due to the microscale at which these processes occur. Understanding what drives calcification is the first step in determining why only some microbial mats calcify, while other mats in comparable environments do not. Microsensor techniques may overcome methodological restrictions imposed by the small spatial arrangement. In a recent study for example, the calcification mechanism in the calcifying coral *Favia* sp. was elucidated by application of

microsensors (Al-Horani et al. 2003; de Beer et al. 2000). In the present study, dynamics of calcium concentration in a calcifying microbial mat were measured for the first time using calcium specific microsensors. Additionally depth profiles of pH, oxygen and dissolved inorganic carbon concentration (DIC), rates of ^{45}Ca incorporation and sulphate reduction rates were determined. These combined small scale determinations were designed to elucidate processes that increase supersaturation of calcium carbonate, and thus promote calcification in hypersaline microbial mats.

Materials and methods

Microbial mat description

Microbial mat samples were collected in May 2001 from 'La Salada de Chiprana' (Lake Chiprana) located in North-eastern Spain (41°14'N, 0°10'W). The lake has a total surface of 31 ha and lies on the Upper Oligocene – Miocene Caspe Formation that is mainly composed of sand- and silt stones. The average salinity of the lake water is around 78 and the ionic composition is dominated by magnesium-sulphate (SO_4^{2-} 500 mM; Mg^{2+} 320 mM). A detailed description of the water composition and the microbial mat community composition was published previously (Jonkers et al. 2003). The mats, collected from a water depth of approximately 40 cm, were composed of visually distinct horizontal layers that were characterised by various species of diatoms, *Chloroflexus*-like bacteria, cyanobacteria and calcium carbonate precipitates (Fig. 1). Abundant populations of aerobic heterotrophic, purple- and colourless sulphur and sulphate-reducing bacteria were also present (Jonkers et al. 2003). Microbial mat samples were transported by plane to Bremen, Germany, and incubated under natural light conditions in a greenhouse in aquaria filled with water from the sampling site. Microsensor measurements of oxygen and photosynthesis profiles, which were routinely measured during the incubation period, were not different from those measured *in situ* under similar light conditions indicating that physiological processes did not change to a major extend during the laboratory incubations.

Microsensor measurements

Microbial mat cores (∅ 5 cm; 1.5 cm thick) taken from the greenhouse-incubated mats were transferred to the laboratory to a temperature controlled flow-through

chamber. The mat pieces were subsequently incubated in the dark or in the light (500, 1000 µmol photons m^{-2} s^{-1}) using a fibre optic lamp (KL 1500, Schott). Microsensor data collection started after steady state oxygen profiles were obtained. Photosynthesis, oxygen and H_2S profiles were measured with Clark-type amperometric glass microsensors with tip diameters around 5, 10 and 15 µm respectively. Calcium and pH dynamics were measured with ion-specific liquid ion-exchange (LIX) glass microsensors with tip diameters of 10 µm (see Kühl & Revsbech (2001) for detailed description of used microsensors). Gross photosynthesis rates were measured in illuminated mats using the light/dark shift method according to Revsbech & Jørgensen (1983). Profiles of all parameters were measured at least three-fold in mats incubated under the specified light conditions.

Estimation of pore water carbonate concentrations

Carbonate concentrations in microbial mat pore water and overlying water were estimated from measured pH profiles and dissolved inorganic carbon (DIC) concentrations. DIC pore water concentrations were measured in aliquots extracted from distinct 1-mm mat slices using a Shimadzu TOC-5050A Total Organic Carbon Analyser. Hereto, intact mat cores were pre-incubated for 5 hours either in the dark or in the light at 500 µmol photons m^{-2} s^{-1}. Cores were subsequently sliced in one millimetre discrete slices and these were immediately centrifuged mildly (10 min × 6000 *g*) in order to obtain supernatant (pore water) without disrupting the cells. The carbonate ion concentration at distinct depth intervals was estimated from the measured pH profiles and DIC concentrations in dark and light (500 µmol photons m^{-2} s^{-1}) incubated mats according to:

$$[CO_3^{2-}] = \frac{[DIC]}{1 + 10^{(-pH+pk_2)}}$$

with a pK_2 value of 9.2 (Stumm & Morgan 1996). The pore water CO_2 concentrations are insignificant at the prevailing pore water pH values and could thus be ignored.

Sulphate reduction rates in dark and light incubated mats

Sulphate reduction rates (SRR) were measured and calculated using a modification of the whole core tracer incubation method (Jørgensen 1978). Microbial mat cores of ∅ 1.5 cm and ≥ 1cm depth were incubated with 2 ml *in situ* water overlying the core at 20ºC either at 500 µmol photons m^{-2} s^{-1} or in the dark. 50 µl radiotracer ($^{35}SO_4^{2-}$; 0.2 Mbq μl^{-1}, Amersham) was injected vertically per core. Ten injections of 5 µl each

were evenly distributed throughout the core to improve label distribution. The homogeneous distribution of label after 10 min was confirmed by imaging the label distribution in 1 mm slices with a Phosphorimager™ (Molecular Dynamics). After incubation (0, 10, 15, 20, 40 and 60 min) sulphate reduction was terminated by placing the intact core in liquid N_2. Cores were subsequently sliced into 1 mm horizontal slices using a cryomicrotom (microm HM 505E, –30ºC) and fixed in 20% ZnAc. Samples were processed using the cold chromium distillation procedure (Kallmeyer 2004) which is based on the single step chromium reduction method as described by Fossing & Jørgensen (1989). Activity of $^{35}SO_4^{2-}$ and TRIS (Total Reduced Inorganic Sulphur) were determined using a liquid scintillation counter (Packard 2500 TR), scintillation cocktail used was Lumasafe Plus® (Lumac BV, Holland). Sulphate was determined by non-suppressed ion-chromatography and conductivity detection (Waters WISP 712).

^{45}Ca radioisotope incubation of mat samples

One-cm thick cores were sampled from the greenhouse-incubated mats using cut off plastic syringes (∅ 1.6 cm). Filtered (0.2 µm; 4 ml) Chiprana lake water was carefully added on top of the mat samples and radioactive incubations were subsequently performed with these cores. Radioactive calcium (^{45}Ca, Amersham Pharmacia Biotech, UK) was added as tracer (3 KBq ml^{-1}) to the water phase and carefully mixed. The amount of radiotracer added was negligible compared to the calcium concentration of the Chiprana water (17 mM). Three series of incubations were run in parallel, two biotic (light and dark) and one killed control (light plus formaldehyde 4% final concentration) at room temperature. Light incubated mats were illuminated with a Schott KL 1500 fibre optic lamb (500 µmol photons m^{-2} s^{-1}). Each series consisted of three mat cores, which were incubated for distinct periods (1.25, 3.25 and 6.25 hours). Biotic incubations were terminated by addition of formaldehyde (4% final concentration) to the water phase. After 5 min the supernatant water of formaldehyde fixed cores was removed and the intact mat cores were washed three times with 4-ml aliquots of 0.2 µm filtered Chiprana-lake water and subsequently frozen overnight (–20°C). Frozen mat samples were vertically cut in 1 mm thick slices which were additionally washed three times in 0.2 µm filtered Chiprana-lake water before being air dried on microscope slides. The originally compact microbial mat slices expanded to almost the double size during washing and microscopic slide preparation. This expansion was corrected for in all presented data. Samples were covered with scintillation foil and analysed by beta microimaging. Three mat slices

were analysed for each experimental condition. Uptake and spatial distribution of radioactive calcium was quantified using a beta emission microimager (Micro Imager, Biospace Mesures, Paris, France). This type of imager allows the quantification of radioactive slides with a spatial resolution of 10 μm, see Laniece et al. (1998) for a detailed description of the beta microimager working principle. The scan time for each sample was fixed at 30 min. Obtained images were analysed with the Betavision software package provided by the manufacturer. In addition to total counts, counts were also horizontally averaged for each depth interval (100 μm) over a width of 4 mm from the mat surface down to 2 mm depth. Because the scan time was fixed and mat sizes comparable for all samples and experimental conditions, obtained total surface counts and depth integrated counts could be directly compared among all samples.

Results

Location and identification of carbonates

A vertical cut through the studied mat (Fig. 1) shows that carbonate crystals in Lake Chiprana mats form discrete layers of approximately 100 µm thickness or are interspersed as grains of up to 500 µm in diameter. The uppermost continuous layers of deposits are located at 1 mm depth and at the mat surface. Deeper layers are found at 4 and 6 mm, the strata that most likely contain older mats layers. FTIR (Fourier Transform infrared spectroscopy) (Böttcher et al. 1997) revealed that 80% of the carbonate fraction from the photic zone (0-3 mm) consisted of aragonite, with a minor fraction of calcite.

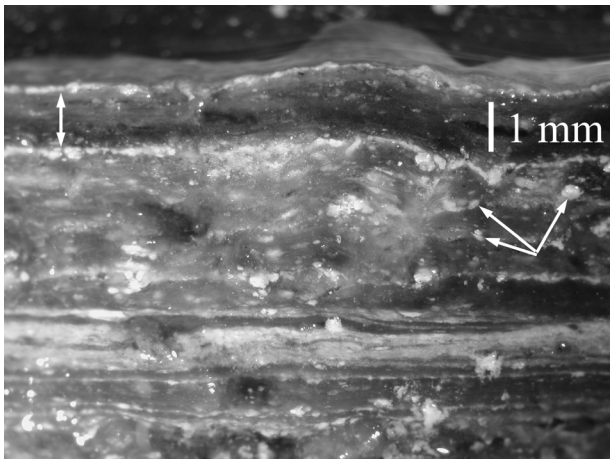

Figure 1 Picture of laminated Lake Chiprana mat with clearly visible calcium carbonate layers (double-headed arrow) and interspersed crystals (single-headed arrows).

Microsensor profiles

Microsensor measurements revealed that the strongest changes between dark and light incubations in pH, Ca^{2+} and O_2 occurred in the top millimetre of the mat (Fig. 2). Photosynthetic oxygen evolution led to a supersaturation of up to five times in the top mm of the mat. The depth of the oxygen peak coincided with the pH maximum of around 9 in the top mm of the mat. Both pH and oxygen concentration increased with increasing light intensity.

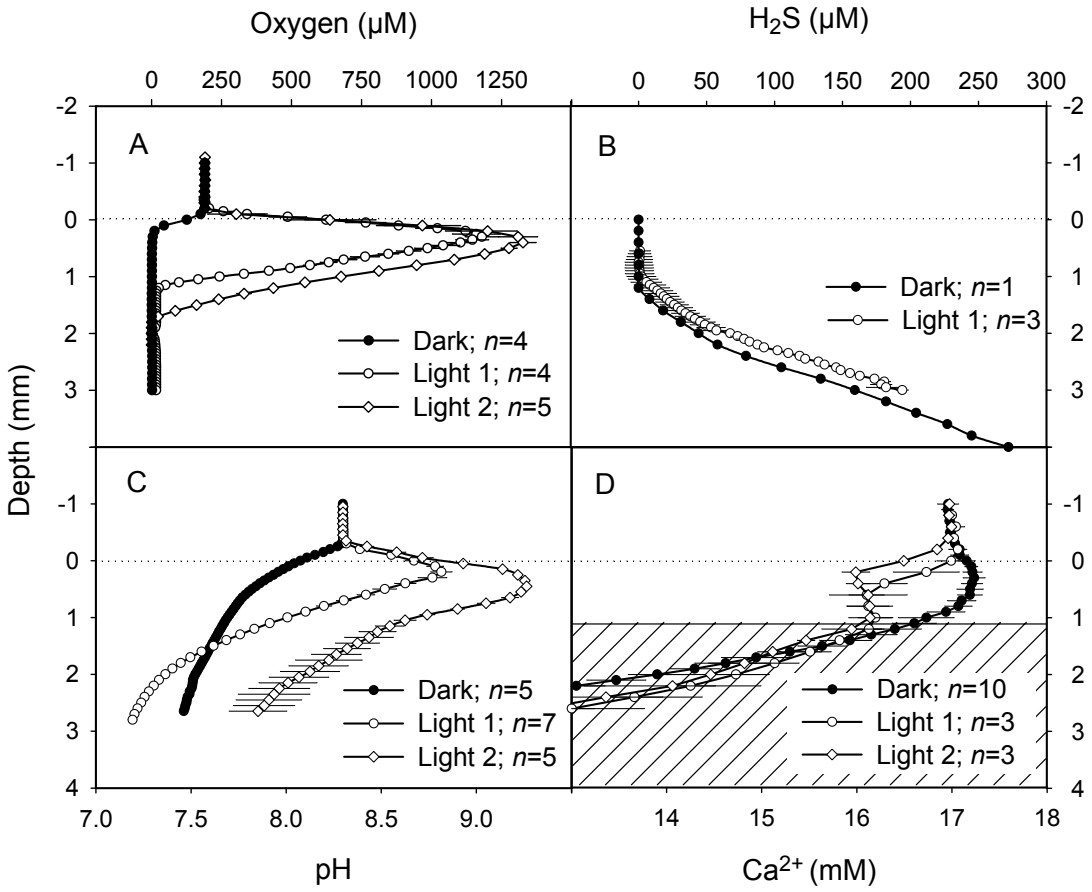

Figure 2 Averaged microprofiles of O_2 (A), H_2S (B) pH (C) and Ca^{2+} (D) ± SD measured in light (o 500µmol photons m^{-2} s^{-1}, ◊ 1000 µmol photons m^{-2} s^{-1}) and dark (•) incubated mats. Number of replicates measured indicated in legend.

The lowest calcium concentrations in the light were found in the same depth as the oxygen and pH peaks. Calcium concentration decreased from 17 mM in the overlying water to approximately 16 mM at 0.4 mm depth with the lowest calcium values measured during incubations at higher light intensities. Unfortunately, measurements of calcium concentration in deeper anoxic layers appeared to be influenced by the presence of sulphide. Tests in calibration solutions confirmed that presence of H_2S induced a strong negative drift of the signal and, therefore, only calcium profiles in sulphide-free mat layers were used for further analysis. Free sulphide could only be detected in deeper layers (> 1mm) of both dark and light incubated mats (Fig. 2B). In the dark, oxygen penetration decreased to 0.3 mm, compared to 1.8 mm at 1000 µmol photons m^{-2} s^{-1} (Fig. 2A). Dark pH profiles revealed a continuous decrease in pH with depth. Calcium concentration in the top millimetre of dark incubated mats showed a slight increase of up to 0.1 mM.

Pore water profiles

Pore water DIC concentration at 500 µE $m^{-2}s^{-1}$ reached the lowest values in the 1 mm horizon (6 mM), compared to 7-8 mM in the overlying water (Fig. 3A). In dark incubated mats DIC concentrations were considerably higher and increased continuously with depth (Fig. 3A). The shape of the calculated CO_3^{2-} concentration profiles (Fig. 3B), however, appeared to be completely different from the DIC profiles.

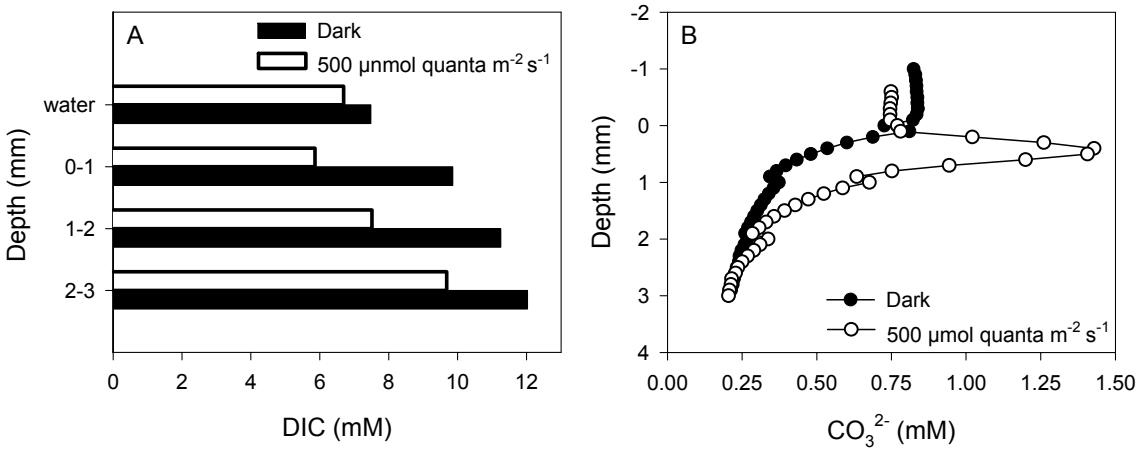

Figure 3 Pore water concentrations of DIC (A) and of CO_3^{2-} (B) measured in dark and light incubated mats.

Maximal CO_3^{2-} concentrations occurred in the top 1 mm layer in light incubated mats, the layer where DIC in the light reached its minimum. The CO_3^{2-} concentration in this layer was twice as high as in any other layer in light or dark incubated mats. In the dark, the highest CO_3^{2-} concentration was found in the overlying water.

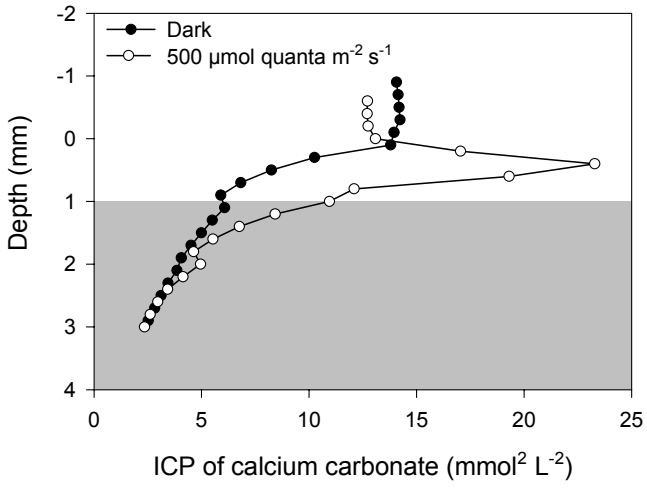

Figure 4 Ion concentration product of calcium carbonate in dark and light incubated mats based on Ca^{2+} microsensor measurements and CO_3^{2-} calculations. Shaded area denotes where Ca^{2+} concentrations where not based on microsensor, but on atomic absorption spectroscopy data.

The profile of the ion concentration product of calcium carbonate ($[Ca^{2+}]*[CO_3^{2-}]$) (Fig. 4) has virtually the same shape as the CO_3^{2-} concentration pore water profile, revealing clearly that the former is chiefly determined by CO_3^{2-} and not by Ca^{2+} concentration. Maximal values were reached at a depth of 0.5 mm in illuminated mats, while in dark incubated mats values were consistently lower than in the overlying water.

Radiotracer incubations

Light incubated mats incorporated significantly more ^{45}Ca radioisotope than dark incubated mats or killed controls (Fig. 5). The spatial distribution of ^{45}Ca showed highest incorporation in the surface layer of light incubated mats (Fig. 5). Dark incubated mats also incorporated radiotracer, but uptake rates were significantly lower than in light incubated mats and comparable to passive adsorption by killed controls.

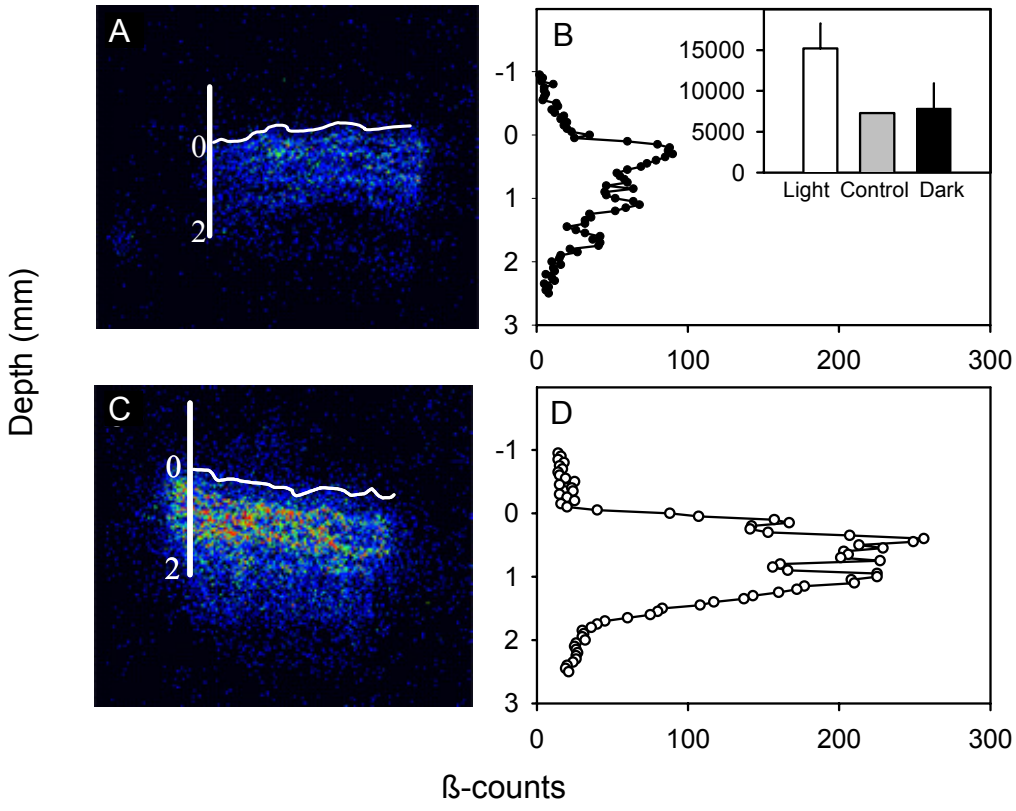

Figure 5 Spatial distribution of incorporated $^{45}Ca^{2+}$ after 6.25 h radiotracer incubation in (A, B) dark and (C, D) light (500 µmol quanta m^{-2} s^{-1}) incubated mats visualized by β-imaging (A, C). For depth profiles of $^{45}Ca^{2+}$ incorporation, signals were averaged over 0.1 × 4 mm (h × w) (B, D). Inset in 5B shows total counts averaged over 2 mm × 4 mm (h × w). The mat expanded during the necessary washing steps and this expansion was corrected for. The white line represents the mat surface.

Sulphate reduction rates

Incubation times of ≤ 1 h were chosen to reduce sulphide reoxidation (Canfield & Des Marais 1991) and indeed incubation times had no discernible effect on sulphate reduction rates (Fig. 6). However, sulphate reduction rates (SRR) showed a high heterogeneity between different cores. This reflects a high spatial variability of SRR, but might also partly be due to the irregular sediment surface, with the consequence that slicing not always followed the layering of the mat. Maximal rates in all replicates, both during light and dark incubation, were around 3 mm depth (Fig. 6).

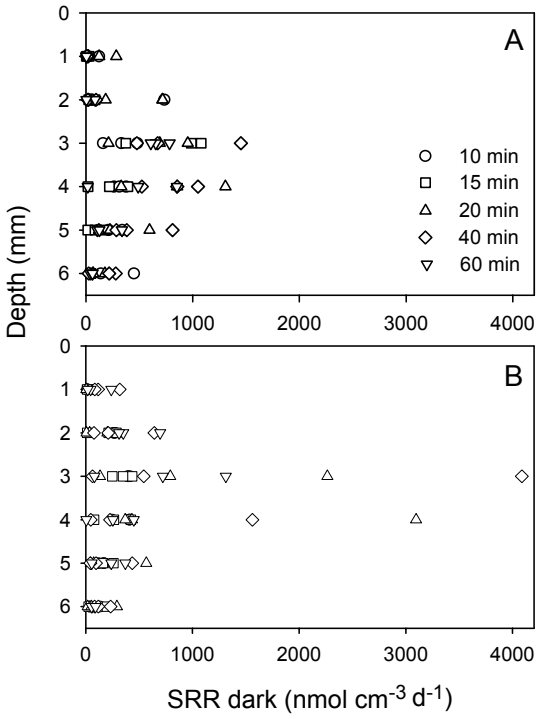

Figure 6 Depth profile of SRR measured in light (500 µE m^{-2} s^{-1}, A) and dark (B) incubated mats using different incubation times (triplicates for each incubation time).

Simultaneously measured oxygen microsensor profiles in replicate cores showed that the oxic zone comprised the first 2-2.5 mm, thus the highest SRR were found at the oxic/anoxic interface. The depth integrated (0-6 mm) SRR averaged over all incubation times amounted to 7 nmol cm^{-2} h^{-1} in the light and 8 nmol cm^{-2} h^{-1} in the dark, while rates for the photic zone (0-3 mm) were 4 and 5 nmol cm^{-2} h^{-1} respectively. Thus, SRR were comparable between light and dark incubated mats. The calculated areal gross photosynthesis rate at 500 µmol photons m^{-2} s^{-1} was 450 nmol O_2 cm^{-2} h^{-1}, which is equivalent to 450 nmol CH_2O units cm^{-2} h^{-1}. SRR in the photic zone of light incubated mats amounted to 4 nmol cm^{-2} h^{-1}, which corresponds to 8 nmol CH_2O units cm^{-2} h^{-1}. Thus, in the photic zone around 60 times more carbon was fixed by photosynthesis, than potentially converted by sulphate reduction.

Discussion

Calcification in microbial mats from "La Salada de Chiprana" is apparently a light driven process, as only in the light was the pore water saturation with respect to calcium carbonate higher than in the overlying water (Fig. 4). Comparing the profile shapes of the ICP profile with the shape of CO_3^{2-} and Ca^{2+} profiles is particularly telling, as it illustrates that the changes in the ICP are predominantly induced by changes in CO_3^{2-} concentration. This strongly suggests that calcification in Chiprana mats is not driven by increased Ca^{2+} concentrations but rather by strongly increased CO_3^{2-} concentrations in light incubated mats. However, Paerl et al. (2001) suggested, that a possible driving force of calcification in recent stromatolites from the Bahamas is a microbial induced increase in pore water calcium concentration. They argued that Ca^{2+} bound to EPS is liberated when EPS is degraded by heterotrophs, as they found that highest metabolic rates of heterotrophs coincided with areas of high $CaCO_3$ precipitation (Paerl et al. 2001). Therefore, a daily calcium dynamic in EPS-rich layers, with relatively low concentrations during the day (Ca^{2+}-binding) and higher concentrations at night (Ca^{2+}-release), can be expected. Interestingly, the measured light and dark profiles of calcium concentration in Lake Chiprana mats, reflect these hypothesised changes. Ca^{2+} concentrations in the photic zone of illuminated mats decreased considerably (about 1 mM), while in dark incubated mats an increase (about 0.2 mM) was measured using Ca^{2+} microsensors (Fig. 2D). The observed uptake of $^{45}Ca^{2+}$ in the light is also in agreement with the EPS theory. However, no liberation of Ca^{2+} high enough to considerably influence the ICP, and thus significantly promote calcification, was measurable in Chiprana mats during any part of the diel cycle (Fig. 2D, Fig. 4). Therefore, we found no evidence that calcification was driven by a liberation of Ca^{2+} from EPS in microbial mats from La Salada de Chiprana.

The microsensor profiles indicate instead, that the increased pH in the light dramatically shifted the carbonate equilibrium towards CO_3^{2-}. This pH increase might be induced by high rates of oxygenic photosynthesis in microbial mats which increase the pH due to the removal of HCO_3^- or CO_2. However, sulphate reduction might also promote calcification in microbial mats by increasing the pH (Visscher et al. 2000; Castanier et al. 1999; Visscher et al. 1998) and has been reported to reach high rates in the fully oxygenated parts of illuminated microbial mats (Jørgensen 1994; Fründ & Cohen 1992;Canfield & Des Marais 1991). We detected high rates of sulphate

reduction in the fully oxygenated upper layer of light incubated Lake Chiprana mats, but rates were comparable to those measured in dark mats. As in the latter no increase in pH was observed (Fig. 2C), the process of sulphate reduction in illuminated mats apparently did not contribute to a major extend to changes in the carbonate equilibrium and thus to changes in ICP values. We therefore conclude that the main causative agent for increasing the saturation of the pore water with respect to $CaCO_3$ was the increase in pH due to oxygenic photosynthesis. The decrease in calcium concentration during light incubation as measured with microsensors, therefore most likely reflects calcification activity. Thus, all our data indicate that a pH-driven calcification occurs in the top 0.5 mm of the mat, the same region where aragonite deposits are indeed found.

Ca^{2+} microsensors, which were for the first time applied in microbial mats, proved to be a valuable tool for assessing the calcification mechanism of hypersaline mats. However, our results also demonstrate, that only an integrative approach that measures both factors that influence the saturation state of calcium carbonate (calcium- and carbonate concentrations) at a micro-scale, will allow the identification of the factor driving calcification.

While oxygenic photosynthesis, rather than sulphate reduction was identified as the driving force of calcification in Lake Chiprana mats, the latter group might still contribute to the calcification process by providing nucleation sites. Nucleation sites have found to be provided by cyanobacteria (Arp et al. 2001) but also by heterotrophic bacteria (Paerl et al. 2001; Chafetz & Buczynski 1992) or the cell surface of sulphate reducers (Van Lith et al. 2003). Sulphate-reducing and other heterotrophic bacteria might therefore play an auxiliary role in calcification of La Salada de Chiprana mats by providing nucleation sites for calcium carbonate precipitation.

Acknowledgements

We are indebted to Tim Ferdelman for help with SRR measurements and thank Michael Böttcher for FTIR analysis. The technicians are thanked for microsensor construction. We thank the local authorities in Chiprana for granting permission to access the lake and taking microbial mat samples and we are particularly grateful to Alfredo Legaz (Guard) for support during field work.

References

Al-Horani, F. A., Al-Moghrabi, S. M., de Beer, D. (2003) The mechanism of calcification and its relation to photosynthesis and respiration in the scleractinian coral *Galaxea fascicularis*. Mar. Biol. 142: 419-426

Arp, G., Reimer, A., Reitner, J. (2001) Photosynthesis-induced biofilm calcification and calcium concentrations in Phanerozoic oceans. Science 292: 1701-1704

Böttcher, M. E., Gehlken, P. L., Steele, D. F. (1997) Characterization of inorganic and biogenic magnesian calcites by Fourier Transform infrared spectroscopy. Solid State Ionics 101: 1379-1385

Canfield, D. E., Des Marais, D. J. (1991) Aerobic Sulfate Reduction in Microbial Mats. Science 251: 1471-1473

Castanier, S., Le Métayer-Levrel, G., Perthuisot, J. P. (1999) Ca-carbonates precipitation and limestone genesis - the microbiogeologist point of view. Sed. Geol. 126: 9-23

Chafetz, H. S., Buczynski, C. (1992) Bacterially induced lithification of microbial mats. Palaios 7: 277-293

de Beer, D., Kühl, M., Stambler, N., Vaki, L. (2000) A microsensor study of light enhanced Ca^{2+} uptake and photosynthesis in the reef-building hermatypic coral *Favia* sp. Mar. Ecol. Prog. Ser. 194: 75-85

Des Marais, D. J. (1990) Microbial mats and the early evolution of life. Trends Ecol. Evol. 5: 140-144

Fossing, H., Jørgensen, B. B. (1989) Measurement of bacterial sulfate reduction in sediments: Evaluation of a single-step chromium reduction method. Biogeochem. 8: 205-222

Fründ, C., Cohen, Y. (1992) Diurnal cycles of sulfate reduction under oxic conditions in cyanobacterial mats. Appl. Environ. Microbiol. 58: 70-77

Garcia-Pichel, F., Al-Horani, F. A., Farmer, J. D., Ludwig, R., Wade, B. D. (2004) Balance between microbial calcification and metazoan bioerosion in modern stromatolitic oncolites. Geobiology. 2: 49–57

Jonkers, H. M., Ludwig, R., de Wit, R., Pringault, O., Muyzer, G., Niemann, H., Finke, N., de Beer, D. (2003) Structural and functional analysis of a microbial mat ecosystem from a unique permanent hypersaline inland lake: 'La Salada de Chiprana' (NE Spain). FEMS Microbiol. Ecol. 44: 175-189

Jørgensen, B. B. (1978) A comparison of methods for the quantification of bacterial sulfate reduction in coastal marine sediments. 1. Measurement with radiotracer techniques. Geomicrobiol. J. 1: 11-27

Jørgensen, B. B. (1994) Sulfate reduction and thiosulfate transformations in a cyanobacterial mat during a diel oxygen cycle. FEMS Microbiol. Ecol. 13: 303-312

Kallmeyer J., Ferdelman, T. G., Weber, A., Fossing, H., Jørgensen, B. B. (2004) A cold chromium distillation procedure for radiolabeled sulfide applied to sulfate reduction measurements. Limnol. Oceanogr. Meth. 2: 171-180.

Krumbein, W. E., Cohen, Y., Shilo, M. (1977) Solar Lake (Sinai). 4. Stromatolitic cyanobacterial mats. Limnol. Oceanogr. 22: 635-656

Kühl, M., Revsbech, N. P. (2001) Biogeochemical microsensors for boundary layer studies. In: Boudreau, B. P., Jorgensen, B. B. (eds) The Benthic Boundary Layer. Oxford University Press, Oxford. pp 180-210

Laniece, P., Charon, Y., Cardona, A., Pinot, L., Maitrejean, S., Mastrippolito, R., Sandkamp, B., Valentin, L. (1998) A new high resolution radioimager for the quantitative analysis of radiolabelled molecules in tissue section. J. Neurosci. Meth. 86: 1-5

Laval, B., Cady, S. L., Pollack, J. C., McKay, C. P., Bird, J. S., Grotzinger, J. P., Ford, D. C., Bohm, H. R. (2000) Modern freshwater microbialite analogues for ancient dendritic reef structures. Nature 407: 626-629

Margulis, L., Barghoorn, E. S., Ashendorf, D., Banerjee, S., Chase, D., Francis, S., Giovannoni, S., Stolz, J. (1980) The microbial community in the layered sediments at Laguna Figueroa, Baja California, Mexico: Does it have Precambrian analogues? Precambrian Res. 11: 93-123

Paerl, H. W., Steppe, T. F., Reid, R. P. (2001) Bacterially mediated precipitation in marine stromatolites. Environ. Microbiol. 3: 123-130

Reid, R. P., Visscher, P. T., Decho, A. W., Stolz, J. F., Bebout, B. M., Dupraz, C., MacIntyre, L. G., Paerl, H. W., Pinckney, J. L., Prufert-Bebout, L., Steppe, T. F., Des Marais, D. J. (2000) The role of microbes in accretion, lamination and early lithification of modern marine stromatolites. Nature 406: 989-992

Revsbech, N. P., Jørgensen, B. B. (1983) Photosynthesis of benthic microflora measured with high spatial resolution by the oxygen microprofile method: Capabilities and limitations of the method. Limnol. Oceanogr. 28: 749-756

Riding, R. (2000) Microbial carbonates: The geological record of calcified bacterial-algal mats and biofilms. Sedimentol. 47: 179-214

Stumm, W., Morgan, J. J. (1996) Aquatic chemistry. Wiley, New York

Van Gemerden, H. (1993) Microbial Mats - A Joint Venture. Mar. Geol. 113: 3-25

Van Lith, Y., Warthmann, R., Vasconcelos, C., McKenzie, J. A. (2003) Microbial fossilization in carbonate sediments: A result of the bacterial surface involvement in dolomite precipitation. Sedimentol. 50: 237-245

Visscher, P. T., Reid, R. P., Bebout, B. M. (2000) Microscale observations of sulfate reduction: Correlation of microbial activity with lithified micritic laminae in modern marine stromatolites. Geology 28: 919-922

Visscher, P. T., Reid, R. P., Bebout, B. M., Hoeft, S. E., MacIntyre, I. G., Thompson Jr., J. A. (1998) Formation of lithified micritic laminae in modern marine stromatolites (Bahamas): The role of sulfur cycling. Am. Mineral. 83: 1482-1493

Chapter 6

Balance between microbial calcification and metazoan bioerosion in modern stromatolitic oncolites

6

Balance between microbial calcification and metazoan bioerosion in modern stromatolitic oncolites

Ferran Garcia-Pichel, Fuad A. Al-Horani, Jack D. Farmer, Rebecca Ludwig, Brian D. Wade

Abstract

Stromatolites date back some 3.5 billion years and constitute the most common and conspicuous fossils through the Proterozoic. These organosedimentary structures decreased dramatically in diversity and abundance by the late Neoproterozoic, a phenomenon often ascribed to destructive grazing by newly evolved metazoans. We investigated the concurrent processes of microbial calcification and metazoan bioerosion in one of the few locations (Rio Mesquites, Cuatro Ciénegas, Coahuila, Mexico) where living freshwater stromatolites, formed by cyanobacteria and diatoms, coexist with significant populations of metazoan grazers. We used microsensor chemical profiling and monitoring of bulk water Ca^{2+} concentrations to determine calcification rates and their dependence on microbial metabolism. The bioerosive impact due to grazing by endemic hydrobiid gastropods was assessed by gravimetric quantification of carbonaceous fecal pellet production. Calcification was clearly light-dependent, reaching maximal rates (saturation) at low incident light intensity, and was surprisingly efficient, with O_2/Ca^{2+} exchange ratios well above unity, and with absolute rates similar to those found in corals. But the erosive action of grazing snails removed most of these carbonate inputs from the oncolites. Thus, a precarious balance between constructive and destructive geobiological processes was at play in the system. The fact that accretion barely exceeded bioerosion in an environment highly conducive to calcification supports the potential impact of faunal grazing as causal agent in the demise of stromatolites in the late Proterozoic. Our findings indicate that a search for fossil evidence of bioerosive grazing in the form of carbonaceous fecal pellets associated with fossil stromatolites may provide a means to test that hypothesis directly.

Introduction

A very diverse, evolutionarily divergent set of organisms is engaged in carbonate precipitation, ranging from bacteria, to algae and to animals. A record of fossil evidence, from Precambrian stromatolites to Holocene marine deposits attests both to the continuity and to the antiquity of this relationship between carbonates and living organisms. Organisms participate in the biological precipitation of either calcite or aragonite from dissolved calcium and carbonate ions in solution, but are also active at the erosional side of the cycle. Grazing on surface biofilms by hard-toothed higher animals and invertebrates (Shachak et al. 1987), as well as the growth of chasmolithic and cryptoendolithic (Friedmann & Weed 1987) microbes can result in significant physical erosion of limestones. Some organisms will tend to chemically dissolve carbonates by virtue of their metabolic activity, and active boring by microorganisms can have significant impact in sedimentary processes at a geological scale (Vogel et al. 2000). With regard to microbial calcification, carbonate precipitation at circumneutral pH in photosynthetic organisms (or photosynthetic microbial communities) is a result of the removal of CO_2 (as bicarbonate) from their immediate vicinity (Golubic et al. 2000) according to the following integrated equation (Stumm & Morgan 1996):

$$Ca^{2+} + 2\ HCO_3^- \rightarrow Ca^{2+} + CO_3^{2-} + CO_2 + H_2O \rightarrow CaCO_3(s) + CH_2O + O_2 \qquad (1)$$

where CO_2 removal tends to increase pH and the precipitation of calcium carbonate tends to decrease it (McConnaughey & Whelan 1997). Microbial aerobic respiration, as the inverse of oxygenic photosynthesis, will tend to dissolve carbonates. The process of microbial calcification is at the base of the formation of many organosedimentary structures, including stromatolites. Stromatolites date back some 3.5 billion years (Hofmann et al. 1999) and constitute not only the oldest form of biological carbonaceous structure, but also the most common and conspicuous fossils through the Proterozoic, decreasing dramatically in diversity and abundance in the fossil record by the late Neoproterozoic (Awramik 1971; Walter et al. 1992b). The near disappearance of stromatolites at this time has been a subject of much conjecture. One of the most commonly held hypotheses states that the stromatolite demise was due to the appearance of a novel ecological force in the form of destructive grazing by newly evolved metazoans (Garret 1970; Awramik 1971; Walter & Heys 1985). The hypothesis is not without controversy (Farmer 1992; Walter et al. 1992a), and other possible causes have been proposed, including competitive exclusion by macroalgae

(Fischer 1965), changes in seawater chemistry (Grotzinger 1990) or sedimentation rates (Pratt 1982). In fact, no quantitative studies have been carried out in modern settings to substantiate the role that small grazers might play on preventing stromatolite accretion.

We present studies on calcification and bioerosion in stromatolitic microbialites from the Cuatro Ciénegas Basin (Coahuila, Mexico). The basin is a complex karstic system in which the underlying Cretaceous limestone, dolomites and gypsum formations are being actively dissolved by an aquifer of distant origin, which results in the formation of innumerable springs, surface and underwater streams, caves and sinkholes, famous for their beauty and the biological diversity they harbour (Grall 1995). Conspicuous stromatolitic microbialites (Burne & Moore 1987) develop in the high-calcium waters of Rio Mesquites, the main river draining the basin, where they form anchored, domal stromatolites, bioherms and detached oncolites (Winsborough & Golubic 1987; Winsborough et al. 1994). Because suspended sediment load in the Rio Mesquites is low, Cuatro Ciénegas stromatolites accrete overwhelmingly by direct calcification, with trapping and binding of allochthonous carbonates being negligible. Accretion of these microbialites often proceeds in the presence of significant populations of grazing gastropods, which is apparently at odds with the grazing hypothesis for stromatolite demise. These stromatolites thus provide an ideal system to investigate in a quantitative manner the relationship between grazing and calcification as opposing forces in net stromatolite accretion.

Materials and methods

Materials

We studied submerged, detached, dendritic, spherical to ovoid oncolites measuring between 5 and 30 cm in diameter from a site along the Rio Mesquites (Wade & Garcia-Pichel 2003) known as Balneario (26°55’ N, 102°06’ W), during visits in January, June, and August, 2002. The oncolites used here consist of cauliflower-like branches that grow radially outward from the centre (Fig.1 A). They were collected from the stream floor by diving and maintained in river water during transport to the laboratory. Natural populations of snails consisted of a mix of two species of hydrobiids endemic to Cuatro Ciénegas (*Nymphophilus minckleyi*, and *Mexithauma quadripaludium*). Specimens used for population manipulations ranged from 18 to

53 mg in (tissue-blotted) wet weight, large enough to be easily traceable, with a population mean of 33.4 g, a mode of 32 g and a standard deviation of 11.6 g.

Microbialite and fecal pellet characterisation

Phase contrast microscopy was carried out to confirm the general composition of the phototrophic microbial community, and a more detailed analysis has been presented elsewhere, including molecular analysis of microbial composition (Wade & Garcia-Pichel 2003). Mineralogy and microfabrics were studied on polished thin sections. Confirmation of mineralogy was done using X-ray powder diffraction in combination with electron microprobe analysis of polished thin sections. X-ray diffraction analysis was carried out using a Siemens automated X-ray diffractometer fitted with a Cu-anode X-ray tube (Cu K alpha 1 = 1.5406 angstroms). The instrument was operated in a summation, step-scan mode at 40 KV (30 mA) and data were obtained over a 2-theta range of 5-90^0 using a 7^0 detector. Mineralogical identifications were made using the ICDD Powder Diffraction data base.

Chemical microprofiling through the benthic boundary layer

Microsensor measurements were performed on freshly collected oncolites in a make-shift laboratory built in the nearby town. Oncolites were incubated in glass aquaria in river water at room temperature; flow, similar to that *in situ*, was maintained by use of submersible pumps. Light was provided by goose-neck fibre-optic illuminators, whose output intensity could be varied without changing spectral composition by means of a diaphragm. Microelectrodes were inserted from above and were driven by computer-controlled motorised micromanipulators (Maerzhäuser, Germany) fixed to heavy metal stands. Profiling was done from the mixed bulk water into and through the benthic boundary layer. Due to the hard nature of the substrate it was not possible to profile into the oncolites themselves. Initial microsensor positioning was aided by observation through binocular microscopes held on boom-stands and focused on the oncolite surface. Oxygen partial pressure was measured with custom-built Clark-type microelectrodes provided with a guard cathode and with sensing tips smaller than 10 µm in diameter (Revsbech 1989). A two-point calibration was carried out using air-bubbled river water (100% air-saturation) and river water amended with local anaerobic sludge (0% air-saturation). Absolute conversion of pO_2 values into O_2 concentrations was achieved after Winkler titrations of the calibration liquids. For pH and Ca^{2+} measurements, we used custom-built liquid-membrane ion-selective (LIX) glass microelectrodes (Jensen et al. 1993). LIX microelectrodes were constructed

according to de Beer et al. (de Beer et al. 1997). For pH we used the ionophore, N, N-dioctadecylmethylamine (Fluka), for Ca^{2+} we used N,N,N',N'-Tetracyclohexyl-3-oxapentanediamide (Fluka). The Ca^{2+} ionophore, has a selectivity of 5x 10^6 over Mg^{2+} (Ammann et al. 1987), the second most common cation in Rio Mesquites water. Modifications to electrode construction and calibration procedure are described in detail elsewhere (de Beer et al. 2000). Due to the short shelf-life of Ca^{2+} microsensors (1-2 days), they were calibrated frequently and exchanged daily. An amperometric sensor was used to check for presence of H_2S (Jeroschewski et al. 1996). It has a detection limit of 3 μmol l^{-1} at pH 8.

Bulk calcification rates

Ca^{2+} concentration in the bulk incubation water was followed during experiments from discrete water samples by graphite furnace atomic absorption. For these experiments, 1-3 oncolites were incubated in small aquaria containing river water and provided with flow. The volumetric ratio for these incubations (oncolite to water volume) was approximately 1:10. Aquaria were kept at room temperature (around 25°C) and provided with light (100 μmol photon m^{-2} s^{-1}) from a tungsten lamp; according to microsensor studies (see results), this light intensity was sufficient to reach maximal rates of calcification. Evaporative water losses were corrected for by daily additions of distilled water. Rates of Ca^{2+} depletion in the water were calculated as the linear regression of calcium concentration vs. time and converted to absolute Ca^{2+} mass using the total water volume in each aquarium. Areal rates were calculated using the added cross-sectional (projectional) areas of all oncolites in the aquarium; these were obtained assuming an ellipsoidal shape for all oncolites, based on measurements of long and short axes (to the nearest mm) for each specimen.

Rates of bioerosion

These were also quantified in laboratory experiments by incubating oncolites containing naturally occurring snail populations. The snail density in the field was 9 ± 0.1 individuals per oncolite, as determined in a homogenous subpopulation of oncolites ca. 10 cm in diameter (Elser et al. 2003). Incubations were carried out at room temperature, with an illumination of 100 μmol photon m^{-2} s^{-1} provided by an incandescent flood lamp and under flow provided by an underwater pump as detailed above. Fecal materials were collected by suction from the aquarium bottom, after gently shaking and turning the oncolite to dislodge loosely adhered particles. The slurry of fecal material was allowed to settle for 10 min in graduated cylinders, pooled

into polypropylene centrifuge tubes and pelleted in a centrifuge at 4100 rpm for 10 min. The pellets were oven dried at 80ºC for 2 to 4 days, and weighed. Acid-resistant (non-carbonaceous) fraction of the pellets was determined in aliquots thereof after a 2-day incubation in 1% HCl, centrifugation and washing twice with distilled water. Incubations to determine rates of bioerosion were performed sequentially for single or groups of 10 oncolites, and run for periods of 1-3 months. Average snail densities remained relatively constant during incubations, with populations increasing maximally to 12 individuals per oncolite, in some incubations, even though a shift in relative abundance to the benefit of *N. minckleyi* did apparently take place.

Results

Light and electron microscopy revealed that oncolites were built by a phototrophic biofilm which was conspicuously bi-layered, as has been determined independently using DNA analyses (Wade & Garcia-Pichel 2003). The biofilm or mat had a lightly mineralised surface community, dominated by large, filamentous heterocystous cyanobacteria (morphologically close to the form-genera *Homeothrix/Calothrix*) and various diatoms, and a deeper community of more heavily mineralised, thin filamentous cyanobacteria morphologically resembling the morpho-genus *Leptolyngbya*. (Fig. 1 C, D). Petrographic thin sections (Fig. 1 B) revealed that the predominant mineral phase making up the oncolites was a carbonate, shown to be calcite by X-ray diffraction analysis.

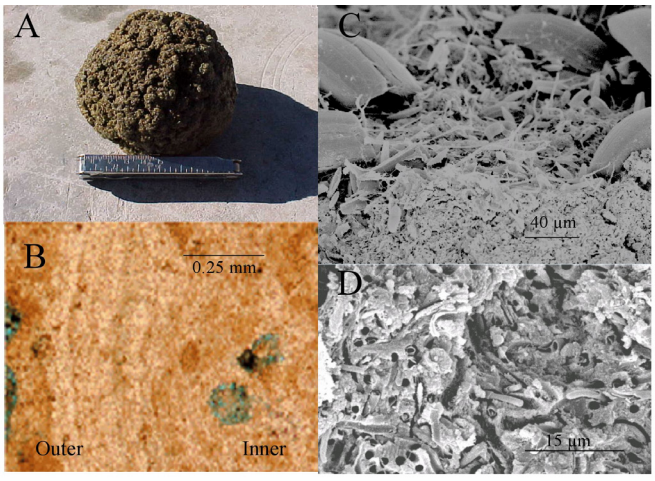

Figure 1: Rio Mesquites Oncolites. A: Appearance of a typical oncolite retrieved from the river, as used for experimentation. Metal tool for scale is approx. 12 cm. B: Petrographic thin section showing the laminated fabric (laminae run top to bottom) within the organosedimentary matrix. C: SEM view of the surface microbial community with cyanobacterial filaments (visible are many terminal hairs of a dominant *Calothrix* spp.), diatoms frustules and loose micritic carbonate. D: SEM view of the heavily calcified deeper community of thin filamentous cyanobacteria. Note here the tight fit between carbonate and the space originally occupied by thin cyanobacterial trichomes, visible as holes.

We studied calcification and its relationship to photosynthesis in aquarium-incubated oncolites by measuring chemical microprofiles of O_2, Ca^{2+}, and pH across the benthic boundary layer (Fig. 2 A, B). This viscous layer witnesses all diffusional mass transport between the active microbial film and the bulk aqueous medium, and the magnitude of the chemical gradients within it can be used to quantify net exchange processes (Jørgensen & Revsbech 1985). Mass transfer rates through the boundary layer were calculated according to Fick's first law of diffusion, where the flux, J, of a given solute is the product of its diffusion coefficient, D, and the magnitude of the concentration gradient, $\delta C/\delta x$, where C is concentration and x is distance. Vertical concentration gradients ($\delta C/\delta x$) were estimated by regression of the linear portions in the profile data above the oncolite surface.

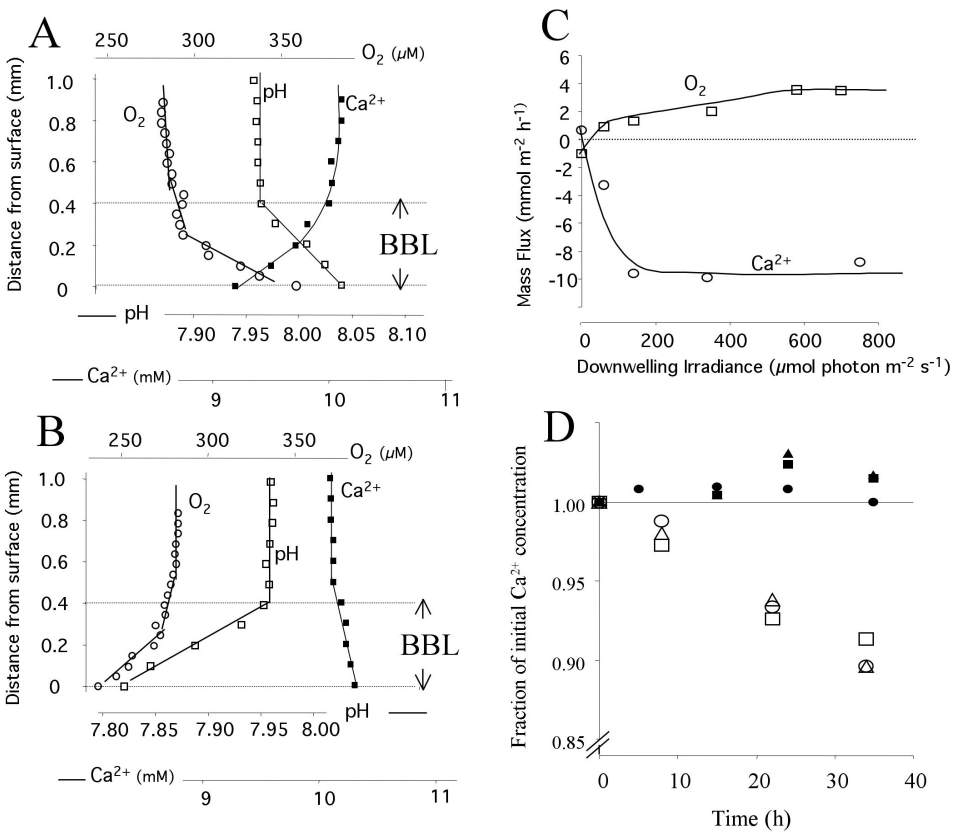

Figure 2: Measurement of calcification by oncolites. A, B: Vertical chemical microprofiles measured across the benthic boundary layer (BBL) above active stromatolitic oncolites incubated in the light (A) and in the dark (B). A decreasing concentration gradient towards the surface indicates import of a chemical species; an increasing gradient indicates net export**.** C: Calcification and net photosynthesis rates as a function of incident light intensity. Sets of profiles such as those shown in A and B were used to define the relationship. D: Calcium depletion (as percentage of initial concentration) from the medium in whole oncolites incubated in river water at saturating light intensities (light symbols) or in the dark (dark symbols). Initial Ca^{2+} concentrations varied between 0.40 and 0.54 g l^{-1}. Each curve depicts a single independent incubation.

When incubated in the light (Fig. 2A), oncolites displayed a net export of photosynthetically derived O_2 (net photosynthesis), which was accompanied by an import of Ca^{2+} from the bulk water (Calcification), and a moderate net proton import. All gradients reversed readily when incubations proceeded in the dark (Fig. 2B), demonstrating the light dependency of calcification and its direct coupling to photosynthesis, even though Ca^{2+} export in the dark was always very weak or undetectable. Using sulphide microelectrodes, we could not detect free H_2S neither in the benthic boundary layer nor in the pore water of microbialite cavities under any conditions. Several series of profile determinations such as those depicted in Fig. 2A, B, but carried out under different light intensities, and condensed in Fig. 2C, demonstrated that both net photosynthesis and calcification rates displayed light-saturation curves. Calcification attained maximum rates (light saturation) at around 5-10% of maximal ambient irradiance (100 µmol photon m^{-2} h^{-1}), whereas net photosynthesis saturated at a much higher irradiance (300 µmol photon m^{-2} h^{-1}).

Despite offering valuable insights into mechanistic aspects of the process, and because of the small area covered, the short times involved, and the necessity to measure in exposed areas of the oncolite, microsensor measurements are not optimal for assessing average accretion rates of macroscopic structures. To obtain estimates that integrated a larger oncolite surface area, including void spaces between branches, we followed the time course of bulk Ca^{2+} concentration in the bathing water during incubations under constant illumination in small aquaria. Ca^{2+} depletion rates in these experiments were linear for at least 3 days (Fig. 2D) and amounted to 3.41 ± 0.35 mmol Ca^{2+} m^{-2} h^{-1}, a value consistent with, if expectedly smaller than, that obtained by microsensor profiling. Oncolite calcification potential *in vitro* was retained for long periods (oncolites kept in incubators for one month yielded 2.79 ± 0.49 mmol Ca^{2+} m^{-2} h^{-1}, if supplied with fresh river water). Even though slow rates of carbonate dissolution in the dark (around 0.6 mmol Ca^{2+} µmol photon m^{-2} h^{-1}; Fig. 2B) could be detected during short-term (minutes to hours) experiments using microsensors, when incubations were extended in the dark for longer periods, rates of calcite dissolution (0.11 ± 0.12 mmol Ca^{2+} m^{-2} h^{-1}; Fig. 2D) were statistically insignificantly different from zero. The short-term effect was thus transient, probably due to dissolution of newly formed, unstable calcite nuclei.

Snail bioerosion

We observed that, during incubations, clean aquarium floors would become quickly covered with sand-sized particles (Fig. 3). Chemical and microscopic analyses revealed that these consisted of 74 ± 3% carbonate by (dry) weight, with the remainder being organic debris, diatom frustules and silicate mineral grains. We suspected that the particles were fecal pellets from grazing snails. We then seeded snail-free oncolites with randomly collected snails (Fig. 3 A, B). As seen in Fig. 3D, the rate of fecal pellet production was a direct linear function of the number of snails present, demonstrating the effectiveness of metazoan grazing in oncolite bioerosion. To determine the rate of fecal pellet production, long-term incubations were then carried out on groups of oncolites without manipulation of their snail populations, which remained relatively constant and similar to those in the natural environment (see materials and methods). The rates of bioerosion thus measured, expressed as dry weight of fecal material, amounted to 1.53 ± 0.2 kg m^{-2} a^{-1}, which translates to 1.13 ± 0.1 kg $CaCO_3$ m^{-2} a^{-1}.

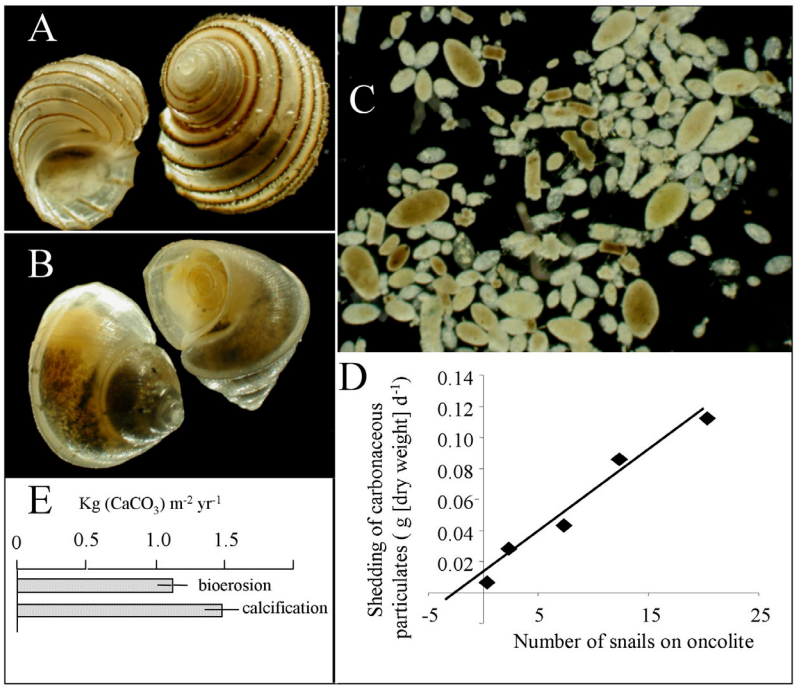

Figure 3: Bioerosion by gastropods during incubation experiments. A: endemic hydrobiid specimens of *Mexithauma quadripaludium* B: endemic hydrobiid specimens of *Nymphophilus minckleyi. C:* Snail fecal pellets produced during incubations. D: the linear dependence of the rate of particulate carbonate shedding by oncolites, relative to the number of snails present during incubations. Snail size was between 3 and 6 mm. E: Estimates of calcification vs. bioerosion in the oncolite/snail system.

Discussion

Instantaneous rates of photosynthesis and calcification

Light-saturated net photosynthesis rates (around 3 mmol O_2 m^{-2} h^{-1}) measured in our oncolites were similar in magnitude to those found in highly productive photosynthetic biofilms in marine (Garcia-Pichel et al. 1999), freshwater (Glud et al. 1992), and terrestrial (Garcia-Pichel & Belnap 1996) settings. But pH gradients across the benthic boundary layer in the light were much subtler than those found in other, non-calcifying photosynthetic biofilms, pointing to the relevance of calcification in our system as a significant buffering process for photosynthetically-mediated alkalinisation. In the dark, however, Ca^{2+} export (which we equate with calcite dissolution) was barely measurable, even though steep gradients could be detected in the light, and buffering of respiration-mediated acidification was not nearly as efficient as buffering of pH increases in the light. While no other measurements of calcification in modern stromatolites exist for direct comparison, instantaneous calcification rates in the light were also very high, similar to those observed in corals. Typical rates in various corals vary between 0.2 and 7 mmol Ca^{2+} m^{-2} h^{-1} (Howe & Marshall 2002), whereas our estimates for the outermost areas of the oncolites based on microsensor measurements, were around 9 mmol Ca^{2+} m^{-2} h^{-1}. Our estimates for whole oncolites, which integrate voids and areas likely to be much more diffusion-limited, were also in the mid range of those from corals (around 3.5 mmol Ca^{2+} m^{-2} h^{-1}). Judging from our microsensor profiles, at light-saturation, and assuming that one carbon atom is biologically fixed for each oxygen molecule produced, 2 to 3 moles of carbonate were precipitated in the system for each mole of carbon fixed into organic matter. Paradoxically, this exceeds the 1: 1 ratio predicted by Eq. 1. However, net photosynthesis as measured by benthic boundary layer gradients is the difference between gross photosynthesis (actual *in situ* oxygen evolution) rates and concurrent respiration rates within the active biofilm. Because part of this oxygen is respired before it can diffuse away into the overlying water, gross photosynthesis in photosynthetic biofilms and microbial mats is typically 2-3 times larger than net photosynthesis (Epping & Jørgensen 1996; Garcia-Pichel et al. 1999). It is likely that specific layers within the stromatolite with high rates of photosynthesis contribute relatively more to the total net import of Ca^{2+}. Because respiratory acidification does not seem to bring about carbonate dissolving effects commensurate with those that

photosynthetically-driven alkalinisation causes with regard to calcification (Fig. 2), the microbial community as a whole may be able to act as a "calcifying ratchet", where gross photosynthesis drives the calcification process at the small scale and respiration is not able to turn around advances in calcification already made. Alternatively, internal processes of sulphate reduction in the oncolite may contribute to the carbonate precipitation, as has been demonstrated in other microbialites (Visscher et al. 2000; Van Lith et al. 2003). Internal budgets of O_2, pH and Ca^{2+} and possibly H_2S would be needed to examine this in more detail. Whatever the mechanism, a very efficient system of mineral formation is present in these complex communities that can exceed the 1:1 ratio measured in single organisms, such as calcareous algae (McConnaughey & Falk 1991).

Long term carbonate inputs and accretion

The mechanistic knowledge obtained from short-term benthic boundary layer profiling, together with the assessment of the instantaneous calcification rates, allows us to obtain long-term estimates for calcification. For this we assumed that daylight periods when calcification does occur are around 12 hours daily, with negligible seasonal variations, due to the low latitude of the setting. We also infer that maximal rates of calcification occur through the daytime, since, according to our light intensity vs. calcification curves (Fig. 2, C), calcification saturates at low light intensities that are reached at low sun elevation angles. Our calculations, in accordance with the data presented, also assume that no dissolution occurs during the night-time. Temperature effects have been neglected as well, since water temperatures in Rio Mesquites vary little seasonally, with daily maxima between 24 and 31°C year round, due to the mildly thermal nature of many of the side springs that feed the stream. Under these assumptions, the oncolites must precipitate an average of 1.49 ± 0.12 kg Calcite m^{-2} a^{-1}. Since oncolites had a specific gravity of 1.9 g cm^{-3}, voids represented about 50% of their surface, and with an internal porosity estimated also at 50%, calcification rates represented a yearly potential vertical accretion rate of 3.1 mm. This is somewhat higher than, but comparable to, estimates for various marine stromatolites that accrete at rates ranging from 0.2 to 2 mm a^{-1} (Rasmussen et al. 1993; MacIntyre et al. 1996; Laval et al. 2000; Reid et al. 2000), chiefly by trapping and binding of sediments, and much higher than estimates for other freshwater microbialites (Laval et al. 2000).

Balance between calcification and bioerosion

The role of gastropod grazing for carbonate erosion and sediment production in marine coastal environments and has been previously demonstrated (Schneider & Toruski 1983). In our case, bioerosion rates of 1.13 ± 0.1 kg $CaCO_3$ m^{-2} a^{-1} constitute not only a significant rate of sediment formation, but also a very significant proportion (76%) of the estimated long-term calcification rates (1.49 ± 0.12 kg Calcite m^{-2} a^{-1}) in the same substrate. The implication is straightforward: in spite of the unusually efficient microbial calcification process at work in the oncolites, and its high overall rates, metazoan grazing was responsible for repackaging much of the newly formed carbonate into fecal material, which was subsequently shed into the carbonate-rich sediments surrounding the oncolites.

Other processes that were not studied may secondarily contribute to bioerosion, such as boring by specialized cyanobacteria, known to occur locally (Seeler & Golubic 1991). It is also likely that some fecal pellets become entrapped in the stromatolite framework, and are not shed to the sediment, but become part of the stromatolite itself. Thus, our estimates for rates of bioerosion must be considered conservative. In spite of these uncertainties, our data clearly demonstrate that the stromatolite/grazer system imposes a precarious balance between net formation and destruction, whose net outcome determines whether macroscopic stromatolitic structures will form. The balance should be very sensitive to environmental parameters that influence either of the two opposing forces. In aquatic habitats with very high levels of calcite supersaturation, such as in Rio Mesquites, calcification rates are sufficiently high to offset the effects of bioerosion. However, in most natural waters they are not, so that even if calcification occurs, net accretion is effectively prevented. Conversely, in habitats where metazoan development is halted or restricted due to extreme conditions, such as hypersalinity, accretion may occur even under slow rates of calcification. In mesic environments, where grazers can develop, some constraints must also exist that limit their continued population growth in order to allow stromatolite growth. Interestingly, predation by members of higher trophic level (fish in the case of Cuatro Ciénegas), limitation due to food quality (Elser et al. 2003), or a combination of both, may be responsible for such ultimate determinants.

Implications for Paleobiology

Our results not only provide evidence for the importance of bioerosion in controlling stromatolite accretion, but also point to the fate of metazoan-bioeroded carbonates, namely incorporation into the surrounding sapropelic sediments. In fact, in springs and streams of the Cuatro Ciénegas basin, sapropelic sediments of this type often accumulate to a thickness in the order of decimetres to meters. While reports of microfossils resembling fecal pellets do exist, dating back to the Early Proterozoic (Robbins et al. 1985), they remain controversial. A study of the preservation potential and diagenesis of highly carbonaceous metazoan fecal materials, and a systematic search for their presence and association with ancient stromatolitic sediments may provide direct evidence of the particular ecological conditions that caused the past global stromatolite decline.

Acknowledgements

All authors contributed equally to this work, which was supported by a grant from NASA's NAI (FGP, JF, BW) and by the Max-Planck-Society (RL, FH). We thank the members of ASU's Cuatro Ciénegas team for field support, Mexico's SEMARNAT for permits and assistance, and Gaby Eickert and Ines Schroeder for electrode construction.

References

Ammann, D., Bührer, T., Schefer, U., Müller, M., Simon, W. (1987) Intracellular neutral-carrier based Ca^{2+} microelectrode with subnanomolar detection limit. Eur. J. Physiol. 409:223-228

Awramik, S. M. (1971) Precambrian columnar stromatolite diversity: Reflection of metazoan appearance. Science 174:825-827

Burne, R. V., Moore, L. S. (1987) Microbialites: Organosedimentary deposits of benthic microbial communities. Palaios 2:241-254

de Beer, D., Kühl, M., Stambler, N., Vaki, L. (2000) A microsensor study of light enhanced Ca^{2+} uptake and photosynthesis in the reef-building hermatypic coral *Favia* sp. Mar. Ecol. Prog. Ser. 194:75-85

de Beer, D., Schramm, A., Santegoeds, C. M., Kühl, M. (1997) A nitrite microsensor for profiling environmental biofilms. Appl. Environ. Microbiol. 63:973-977

Elser, J. J., Schampel, J. H., Garcia-Pichel, F., Wade, B. D., Souza, V., Eguiarte, L., Escalante, A., Farmer, J. D. (2003) Effects of phosphorus enrichment and grazing snails on modern stromatolitic microbial communities. under review

Epping, E. H. G., Jørgensen B. B. (1996) Light-enhanced oxygen respiration in benthic phototrophic communities. Mar. Ecol. Prog. Ser. 139:193-203

Farmer, J. D. (1992) Grazing and bioturbation in modern microbial mats. In: Schopf, J.W., Klein, C. (eds) The Proterozoic Biosphere: A Multidisciplinary Study. Cambridge Univ. Press, Cambridge, pp 295-297

Fischer, A. G. (1965) Fossils, early life and atmospheric history. Proc. Natl. Acad. Sci. USA 53:1205-1215

Friedmann, E. I., Weed, R. (1987) Microbial trace-fossil formation, biogenous and abiotic weathering in the Antarctic cold desert. Science 236:703-705

Garcia-Pichel, F., Belnap, J. (1996) Microenvironments and microscale productivity of cyanobacterial desert crusts. J. Phycol. 32:774-782

Garcia-Pichel, F., Kühl, M., Nübel, U., Muyzer, G. (1999) Salinity-dependent limitation of photosynthesis and oxygen exchange in microbial mats. J. Phycol. 35:227-238

Garret, P. (1970) Phanerozoic stromatolites: Noncompetitive ecologic restriction by grazing and burrowing animals. Science 169:171-173

Glud, R. N., Ramsing, N. B., Revsbech, N. P. (1992) Photosynthesis and photosynthesis-coupled respiration in natural biofilms quantified with oxygen microsensors. J. Phycol. 28:51-60

Golubic, S., Seong-Joo, L., Browne, K. M. (2000) Cyanobacteria: Architects of sedimentary structures. In: Riding RE, Awramik SM (eds) Microbial Sediments. Springer-Verlag, Heidelberg, pp 57-67

Grall, G. (1995) Cuatro Ciénegas: Mexico's desert aquarium. National Geographic 188:85-97

Grotzinger, J. P. (1990) Geochemical model for Proterozoic stromatolite decline. Am. J. Sci. 290A:80-103

Hofmann, H. J., Grey, K., Hickman, A. H., Thorpe, R. I. (1999) Origin of 3.45 Ga coniform stromatolites in Warrawoona Group, Western australia. Geol. Soc. Am. Bull. 111:1256-1262

Howe, S. A., Marshall, A. T. (2002) Temperature effects on calcification rate and skeletal deposition in the temperate coral, *Plesiastrea versipora* (Lamarck). J. Exp. Mar. Biol. Ecol. 275:63-81

Jensen, K., Revsbech, N. P., Nielsen, L. P. (1993) Microscale distribution of nitrification activity in sediment determined with a shielded microsensor for nitrate. Appl. Environ. Microbiol. 59:3287-3296

Jeroschewski, P., Steuckart, C., Kühl, M. (1996) An amperometric microsensor for the determination of H_2S in aquatic environments. Anal. Chem. 68:4351-4357

Jørgensen, B. B., Revsbech, N. P. (1985) Diffusive boundary layers and the oxygen uptake of sediments and detritus. Limnol. Oceanogr. 30:111-122

Laval, B., Cady, S. L., Pollack, J. C., McKay, C. P., Bird, J. S., Grotzinger, J. P., Ford, D. C., Bohm, H. R. (2000) Modern freshwater microbialite analogues for ancient dendritic reef structures. Nature 407:626-629

MacIntyre, I. G., Reid, R. P., Steneck, R. S. (1996) Growth history of stromatolites in a Holocene fringing reef, Stocking Island, Bahamas. J. Sed. Res. 66:231-242

McConnaughey, T. A., Falk, R. H. (1991) Calcium-proton exchange during algal calcification. Biol. Bull. 180:185-195

McConnaughey, T. A., Whelan, J. F. (1997) Calcification generates protons for nutrient and bicarbonate uptake. Earth Sci. Rev. 42:95-117

Pratt, B. R. (1982) Stromatolite decline: A reconsideration. Geology 10:512-515

Rasmussen, K. A., MacIntyre, I. G., Prufert, L. (1993) Modern stromatolites reefs fringing a brackish coastline, Chetumal Bay, Belize. Geology 21:199-202

Reid, R. P., Visscher, P. T., Decho, A. W., Stolz, J. F., Bebout, B. M., Dupraz, C., MacIntyre, I. G. Paerl, H. W., Pinckney, J. L., Prufert-Bebout, L., Steppe, T. F., Des Marais, D. J. (2000) The role of microbes in accretion, lamination and early lithification of modern marine stromatolites. Nature 406:989-992

Revsbech, N. P. (1989) An oxygen microelectrode with a guard cathode. Limnol. Oceanogr. 34:474-478

Robbins, E. I., Porter, K. G., Haberyan, K. A. (1985) Pellet microfossils: Possible evidence for metazoan life in early Proterozoic time. Proc. Natl. Acad. Sci. USA 82:5809-5813

Schneider, J., Torunski, H. (1983) Biokarst on limestone coasts, morphogenesis and sediment production. Mar. Ecol. 4: 45-63

Seeler, J.-S., Golubic, S. (1991) *Lyengariella endolithica* sp. nov., a carbonate boring stigonematalean cyanobacterium from a warm spring-fed lake; nature to culture. Arch. Hydrobiol. Suppl. 92:399-410

Shachak, M., Jones, C. G., Granot, Y. (1987) Herbivory in rocks and the weathering of a desert. Science 236 (4805):1098-1099

Stumm, W., Morgan, J. J. (1996) Aquatic Chemistry, 3rd Edition, John Wiley & Sons, New York

Van Lith, Y., Warthmann, R., Vasconcelos, C., McKenzie, J. A. (2003) Sulphate-reducing bacteria induce low-temperature Ca-dolomite and high Mg-calcite formation. Geobiol. 1:71-79

Visscher, P. T., Reid, R. P., Bebout, B. M (2000) Microscale observations of sulfate reduction: Correlation of microbial activity with lithified micritic laminae in modern marine stromatolites. Geology 28:919-922

Vogel, K., Gektidis, M., Golubic, S., Kiene, W. E., Radtke, G. (2000) Experimental studies on microbial bioerosion at Lee Stocking Island, Bahamas and One Tree Island, Great Barrier Reef, Australia: Implications for paleoecological reconstructions. Lethaia 33:190-204

Wade, B., Garcia-Pichel, F. (2003) Evaluation of DNA extraction methods for molecular analysis of microbial communities in modern calcareous microbialites. Geomicrobiol. J. 20:549-561

Walter, M. R., Bauld, J., Des Marais, D. J., Schopf, J. W. (1992a) A general comparison of microbial mats and microbial stromatolites: Bridging the gap between the modern and the fossil. In: Schopf JW., Klein, C. (eds.) The Proterozoic Biosphere: A Multidisciplinary Study. Cambridge University Press, Cambridge, pp 335-338

Walter, M. R., Grotzinger, J. P., Schopf, J. W. (1992b) Proterozoic Stromatolites. In: Schopf, J.W., Klein, C. (eds.) The Proterozoic Biosphere: A Multidisciplinary Study. Cambridge University Press, Cambridge, pp 253-260

Walter, M. R., Heys, G. R. (1985) Links between the rise of the Metazoa and the decline of stromatolites. Precambrian Res. 29:149-174

Winsborough, B. M., Seeler, J.-S., Golubic, S., Folk, R. L., Maguire Jr., B. (1994) Recent fresh-water lacustrine stromatolites, stromatolitic mats and oncoids from Northeastern Mexico. In: Bertrand-Sarfati J, Monty C (eds.) Phanerozoic Stromatolites II. Kluwer Academic Publishers, Amsterdam, pp 71-100

Winsborough, B. M., Golubic, S. (1987) The role of diatoms in stromatolite growth: Two examples from modern freshwater settings. J. Phycol. 23:194-201

Discussion

Relationship between microbial primary production and biomass accretion

Phototrophic microbial mats belong to the world's most productive ecosystems (Jørgensen et al. 1979). Daily oxygenic photosynthesis rates of 156 mmol O_2 m^{-2} have been reported (Revsbech et al. 1983) and microbial mat primary productivity has been considered comparable to tropical rain forests (Stal 2000, Guerrero & Mas 1989). Indeed, when photosynthesis rates of microbial mats are converted to carbon yield, assuming a photosynthetic ratio of one and a photoperiod of 12 hours, these values (1900-2500 mg C m^{-2} d^{-1} for gross photosynthesis (Jørgensen et al. 1983) and up to 1800 mg C m^{-2} d^{-1} for net photosynthesis (Wieland & Kühl 2000)) are comparable to estimates of total net primary productivity of tropical forests (median 1900-3500 mg C m^{-2} d^{-1}, Clark et al. 2001). Like in rain forests, net growth in mature mats is much lower than potentially possible when compared to the high rates of primary production (Nold & Ward 1996; Van Gemerden 1993; Krumbein et al. 1977). This raises two questions: i) What is the fate of photosynthetically fixed carbon? and ii) what restricts the conversion of photosynthetically fixed CO_2 into biomass in systems with low grazing pressure? To answer the latter question, a wide array of compounds (inorganic carbon, organic carbon and nutrients) were screened for their potential to stimulate community gross photosynthesis, net photosynthesis and respiration (chapter 3). A short-term approach was chosen to avoid a shift in community composition towards opportunistic organisms. Phosphate and amino acids were identified as compounds which limit both processes, gross photosynthesis and respiration, while net photosynthesis remained constant. Net photosynthesis (NP), includes organic carbon not respired in the mat i.e. biomass, the recalcitrant part of extracellular polymeric substances (EPS) and organic carbon lost to the overlying water. The combination of unchanged NP and stimulation of photosynthesis and respiration could be explained by a change in carbon partitioning: During nutrient limitation, organic carbon is mostly excreted by phototrophs (Staats et al. 2000; Berman-Frank & Dubinsky 1999; Myklestad et al. 1989). In mats from "La Salada de Chiprana" this excreted organic carbon was apparently not completely metabolised by heterotrophic bacteria, as the DOC content in the mats was high and organic carbon was partially lost to the overlying water, as indicated by *in situ* fatty acid fluxes (chapter 2). If this organic carbon is instead used for growth, as may be the case after

relieve of nutrient limitation, no change in NP will result. Thus, in the case of microbial mats from La Salada de Chiprana, low accretion rates might be attributable to nutrient limitation which directly affects two key processes of the carbon cycle, oxygenic photosynthesis and respiration (chapter 3). Why do microbial mats accrete biomass at all despite presumed nutrient limitation? For accretion of biomass at low growth rates, a reduced grazing pressure has to be assumed which is indeed usually the case in extreme environments (Fenchel & Kühl 2000; Stal 2000).

The relationship between calcium carbonate accretion (calcification) and removal by metazoan grazers was investigated in chapter 6 using stromatolitic oncolites. In this system, stromatolites coexist with a significant population of grazers, i.e. endemic gastropods (hydrobiids). It was demonstrated that calcification in this system occurred at high rates (3.5 mmol Ca^{2+} m^{-2} h^{-1}), comparable to rates measured in stony corals. These high calcification rates sustained oncolite accretion, even though bioerosion removed 76% of the calcium carbonate precipitated. Interestingly, (Elser et al. submitted) found evidence that oxygenic phototrophs in this system were limited by phosphate, as was also found for Chiprana mats (chapter 3). The low P content of phototrophs apparently induced P limitation in these grazers likely resulting in modest grazing impacts. As microbial mats are often found in nutrient poor environments (Paerl et al. 2000; Stal 1995), nutrient limitation of the grazing community might contribute to the low grazing pressure in these systems.

In future studies, in order to better quantify the amount of C excreted as well as the flow of carbon in microbial mats in general, microsensor measurements of gross photosynthesis rates should be combined with $^{14}CO_2$ labelling experiments. The latter should be used to localise and quantify (using β-imaging) the ratio of $^{14}CO_2$ photosynthetically fixed into biomass versus the amount of label excreted as DOC.

Coupling of community structure and function

Certain aspects of the relationship between community structure (localisation of mat organisms) and function (metabolism of mat organisms) of different functional groups of bacteria were revealed in this thesis. Firstly, it was observed that *Chloroflexus*-like bacteria dominated the uppermost layer in mats of La Salada de Chiprana (chapter 2). The functional analysis revealed that the upward flux of organic carbon to this layer was highest, which presumably supported photoheterotrophic growth of *Chloroflexus*-like bacteria. Irradiances around solar noon (>1400 µmol photons m^{-2} s^{-1}) were found to be inhibitory to oxygenic phototrophs, evoking downward migration of

cyanobacteria resulting in a reduction of areal gross photosynthesis. The top layer of *Chloroflexus*-like bacteria is likely to reduce the irradiance reaching the underlying layer dominated by cyanobacteria. Therefore *Chloroflexus*-like bacteria are expected to profit from cyanobacterial excretion products, while cyanobacterial exposure to high light intensities is reduced.

Sulphate-reducing bacteria were found in high abundance throughout the investigated depth (0-6 mm). Their activity, measured as sulphate reduction rates (chapter 5), however, was highest in the oxic/anoxic interface around 3 mm and not in the layer with maximal fatty acid concentration. The highest activities were thus found where oxygen pressure was low, but substrate was still amply available.

A close coupling between two processes, photosynthesis and respiration, was revealed by the response to additions of rate-limiting compounds (chapter 3). Addition of limiting compounds apparently stimulated photosynthesis and respiration always to the same extent. While this may indicate that both groups were limited by the same compounds, this finding might also suggest that one group is dependent on the other. As pointed out in chapter 3, phototrophs might depend on heterotrophs as these decrease oxygen supersaturation or moderate pH increases due to CO_2 production. The study presented in chapter 4 demonstrates that limitation of photosynthesis can indeed be induced by increased oxygen partial pressure. Furthermore it was shown that high salt concentrations limited photosynthesis in benthic but not in planktonic systems: With increasing salinity, oxygen solubility and diffusive exchange with the overlying water decrease, which induced high oxygen partial pressures. This salinity-dependent oxygen supersaturation only occurs in diffusion-limited benthic cultures. This study showed that the removal of oxygen from the mat, e.g. by aerobic heterotrophic respiration may be important for the functioning of hypersaline mats. During this PhD study it was planned to further investigate the interdependence of photosynthesis and respiration using model organisms in simulated mat gradients in benthic gradient chambers (BGC). The latter are devices that allow the culturing of model organisms in a sand core with gradients of light, oxygen and H_2S under sterile conditions. However, several attempts to culture filamentous cyanobacteria in the sand core were not successful as cyanobacteria developed biofilms in the fully oxygenated water instead. In these experiments it was planned to compare gross and net photosynthesis as well as respiration rates in axenic cyanobacterial cultures with those of defined mixed cultures of cyanobacteria and aerobic heterotrophs to further clarify metabolic interactions between these groups.

In order to identify the organisms involved in the carbon cycle of "La Salada de Chiprana", a clone library was constructed. The 16S rRNA clone library was constructed by amplifying the almost complete gene (~1500 bp) from environmental DNA using the primer pair GM3F and GM4R (Muyzer et al. 1995). DNA was extracted from the oxic (0-3 mm) and anoxic (3-6 mm) horizon of Lake Chiprana mats in order to find out whether species composition in these two layers was influenced by the different environmental conditions. The PCR products were cloned using TOPO TA Cloning® Kit (Invitrogen Ltd, UK) according to manufacturer's instruction. Around 20 clones for each depth were obtained and partially sequenced using the vector primer M13F. Sequences were aligned with help of the program BioEdit (http://www.mbio.ncsu.edu/BioEdit /bioedit.html). However, the number of clones obtained per depth so far are not sufficient to get a representative picture of mat species. Therefore the cloning process has to be repeated in order to obtain a higher number of clones. 50% of the clones obtained were cyanobacteria, of which 99% belonged to the genus *Microcoleus.* Species of this genus were in fact identified by fluorescence microscopy (chapter 2) to be the most abundant cyanobacteria in Lake Chiprana mats.

Calcification

Photosynthetic increase in pH is one process that promotes calcification, which in turn buffers the pH increase induced by photosynthesis. These processes thus link calcification to the carbon cycle. While all microbial mats are characterised by high primary production rates, only some do calcify. As a first step to explain this phenomenon, the mechanisms by which microbes promote calcification must be identified. The results presented in chapters 5 and 6, clearly suggest that calcification is driven by a pH increase induced by photosynthesis. Chapter 5 provides evidence that photosynthesis rather than sulphate reduction induces calcification in the studied hypersaline mats. Firstly, sulphate reduction rates were substantially lower than oxygenic photosynthesis rates. Secondly, dark sulphate reduction rates were comparable to those in the light, but failed to induce a pH increase in the zone were calcification took place. Measurements in calcifying oncolites (chapter 6) demonstrated the effectiveness of calcification as a pH buffer. The pH increase in the DBL induced by photosynthesis was smaller than the pH decrease due to respiration in the light. Simultaneously measured Ca^{2+} gradients showed that calcification was highly efficient in the light, while in the dark the respiratory decrease in pH was not sufficient to induce calcium dissolution. The data presented in chapter 6 support the

hypothesis that calcification of the oncolites was induced by photosynthesis, the same mechanism that induced calcification of microbial mats from "La Salada de Chiprana". Thus in two different systems, calcification was shown to be driven by an increase of pH due to photosynthesis. This finding suggests that oxygenic photosynthesis may be the driving factor regulating calcification in mats, as it is the factor that largely controls pH changes. Further investigations concerning the question of why certain mats calcify and others do not should therefore focus on this key process.

References

Berman-Frank, I., Dubinsky, Z. (1999) Balanced growth in aquatic plants: Myth or reality? Biosci. 49: 29-37

Clark, D. A., Brown, S., Kicklighter, D. W., Chambers, J. Q., Thomlinson, J. R., Ni, J., Holland, E.A. (2001) Net primary production in tropical forests: An evaluation and synthesis of existing field data. Ecol. Appl. 11, 371-384

Elser, J., Schampel, J., Garcia-Pichel, F., Wade, B., Souza, V., Eguiarte, L., Escalante, A., Farmer, J. (submitted)

Fenchel, T., Kühl, M. (2000) Artificial cyanobacterial mats: Growth, structure, and vertical zonation patterns. Microb. Ecol. 40: 85-93

Guerrero, R., Mas, J. (1989) Multilayered microbial communities in aquatic ecosystems: Growth and loss factors In: Microbial mats - Physiological ecology of benthic microbial communities (Cohen, Y. & Rosenberg, E., Eds.), pp. 37-51. American Society for Microbiology, Washington DC.

Jørgensen, B. B., Revsbech, N. P., Blackburn, T. H., Cohen, Y. (1979) Diurnal cycle of oxygen and sulfide microgradients and microbial photosynthesis in a cyanobacterial mat system. Appl. Environ. Microbiol. 38: 46-58

Jørgensen, B. B., Revsbech, N. P., Cohen, Y. (1983) Photosynthesis and structure of benthic microbial mats: Microelectrode and SEM Studies of four cyanobacterial communities. Limnol. Oceanogr. 28, 1075-1093

Krumbein, W. E., Cohen, Y., Shilo, M. (1977) Solar Lake (Sinai). 4. Stromatolitic cyanobacterial mats. Limnol. Oceanogr. 22: 635-656

Muyzer, G., Teske, A., Wirsen, C. O., Jannasch, H. W. (1995) Phylogenetic relationships of *Thiomicrospira* species and their identification in deep-sea hydrothermal vent samples by denaturing gradient gel-electrophoresis of 16S rDNA fragments. Arch. Microbiol. 164: 165-172

Myklestad, S., Holm-Hansen, O., Varum, K. M., Volcani, B. E. (1989) Rate of release of extracellular amino acids and carbohydrates from the marine diatom *Chaetoceros affinis*. J. Plankton Res. 11: 763-773

Nold, S. C., Ward, D. M. (1996) Photosynthate partitioning and fermentation in hot spring microbial mat communities. Appl. Environ. Microbiol. 62: 4598-4607

Paerl, H. W., Pinckney, J. L., Steppe, T. F. (2000) Cyanobacterial-bacterial mat consortia: Examining the functional unit of microbial survival and growth in extreme environments. Environ. Microbiol. 2: 11-26

Revsbech, N. P., Jørgensen, B. B., Blackburn, T. H., Cohen, Y. (1983) Microelectrode studies of the photosynthesis and O_2, H_2S, and pH profiles of a microbial mat. Limnol. Oceanogr. 28: 1062-1074

Staats, N., Stal, L. J., Mur, L. R. (2000) Exopolysaccharide production by the epipelic diatom *Cylindrotheca closterium*: Effects of nutrient conditions. J. Exp. Mar. Biol. Ecol. 249: 13-27

Stal, L. J. (2000) Cyanobacterial mats and stromatolites. In: Whitton, B., Potts, M. (eds) The Ecology of Cyanobacteria. Kluwer Academic, pp 61-120

Stal, L. J. (1995) Physiological ecology of cyanobacteria in microbial mats and other communities. New Phytol. 131: 1-32

Van Gemerden, H. (1993) Microbial Mats - A Joint Venture. Mar. Geol. 113: 3-25

Wieland, A., Kühl, M. (2000) Short-term temperature effects on oxygen and sulfide cycling in a hypersaline cyanobacterial mat (Solar Lake, Egypt). Mar. Ecol. Prog. Ser. 196, 87-102

Summary

Phototrophic microbial mats are laminated aggregations of microorganisms that thrive in extreme and oligotrophic environments. Primary production rates by oxygenic phototrophs are extremely high. Primary producers supply heterotrophic mat members with organic carbon, which in turn regenerate CO_2 needed for autotrophic carbon fixation. Another potential source of CO_2 is calcification, which is known to shift the carbonate equilibrium towards CO_2. This thesis investigated the carbon cycle of microbial mats and stromatolitic oncolites, with special emphasis on oxygenic photosynthesis and calcification.

Microbial mats from "La Salada de Chiprana", which were used for three studies (chapters 2, 3 & 5), were characterised combining *in situ* and laboratory analyses (chapter 2). Maximal *in situ* gross photosynthesis rates of 0.44 nmol O_2 cm^{-2} s^{-1} were only reached during early morning and late afternoon, higher light intensities around noon (2500 μmol photons m^{-2} s^{-1}) inhibited gross photosynthesis. HPLC pigment analysis revealed that the phototrophs migrated downwards during the day, apparently to avoid high light intensities. It was calculated that up to 14% of carbon fixed by gross photosynthesis diffused to the overlying water in the form of low molecular weight fatty acids. The high abundances of *Chloroflexus*-like bacteria and sulphate-reducing bacteria found in the top layers of the mat are probably linked to the upward flux of these compounds, as they represent typical substrates for these bacteria.

Lake Chiprana mats were also used to investigate why high primary production rates in microbial mats do not necessarily result in high growth rates (chapter 3). The response of gross photosynthesis and respiration rates to short-term additions of potentially rate-limiting compounds revealed that both processes were limited by phosphate and organic nitrogen. As net photosynthesis was not stimulated, it remains to be clarified whether the observed increased process rates did in fact induce biosynthesis, and if so, whether biosynthesis occurred at the expense of organic carbon excretion rates. Interestingly, gross photosynthesis and respiration were apparently closely coupled as both processes were always stimulated to the same extent.

The experiment presented in chapter 4 revealed that certain physicochemical conditions might influence metabolism of planktonic and benthic ecosystems differently. High salinity limited oxygenic photosynthesis and respiration in benthic

but not in planktonic cultures of *Halothece* sp. Evidence is presented that benthic cultures at high salinity reached inhibitory oxygen partial pressures (pO_2) at lower photosynthesis rates due to the combination of decreased oxygen solubility and diffusive transport. The finding that high pO_2 restricted photosynthesis indicates that the close coupling between photosynthesis and respiration, as was observed in chapter 3, might at least partially be due to the dependence of phototrophs on oxygen removal by heterotrophic respiration.

Chapter 5 presents evidence that calcification in microbial mats from "La Salada de Chiprana" is induced by photosynthesis and not by sulphate reduction. The ion concentration product (ICP) of calcium carbonate was only increased in the light and pore water analysis indicated that the ICP was mainly influenced by changes in CO_3^{2-} concentration. The pH increase that shifted the carbonate equilibrium towards CO_3^{2-} was found to be caused by oxygenic photosynthesis and not by sulphate reduction.

Calcification in stromatolitic oncolites was also shown to be induced by a photosynthetically induced shift in the carbonate equilibrium (chapter 6). Microsensor measurements revealed that calcification was very high (1.49 kg $CaCO_3$ m^{-2} a^{-1}), which allowed accretion of oncolites despite grazing pressure (1.13 kg $CaCO_3$ m^{-2} a^{-1}) by metazoans.

Zusammenfassung

Phototrophe mikrobielle Matten sind zusammenhängende Bakteriengemeinschaften mit deutlicher Zonierung, die unter extremen und oligotrophen Umweltbedingungen existieren können. Die Primärproduktion durch oxygene Phototrophe ist außergewöhnlich hoch. Die Primärproduzenten versorgen heterotrophe Mattenorganismen mit organischem Kohlenstoff, welche wiederum CO_2 regenerieren, das für die autotrophe Kohlenstoffixierung benötigt wird. Eine andere mögliche CO_2-Quelle stellt die Kalzifizierung dar, da sie das Karbonatgleichgewicht zugunsten des CO_2 verschiebt. In dieser Doktorarbeit wurde der Kohlenstoffkreislauf in mikrobiellen Matten und stromatolitischen Oncoliten untersucht. Dabei stellten oxygene Photosynthese und Kalzifizierung zwei Schwerpunkte dar.

Drei Untersuchungen (Kapitel 2, 3 & 5) wurden an mikrobiellen Matten von "La Salada de Chiprana" durchgeführt, welche mithilfe von *in situ*- und Laboranalysen charakterisiert wurden (Kapitel 2). Maximale Bruttophotosyntheseraten von bis zu 0.44 nmol O_2 cm^{-2} s^{-1} wurden im Freiland während der frühen Morgen- und späten Abendstunden erreicht. Vermutlich vermeiden phototrophe Organismen höhere Lichtintensitäten (bis zu 2500 µmol Photonen m^{-2} s^{-1}) durch Migration in tiefere Mattenschichten, wie mittels Pigmentanalysen an der HPLC gezeigt werden konnte. Bis zu 14% der Bruttophotosynthese diffundierte in Form niedermolekularer Fettsäuren ins überliegende Wasser. Da diese Komponenten typische Substrate für *Chloroflexus*-ähnliche und sulfatreduzierende Bakterien darstellen, bilden sie vermutlich die Grundlage für hohe Abundanzen dieser Bakterien in den oberen Mattenschichten.

Anhand der gleichen Matten wurde untersucht, warum sich die hohe Primärproduktion mikrobieller Matten nicht in hohen Wachstumsraten niederschlägt (Kapitel 3). Durch Zugabe von Phosphat und organischem Stickstoff konnten die Bruttophotosynthese- und Respirationsraten gesteigert werden, was auf eine Limitierung durch diese Substanzen hindeutet. Die beiden Prozesse scheinen eng gekoppelt zu sein, da sie stets im gleichen Ausmaß stimuliert wurden. Die Nettophotosynthese wurde durch die Zugaben nicht gesteigert. Falls die beobachtete Zunahme der Raten also tatsächlich zu einer erhöhten Biosynthese führt, müsste diese zulasten der Exkretionsraten stattgefunden haben.

Das Experiment in Kapitel 4 zeigt, dass planktonische und benthische Systeme unterschiedlich auf identische physikochemische Einflüsse reagieren. Limitierung von

Photosynthese und Atmung durch hohe Salinitäten trat in benthischen, nicht jedoch in planktonischen Kulturen von *Halothece* sp. auf. In benthischen Systemen führte die Kombination von reduzierter Sauerstofflöslichkeit und Diffusivität bei erhöher Salinität dazu, dass ein inhibitierender Sauerstoffpartialdruck (pO_2) schon bei niedrigeren Photosyntheseraten erreicht wurde. Diese photosynthesehemmende Wirkung eines erhöhten pO_2 deutet darauf hin, daß die in Kapitel 3 beobachtete enge Kopplung von Photosynthese und Atmung zumindest zum Teil auf der Abhängigkeit phototropher Organismen von der Entfernung des Sauerstoffs beruhen könnte.

Kapitel 5 zeigt, dass die Kalzifizierung in mikrobiellen Matten von "La Salada de Chiprana" durch Photosynthese und nicht durch Sulfatreduktion induziert wird. Eine Steigerung des Ionenkonzentrationsproduktes (ICP) des Kalziumkarbonats erfolgte nur im Licht. Porenwasseranalysen deuteten darauf hin, dass das ICP hauptsächlich von der CO_3^{2-} -Konzentration beeinflusst wurde. Oxygenische Photosynthese und nicht Sulfatreduktion verursachte den pH-Anstieg, der das Karbonatgleichgewicht zugunsten von CO_3^{2-} verschob.

Auch die Kalzifizierung in stromatolitischen Oncoliten wurde durch eine photosythesebedingte Verschiebung des Karbonatgleichgewichtes angeregt, wie in Kapitel 6 dargestellt wird. Messungen mit Mikrosensoren offenbarten eine sehr hohe Kalzifizierung (1.49 kg $CaCO_3$ m^{-2} a^{-1}), die trotz des hohen Fraßdrucks durch Metazoen (1.13 kg $CaCO_3$ m^{-2} a^{-1}) ein Wachstum der Oncoliten ermöglichte.

Danksagung

This thesis work would not have been possible without the help of numerous people, which I gratefully acknowledge. First of all I would like to thank Olivier and Henk for giving me the opportunity to work on microbial mats. Thanks to Bo for his advice during this thesis and for refereeing it. I would like to say a warm thank you to everyone participating in the field trips to "La Salada de Chiprana", for the excellent working atmosphere and the fruitful discussions over one or two glasses of Patxaran and some Tapas. Merci beaucoup aussi à Astrid et Dorothée (LOB Arcachon).

The field trip to Mexico was also very enjoyable. Therefore, my very warm thank you to Ferran, for asking me to participate and also to Susanne and Marlene for the hospitality. Thanks to Fuad for the pleasant co-operation and to James, John, Jack and Brian for the nice working atmosphere.

Mein Dank gilt auch Rudi, der mir die Exkursion in die Molekularökologie ermöglicht hat und allen Mollis, die mir dabei geholfen haben, insbesondere Anna, Silke und Jörg. Tim danke ich für seine Hilfe bei der Vorbereitung der Sulfatreduktionsmessung.

Hans bekommt ein besonders großes Dankeschön, nicht nur für all die beantworteten Fragen und hilfreichen Ratschläge im Laufe der Doktorarbeit, sondern besonders für die unerwartete Hilfe in letzter Minute. Auch an Peter, Miriam, Fanni und Eli ein herzliches Dankeschön für die Unterstützung in dieser Zeit.

Die Hilfsbereitschaft, die ich in meiner Zeit am MPI erlebt habe, war enorm und so viele Leute haben eine entscheidende Kleinigkeit beigetragen. Stellvertretend möchte ich mich bei Elze bedanken, die die Mikrosensorgruppe bei Stimmung gehalten hat, und bei den TAs für die unermüdliche Arbeit im Hintergrund und die tolle Unterstützung. Björn kam oft zur Rettung, wenn die Computer nicht so richtig wollten. Noch wertvoller für mich war aber seine Gabe mathematische oder physikalische Sachverhalte zu erklären.

Ein besonderes Dankeschön geht an Eli für sein offenes Ohr, die klasse Kaffeepausen und dafür mich überzeugt zu haben, daß Steine nicht langweilig sind.

Klasse war auch, daß ich mit Dörte, Uschi und Felix die 'besten Bürogenossen wo gibt' hatte: Ihr wart immer da, um größere und kleinere Probleme zu lösen und meine Fragen zu beantworten. Vor allem möchte ich mich aber für die tolle Stimmung und gute Arbeitsatmosphäre bedanken. Dickes Lob! Das fetzte! Uschi, die die heiße Phase mit mir alleine durchstehen mußte, bekommt für die konstruktive Hilfe und den tollen Einsatz ein besonders dickes Dankeschön.

Bedanken möchte ich mich bei Bernd für den freundlichen und unermüdlichen Literaturservice - selbst dann noch, als unser Zimmer sein ästethisches Empfinden verletzt hat. Den Elektronikwerkstättlern möchte ich auch danken (insbesondere für die Ferndiagnose am Freitagnachmittag).

Bei Dirk möchte ich mich bedanken für so manche konstruktive Kritik, aber besonders dafür, daß er mich ermutigt hat ein zweimonatiges Stipendium in den USA anzutreten. Es war eine wirklich tolle Erfahrung! Herrn Kirst sei gedankt für die Begutachtung dieser Arbeit und Frau Koenig für ihre Bereitschaft als Prüferin zu fungieren.

Zum Schluß möchte ich mich besonders bei meinem Betreuer Henk bedanken, der mir durch seine positive und optimistische Art und seinen Einsatz in den letzten Wochen sehr geholfen hat. Dank je wel!

Da es tatsächlich auch ein Leben außerhalb des MPI's gibt, möchte ich all denen danken, die mich von außerhalb unterstützt haben: Ny, Esther, Frank und Manou. Bei meiner Familie bedanke ich mich für das mir entgegengebrachte Verständnis. Ganz besonders habe ich mich aber darüber gefreut, daß ihr nie aufgegeben habt zu verstehen, was um alles in der Welt ich denn den ganzen Tag mache! Mein Dank an die Rugbymannschaften von Union Bremen und Welfen Braunschweig, die dafür gesorgt haben, daß ich regelmäßig Dampf ablassen konnte und somit wieder entspannt an die Arbeit gehen konnte.

Danke Stefan für einfach alles!

Manuscripts presented in this thesis

Structural and functional analysis of a microbial mat ecosystem from a unique permanent hypersaline inland lake: 'La Salada de Chiprana' (NE Spain)
Henk M. Jonkers, Rebecca Ludwig, Rutger de Wit, Olivier Pringault, Gerard Muyzer, Helge Niemann, Niko Finke, Dirk de Beer
FEMS Microbiology Ecology (2003) 44 (2): 175-189

Limitation of oxygenic photosynthesis and respiration by phosphate and organic nitrogen in a hypersaline mat: A microsensor study
Rebecca Ludwig, Olivier Pringault, Rutger de Wit, Dirk de Beer, Henk Jonkers
To be submitted to FEMS Microbiology Ecology

Reduced gas diffusivity and solubility limit metabolic rates in benthic phototrophs at high salinities
Rebecca Ludwig, Ferran Garcia-Pichel
In preparation for submission to L&O

Photosynthesis controlled calcification in a hypersaline microbial mat
Rebecca Ludwig, Fuad A. Al-Horani, Dirk de Beer and Henk M. Jonkers
To be submitted to L&O

Balance between microbial calcification and metazoan bioerosion in modern stromatolitic oncolites
Ferran Garcia-Pichel, Fuad A. Al-Horani, Jack D. Farmer, Rebecca Ludwig, Brian D. Wade
Geobiology (in press)